Democratic and Popular Republic of Algeria

Ministry of Higher Education and Scientific Research

University Ahmed Draia - Adrar

Faculty of Sciences and Technology

Department of Electrical Engineering

A Dissertation Presented to Fulfill the Doctoral Degree in Electrical
Engineering

Option: Electrical Engineering

Title

Modeling Losses of Mobile Networks using Artificial Intelligence Methods

Prepared by
Mr. Alnatoor Moamen

The Jury Members:

Pr. Messaoud Hamouda	*President*
Pr. Mohammed Omari	*Supervisor*
Dr. Mohammed Kaddi	*Examiner*
Dr. Ramadhan Masmoudi	*Examiner*
Dr. Ammar Necaibia	*Examiner*

Academic Year 2022/2023

بِسْمِ اللهِ الرَّحْمٰنِ الرَّحِيمِ

قُلْ إِنَّ صَلَاتِي وَنُسُكِي وَمَحْيَايَ وَمَمَاتِي لِلَّهِ رَبِّ الْعَالَمِينَ ﴿١٦٢﴾

صَدَقَ اللهُ الْعَظِيمُ

١

Dedication

To the first teacher in my life, to the one who once said to me: "Knowledge is your only weapon in this world"...my father.

To the one who covered me with her tenderness and supplication since I was little, to the one who used to build me on her carpet when the world was destroying me, and who took my hand when I got lost in this world.... my mother.

To the only star that stayed lit when the entire universe went dark....my sister Israa.

To my little child and my great teacher, my psychological comfort....my brother Noureddine

To the one who was and still is the bond and honor, to him is the companion of alienation and homeland... My brother Mohammed.

To my old brother and my first role model...Ahmed.

To the companions of the path, the companions of the way, those who continued on the covenant and left on that... my friends.

To that place that taught me that exile is the food of men.

To that noble heart that accompanied me on my way.

I dedicate this work.

Acknowledgments

First and all, I want to thank ALLAH for giving me the strength and patience to finish my studies.

Through this modest work,

I thank my supervisor: Prof. Mohammed OMARI, for his invaluable guidance, suggestions, financial support. I also thank him for the precious time he offered me and for his understanding and patience, which created the ideal working environment for me.

Special thanks to Professor Messaoud Hamouda, director of the LDDI laboratory, for the facilities he provided us during the completion of this dissertation.

My heartfelt gratitude goes to the jury members for agreeing to examine and evaluate this work.

For their devotion and hard work, I extend my sincere gratitude to all of the professors in the laboratory of sustainable energy and computer science LDDI.

I need also to thank the research center for renewable energies in the middle of the desert, which allowed me to use its equipment while completing this work.

Without failing to express my heartfelt gratitude to everyone who helped make this work a reality, especially to Pr. Saifi Mechaour, Dr. Abdalghani Dahou, Dr. Ebrahim Alkebsi, Dr. Fadila Tahiri, Dr. Abdallah Laidi, mr. Mohammed Abdeldjabar, and Dr. Chahrazad Lkrim.

Abstract

One of the most critical problems in a communication system is losing information between the transmitter and the receiver. WiMAX (Worldwide Interoperability of Microwave Access) technology is gaining popularity and recognition as a Broadband Wireless Access (BWA) solution. At frequencies below 11 GHz, WiMAX can operate in line-of-sight (LOS) and non-line-of-sight (NLOS) scenarios. The implementation of WiMAX networks will be rushed worldwide. Estimating path loss is crucial in the early stages of wireless network deployment and cell design. To anticipate propagation loss, several path loss (PL) models are available (e.g., Okumura Model Hata Model), but they are all bound by particular parameters. In this dissertation , we propose an MLP neural network-based path loss model with a well-structured implementation network design and grid search-based hyperparameter tweaking. The proposed model optimally approximates mobile and base station path losses. Therefore, neuron number, learning rate, and hidden layer number are investigated to obtain the best model in terms of prediction accuracy. Path loss data is collected based on 14 networks in different microcellular settings. Simulations under MATLAB environment showed that prediction errors were lower than standard log-distance-based path loss models.

Keywords: Mobile networks, prediction models, urban, suburban and rural environments, artificial neural networks.

Résumé

L'un des problèmes les plus critiques dans un système de communication est la perte d'informations entre l'émetteur et le récepteur. La technologie WiMAX (Worldwide Interoperability of Microwave Access) gagne en popularité et en reconnaissance en tant que solution d'accès sans fil à large bande (BWA). À des fréquences inférieures à 11 GHz, le WiMAX peut fonctionner dans des scénarios en visibilité directe (LOS) et sans visibilité directe (NLOS). La mise en œuvre des réseaux WiMAX sera précipitée dans le monde entier. L'estimation de la perte de chemin est cruciale dans les premières étapes du déploiement du réseau sans fil et de la conception des cellules. Pour anticiper la perte de propagation, plusieurs modèles de perte de propagation (PL) sont disponibles (par exemple, Okumura Model Hata Model), mais ils sont tous liés par des paramètres particuliers. Dans cette thèse, nous proposons un modèle de perte de chemin basé sur un réseau de neurones MLP avec une conception de réseau de mise en œuvre bien structurée et un ajustement d'hyperparamètres basé sur la recherche de grille. Le modèle proposé se rapproche de manière optimale des pertes de trajet de la station mobile et de la station de base. Par conséquent, le nombre de neurones, le taux d'apprentissage et le nombre de couches cachées sont étudiés pour obtenir le meilleur modèle en termes de précision de prédiction. Les données de perte de trajet sont collectées sur la base de 14 réseaux dans différents paramètres micro cellulaires. Les simulations sous l'environnement MATLAB ont montré que les erreurs de prédiction étaient inférieures aux modèles standard de perte de trajet basés sur la distance logarithmique.

Mots clés : Réseaux mobiles, modèles de prédiction, environnements urbains, suburbains et ruraux, réseaux de neurones artificiels.

الملخص

من أهم المشاكل في نظام الاتصال هو فقدان المعلومات بين المرسل والمستقبل. تكتسب تقنية WiMAX (قابلية التشغيل البيني في جميع أنحاء العالم للوصول إلى الميكروويف) شعبية واعترافًا كحل للوصول اللاسلكي عريض النطاق (BWA). عند الترددات التي تقل عن 11 جيجاهرتز ، يمكن أن تعمل WiMAX في سيناريوهات خط البصر (LOS) وغير خط البصر (NLOS). سيتم التعجيل بتنفيذ شبكات WiMAX في جميع أنحاء العالم. يعد تقدير خسارة المسار أمرًا بالغ الأهمية في المراحل الأولى لنشر الشبكة اللاسلكية وتصميم الخلايا. لتوقع خسارة الانتشار ، تتوفر عدة نماذج لخسارة المسير (PL) على سبيل المثال ، نموذج (Okumura Model Hata) ، لكنها كلها مرتبطة بمعلمات معينة. في هذه الأطروحة ، نقترح نموذج خسارة المسار المعتمد على الشبكة العصبية MLP مع تصميم شبكة تنفيذ جيد التنظيم وتعديل المعلمات الفائقة المستند إلى البحث في الشبكة. يقترب النموذج المقترح على النحو الأمثل من خسائر المسار المتنقلة والمحطة الأساسية. لذلك ، يتم التحقق من عدد الخلايا العصبية ومعدل التعلم ورقم الطبقة المخفية للحصول على أفضل نموذج من حيث دقة التنبؤ. يتم جمع بيانات فقدان المسار بناءً على 14 شبكة في إعدادات مختلفة من الخلايا الدقيقة. أظهرت عمليات المحاكاة في بيئة MATLAB أن أخطاء التنبؤ كانت أقل من النماذج القياسية لخسارة المسير القائمة على لوغاريتم المسافة.

الكلمات المفتاحية: شبكات المحمول ، نماذج التنبؤ ، البيئات الحضرية والضواحي والريفية ، الشبكات العصبية الاصطناعية.

Table of Contents

<u>Chapter 3 : Related works</u>

List of Figures

List of Tables

List Abbreviations and Acronyms

WiMAX	Worldwide Interoperability of Microwave Access
GSM	Global System for Mobile Communications
BWA	Broadband Wireless Access
LOS	line-of-sight
NLOS	non-line-of-sight
PL	path loss
BSS	Base Station Sub-system
NSS	Network Sub System
OSS	Operation Sub-System
MSC	Mobile Switching Center
HLR	Home Location Register
AUC	Authentication Center
VLR	Visitor Location Register
EIR	Equipment Identity Register
OMC	Operations and Maintenance Centre
NMC	Network and Management Centre
IMSI	International Mobile Subscriber Identity
KI	encryption key
IMEI	International Mobile station Equipment Identity
GPRS	General Packet Radio Service
SGSN	The Service Node
GGSN	Gateway Node
3G	the third generation of mobile network
UMTS	Universal Mobile Telecommunications System
LTE	Long-Term Evolution
OFDMA	Orthogonal Frequency Division Multiple Access
SC-FDMA	Single Carrier – Frequency Division Multiple Access
EPS	Evolved Packet System
EPC	Packet Core Evolved
ITU	International Telecommunication Union
AN	access network
UE	user equipment
UHF	ultra-high frequency
FAF	floor attenuation factor
FSPL	Free Space Path Loss
WI	Walfisch-Ikegami
SUI	Stanford University Interim
MMDS	Multipoint Microwave Distribution System
MAC	medium access control
PDF	probability density function of signal
BPSK	binary phase-shift keying
UGV	unmanned ground vehicle
WSNS	wireless sensor networks is presented
UAB	uniformly attenuated buildings
RSS	receiver signal strength
WHIPP	Wicca Heuristic Indoor Propagation Prediction
DOA	direction of arrival

TOA	the time of arrival
NF	Neuro-Fuzzy
FL	fuzzy logic
BS	base station
MS	mobile station
EIRP	adequate isotropic radiated power
ANN	Artificial Neural Network
MLP	multi-layer perceptron
SVM	Support Vector Machines
CSI	channel state information
BW	bandwidth of transmission
Dist	distance between the gateway and the end-device
Floor	number of floors between gateway and end-device
Freq	frequency used for transmission
Lat	latitude extracted from Payload
Long	longitude extracted from Payload
Prx	power received at the gateway
RSSI	received signal strength Indicator
Seq	sequence of the packet
SF	spreading factor
SNR	signal-to-noise ratio
Wall	number of walls between gateway and end-device
MSE	Mean Squared Error
$\mathbf{H_{base}, h_b}$	antenna height of the base station, the height of the roof Hmobile
$\mathbf{h_r}$	height of the roof- antenna height of the mobile station
d	distance between the transmitter and the receiver
f	frequency of signal propagation
B	distance between buildings
W	street width
θ	street orientation angel 30 degree
s	fading standard deviation

General Introduction

People can now wirelessly use the internet for phone, radio, and TV services, whether in a fixed location or moving around. Because the wireless internet is overgrowing, people want to connect to the World Wide Web quickly. The IEEE 802.16 working group developed a new broadband wireless access technology called "WiMAX," which stands for Worldwide Interoperability for Microwave Access. This was done to meet the demand for access to the internet "anywhere, anytime" and to ensure the service was good. In an ideal situation, WiMAX recommends a bit rate of up to 75 Mbps and a range of up to 50 km between the transmitter and the receiver along the line of sight. However, in the real world, measurements show significant differences from the ideal situation: a bit rate of up to 7 Mbps and a coverage area of between 5 and 8 km. To reach the best goal, researchers found the following things that make it hard for the signal to get from the transmitter to the receiver: Path loss, fading, multipath delay spread, and doppler spread.

To resolve these issues at the first phase of network development, propagation models are often employed for feasibility studies. Numerous propagation models are available to predict the path loss (e.g., Okumura Model, Hata Model), but they tend to be limited to the lower frequency bands (up to 2 GHz) (e.g., COST 231 Hata model, ECC-33 model, SUI model, Ericsson model and COST 231 Walfish-Ikegami (W-I) model), which have been proposed in urban, suburban, and rural environments with varying antenna heights. During initial network deployment, propagation models calculate electromagnetic field intensity for wireless network design. It represents signal attenuation from the transmitter antenna to the reception antenna as a function of distance, carrier frequency, antenna heights, and other critical characteristics such as terrain profile (e.g., urban, suburban, and rural).

Models such as the Harald.T. Friis free space model are used to forecast the signal strength at the receiver end under line-of-sight conditions between the transmitter and receiver. The traditional Okumura model is utilized for initial coverage deployment in urban, suburban, and rural regions from over 200 MHz to 1920 MHz. The Hata-Okumura model, commonly known as the Hata model, is a refined version of the Okumura model widely used over the frequency range of 150 MHz to 2000 MHz in urban areas. Numerous academics have examined the comparison of path loss models from various angles. Researchers explored empirical propagation models in various terrains as a function of antenna height parameters.

Our objective in this dissertation is to investigate another approach to modeling a system: artificial neural networks. The latter derive their modeling power from their ability to capture high-level dependencies, i.e., which involve several variables simultaneously. The applications are numerous, and all share a common point essential to the usefulness of neural networks: the processes for which one wishes to make predictions include many explanatory variables; above all, there are possibly non-linear dependencies between these variables which, if they are discovered and exploited, can be used to improve the prediction of the process. The fundamental advantage of neural networks over traditional statistical models is that they can automate the discovery of the most critical dependencies from the point of view of process prediction. The interest of these networks is their ability to react automatically to a complex environment such as telecommunication systems. We will take as an example of illustration, in our work, the estimation of signal losses in a physical channel.

In this context, our dissertation describes the mobile network system and studies the physical behavior of the signals in the mobile channel. We will then proceed to the simulation of our prediction models to calculate the attenuation. Finally, a comparative study will be conducted between the proposed and other empirical models to validate our model's applicability.

This work is divided into five chapters, a general conclusion, and bibliographical references:

The first chapter focuses on a reminder of mobile networks telecommunication networks, the architecture of this type of network, planning, and coverage prediction.

The second chapter presents some prediction models to use later in the simulation. The third chapter is some previous related work with analysis and comparison.

A general introduction to neural networks, their definition, theory and different types of networks, and learning techniques are represented in chapter four.

The last chapter is divided into two parts. The first part is conducting the empirical models in three different environments in Algeria. The second part is the interpretation of the neural networks models results obtained and the comparison with the empirical models.

A general conclusion allows us to situate the strengths of our study.

Chapter 1:
General information on mobile networks

1.1. Introduction

Every business nowadays needs one or more communications networks that transmit the varied data required for its survival and growth. These systems are grouped into networks, defined as collections of equipment and transmission mediums to facilitate information flow. We have entered a period of communication in which the amount and variety of information are increasing .

In the 1980s, this diversity led to the adoption of distinct and different communication solutions depending on the nature of the information to be transmitted: telephone networks for voice transmission, networks specialized in long-distance data transmission such as Trans Pac in France, or over a short distance such as company local area networks, Hertzian network or cable for television.

Technological advances make it possible to process information of different kinds on the same computer: video and sound sequences and presentation of documents. This is the domain of multimedia.

In addition, progress in transmission techniques makes it possible to transfer this varied information on the same medium (an optical fiber, for example). The boundaries between the different networks tend to blur. For example, initially intended exclusively for data transmission, the global Internet network transmits telephone communications. There are many solutions to a communication need, and technical progress has made the field of networks abounding.

In this chapter, the cellular concept, the general architecture, and all that encompass the essential notions of a mobile network, as well as the problems which confront the latter at the level of the deployment and planning of the infrastructures, ensure a good cost/quality ratio has been explored.

1.2. Types of mobile networks

A communication network is all the hardware and software resources involved in data transmission and exchange between different entities. Networks are subject to various specifications and standards based on their structure, architecture, distances, transmission speeds, and the type of information transferred (Augustin 2016).

1.3. GSM network

I.3.1. Definition

GSM for voice communications and GPRS or EDGE for data transport, the 2G network (for the 2nd generation of mobile network) is at the origin of the launch of the mobile internet by allowing the transfer of data by packets. 2G allows a theoretical maximum throughput of 384 Kbit/s (Halonen 2004).

1.3.2. Presentation of the infrastructure of a GSM network

The GSM network's principal function is to permit communication between GSM subscribers and RTC (fixed network) subscribers. The GSM network contains switches and connects to the PSTN network. The radio connection distinguishes the GSM network from other networks.

The GSM network is made up of three subsets:

- The radio subsystem – BSS Base Station Sub-system provides and manages radio transmissions.
- The routing subsystem – NSS Network Sub System (we also speak of SMSS Switching and Management Sub-System to talk about the routing subsystem).
- The NSS includes all the functions necessary for calls and mobility management.
- The operation and maintenance subsystem – OSS Operation Sub-System) allows the operator to operate his network.
- Implementing a GSM network (in-circuit mode) will allow an operator to offer "Voice" type services to its customers by giving access to mobility while maintaining an interface with the fixed network. Existing PSTN (Laipio 2008).

1.3.3. BSS subsystem hardware architecture

The BSS includes the BTSs, transceivers with a minimum of intelligence, and the BSCs, which control a set of BTSs and allow a first concentration of the circuits (Gobbo 2013).

The BTS base station

The BTS is a set of transceivers called TRX. The function of the BTS is to manage radio transmissions (modulation, demodulation, coding equalization, and error correction). The BSC carries out the exploitation of the data collected by the BTS. The BTS manages the data link

layer to exchange signaling between mobiles and the operator's network infrastructure (Aggelou 2001).
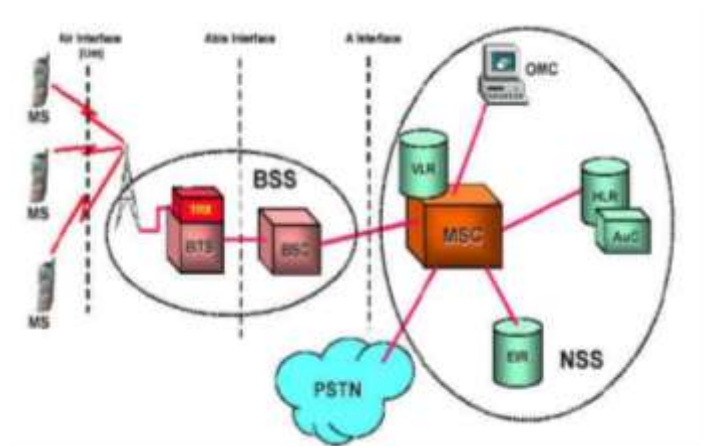
Figure 1. 1. Architecture of a GSM network (Halonen 2004).

The maximum capacity of a BTS is 16 carriers (technical limit rarely reached for reliability reasons). Thus, a BTS can manage a maximum of one hundred simultaneous communications.

There are different types of BTS offered to meet different needs. These stations are designed by manufacturers who strictly adhere to the GSM standard so that equipment from different manufacturers can be compatible. The BTS is of variable power to avoid interference between two cells, and it is crucial to regulate the power of the portable to avoid this same interference (Fernandes 2013).

The radiant BTS

They are ideal for covering sites where the density of subscribers is low. They are located on strategic points (summits, pylons). These stations transmit in all directions: they are the most visible stations. They cover macrocells. They are found in abundance along the highways. These BTS cannot be used in high-density areas because they transmit and occupy network bandwidth over a long distance (up to 20 Km/s) (Ohyane 2007).

The targeted BTS

They are often placed in areas with a higher number of subscribers than radiating BTSS. They are found in town, for example. They are relatively elongated in shape and allow transmission at an exact angle: thanks to this, it is possible to easily reuse the same channel in another nearby cell (SAUNDERS 2007).

Micro BTS

Micro BTS are base stations with low transmission power and sensitivity compared to conventional BTSs; this makes it possible to set up microcells that integrate into the existing network. These microcells have as fundamental characteristics a tiny size (a radius of about 400 m) and a low installation cost (the antennas can be installed below the level of the building). The multiplication of these cells allows more efficient distribution of available frequencies over densely populated areas. Micro BTS also offers the possibility of use inside a building, for example, in factories or airports (GOLDSMITH 2005).

1.3.4. BSC Functions

The BSC is the intelligent organ of the radio subsystem. The base station controller manages one or more stations and performs various communication and operating functions. The BSC is a database for software versions and configuration data uploaded by the operator to the BTS. Finally, the BSC controls the transfers between two cells; on the one hand, it notifies the new BTS, which will take charge of the "mobile" subscriber while informing the back-end system, here the HLR, of the subscriber's new location. The BTS is "contacted" by the maintenance and operations center through the BSCs, which play this relay role (BALLARD 1990). The BTSs are connected to their BSC controller (Figure 1. 1):

- either star (1 MIC per BTS.)
- either in a chain (several BTS share 1 MIC).
- Either in a loop (closed chain link allowing redundancy: a cut MIC link does not isolate the BTS).

1.3.5. NSS subsystem hardware architecture

The network subsystem, called Network Switching Center (NSS), plays a vital role in a mobile network. While the radio sub-network manages the radio access, the NSS elements take care of all the control and analysis of information in databases necessary for establishing connections using one or more of the following functions: encryption, authentication, or roaming.

The primary role of this subsystem is to manage communications between subscribers and users who may be other subscribers, users on the ISDN network, or users of fixed telephone networks (GU 2010).

The NSS is made up of:the following

- Mobile Switching Center (MSC)
- Home Location Register (HLR) / Authentication Center (AUC)
- Visitor Location Register (VLR)
- Equipment Identity Register (EIR) (GU 2010).

HLR functions

The HLR is a subscriber location and characteristics database. A network may have several HLRs depending on machine capacity, reliability, and operational criteria. The HLR is the nominal location register as opposed to the VLR, which is the visitor location register.

VLR functions

This database only contains dynamic information and is linked to an MSC. There are, therefore, several in a GSM network. It contains dynamic data transmitted by the HLR, which communicates when a subscriber enters the coverage area of the mobile switching center to which it is attached. When the subscriber leaves this coverage area, his data is transmitted to another VLR and follows the subscriber (GHRIBI 2000).

The difference between HLR and VLR

HLR and VLR have their functionality in the GSM architecture. According to the GSM architecture, there is also a communication interface between HLR and VLR. The number of communications is done within the HLR and VLR nodes to share their information. For example, when subscribers move from one VLR area to another, their locations are updated in the VLR, and the new VLR information is updated in the HLR. However, if a subscriber moves to the same VLR area, no interaction with the HLR is necessary. HLR and VLR store subscriber information according to GSM architecture to provide mobile communication services to subscribers registered in the network. HLR contains information about all subscribers within a network, while VLR contains more dynamic information relevant to subscribers roaming within the VLR area. This may vary depending on the design of the network architecture, as in most cases, HLRs act as centralized nodes while VLRs are primarily geographically diverse nodes. HLR acts as a fixed reference point at a given mobile station (subscriber), while its VLR may vary depending on mobility and network design (HUBBEL 1997).

MSC functions

MSCs are mobile switches typically associated with VLR databases. The MSC provides an interconnection between the mobile network and the fixed public network. The MSC manages the establishment of communications between mobile and another MSC, transmitting short messages. The MSC can also have a gateway function, GMSC (Gateway MSC), activated from a fixed subscriber to a mobile subscriber at the start of each call. A couple of MSC / VLR generally manages a hundred thousand subscribers (CAPLAN 2017).

Functions of OMC and NMC

Two levels of hierarchy are defined in the GSM standard. The OMC (Operations and Maintenance Centre) and the NMC (Network and Management Centre). This organization was defined to allow telecom operators to manage the multiplicity of equipment (transmitters, receivers, databases, switches, Etc.) and suppliers.

The NMC allows the general administration of the entire network through centralized control. The OMCs allow local supervision of the equipment (BSC / MSC / VLR) and transmit to the NMC the major incidents occurring on the network. The various CMOS perform a mediation function (ATHANASOPULOS 1989).

AUC functions

This database is associated with the HLR. The subscriber is identified by his Sim card, which transmits the information of The IMSI (International Mobile Subscriber Identity) and the KI (encryption key). The HLR manages the IMSI (the IMSI gives information on the network of origin and the country, among others) and the KI, which is managed by the database AUC data (GIANNATTASIO 2009)

Functions of the EIR

Despite the mechanisms introduced to secure network access and communications content, the mobile telephone could accommodate any SIM card from any network. It is, therefore, conceivable that a thief could use a terminal without him being able to be spotted.

To combat this risk, each terminal receives a unique identifier (International Mobile station Equipment Identity, IMEI) which cannot be modified without altering the terminal. Depending on data about a terminal, an operator can decide to refuse access to the network. Not all operators implement such a database (SPINELLIS 2000).

1.3.6. The architecture of the OSS Subsystem
 Network Administration

The administration of the network includes all the activities which make it possible to memorize and control the performance of resource use to offer the users a correct level of quality.

System configuration control

Software upgrades, the introduction of new equipment, or new functionalities. The GSM network administration system is close to the TMN concept, which aims to rationalize the organization of communication and maintenance operations and define the technical conditions for economic and efficient supervision of the quality of service (Liitsalo 2000).

1.3.7. The Pros and Cons of a GSM network

It can be concluded that setting up a GSM network represents a considerable investment. At present, GSM networks are constantly evolving in order to ensure an ever-increasing quality of coverage. The network's coverage is ensured by multiplying the BTS – BSC sets. We will see later that the GSM network is a basis for setting up GPRS and UMTS networks. Even if the UMTS network is beyond the high cost of purchasing licenses, we will see that the BTS – BSC set – MSC will need to be changed or modified at the base. Let us quickly recall here that a BTS covers approximately 500m of an area in town and 10 km of area in the countryside (MEDDOUR 2011).

1.4. The GPRS network (General Packet Radio Service)

1.4.1. Overview of Network Infrastructure

A GPRS network is primarily an IP network. The network is therefore made up of IP routers. The introduction of mobility also requires the specification of two new entities:

- The Service Node – the SGSN.
- The Gateway Node – the GGSN.
- A third entity – the BG, plays an additional security role.

The GPRS network adds a certain number of "modules" to the GSM network without changing the existing network. Thus, all the modules of the GSM architecture are kept. We will also see that some GSM modules will be used to operate the GPRS network.

Implementing a GPRS network will allow an operator to offer customers new "Data" type services. GPRS is in packet mode (CAI 1997).

1.4.2. The advantages and disadvantages of a GPRS network

- WAP access (lightweight internet).

- Billing by data. A permanent connection is possible.

- Support for multiple levels of QoS. No global internet access.

- GSM network is already saturated. No decisive application for the general public.

- It can be concluded that the GPRS service makes it possible to consider the GSM network as a packet data transmission network with radio access and mobile terminals. The GPRS network is compatible with IP and X.25 protocols. Specialized routers SGSN and GGSN are introduced on the network.

- Packet transmission on the radio channel saves radio resources: a terminal can receive or transmit data anytime without a radio channel being permanently monopolized, as in a network GSM (CAI 1997).
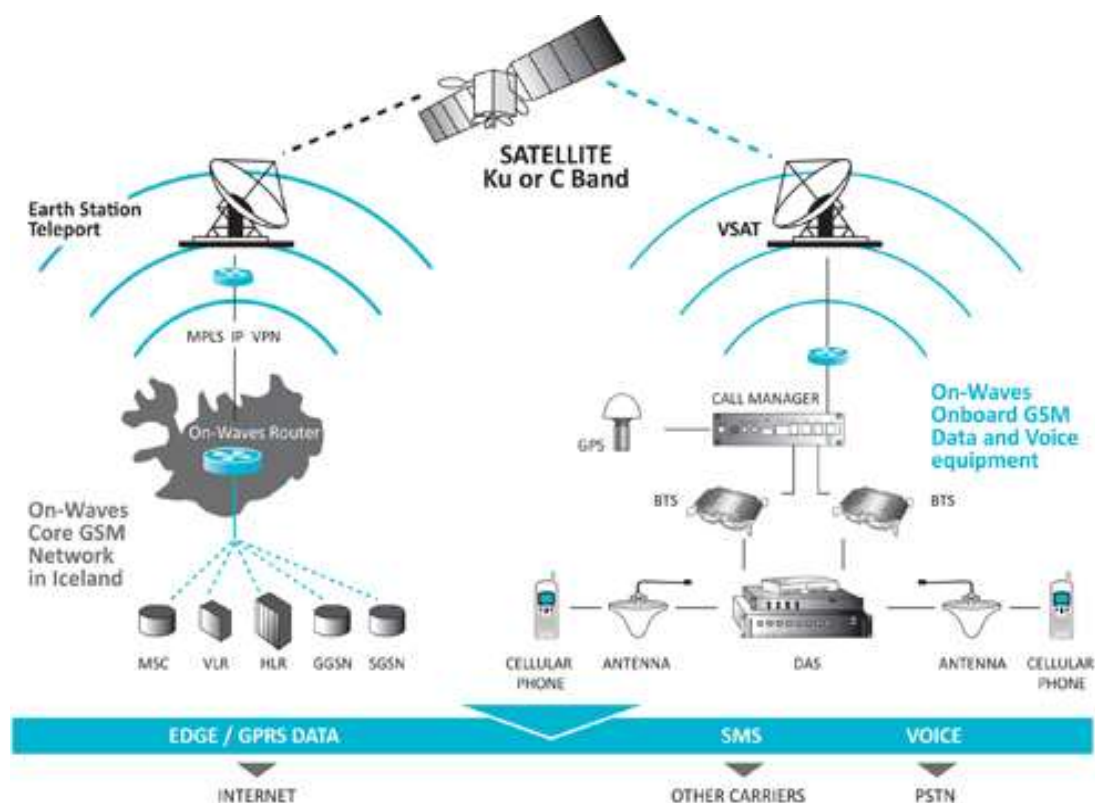
Figure 1. 2. Architecture of a GPRS network (Halonen 2004).

The maximum instantaneous speed announced for GPRS is 171.2 Kbit/s, even if it is limited to 48 Kbit/s in downlink mode. (Current limit of GPRS terminals). Implementing a GPRS network allows an operator to offer new Data type services with a data rate 5 to 10 times higher than the theoretical maximum rate of a GSM network. (Reminder maximum speed in GSM: 9.6 Kbit/s). The GPRS network is finally a step toward the UMTS network (ERMEL 2002).

1.5. 3G network (the third generation of mobile network)

The 3G network and its evolutions (3G+, H+) offer a speed much higher than the 2G network. Downloading data is more efficient, and browsing the internet is more comfortable. You can seamlessly use your applications, send and receive emails with attachments or watch videos in standard definition. 3G and its developments allow a theoretical maximum throughput of 42 Mbit/s (Jalal 2007).

1.6. The UMTS network (Universal Mobile Telecommunications VI. System)
1.6.1. Overview of Network Infrastructure
The UMTS network is combined with existing networks.

The existing GSM and GPRS networks provide respective Voice and Data functionalities; the UMTS network then brings the Multimedia functionalities. It is important to note that:

- The high cost of setting up a UMTS system (purchase of license + significant if not a total modification of the essential elements of the network (station/antenna) distributed in a massive way over a national territory.(

- The difficulty in precisely defining the architecture of a future UMTS network insofar as 3GPP and UMTS are still working today on the definition of standards and technical specifications.

Implementing a UMTS network will allow an operator to supplement its existing offer by providing new services in packet mode, thus complementing the GSM and GPRS networks (KHAN 2010).
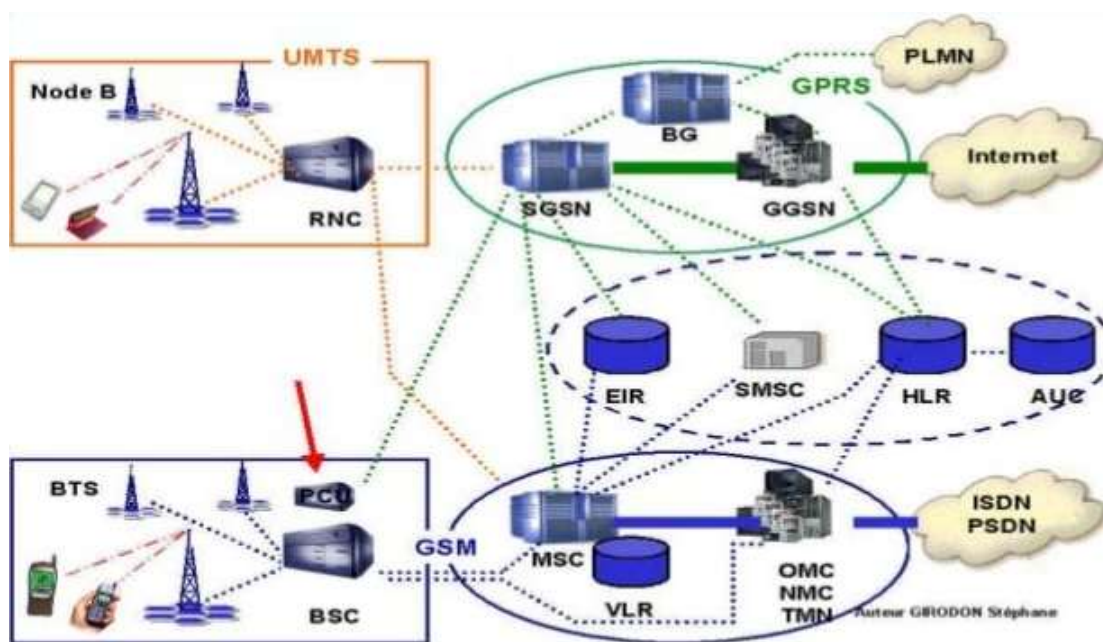
Figure 1.3. The architecture of a UMTS network (Jalal 2007).

1.6.2. UMTS Network Equipment

Setting up the UMTS network involves setting up new elements on the network.

Node B

Node B is an antenna. Geographically distributed throughout the territory, the Nodes B are to the UMTS network and what the BTS is to the GSM network. Node Bs manage the physical layer of the radio interface. Node B governs channel coding, interleaving, rate adaptation, and spreading. Node Bs communicate directly with the mobile (ROXIN 2007)

The NCR

The RNC is a Node B controller. The RNC is, again here, the equivalent of the BCS in the GSM network. It controls and manages radio resources using the RRC (Radio Resource Control) protocol to define procedures and communication between mobiles (via Node B) and the network. The RNC interfaces with the network for packet mode and circuit mode transmissions. The RNC is directly connected to Node B (Rosa 2004). It then manages:

- Load and congestion control of the different Node B.
- Admission control and allocation of codes for new radio links (entry of mobile into the zone of managed cells, Etc.).

There are two types of RNCs:

- The Serving RNC acts as a gateway to the network.
- The Drift RNC, whose primary function is data routing.

NB: All Node B and RNCs constitute the equivalent of the BSS sub-architecture seen previously in the GSM network. In a UMTS network, we will speak of the UTRAN sub-architecture (Rosa 2004).

1.6.3. The advantages and disadvantages of a UMTS network

We conclude that the UMTS network complements the GSM and GPRS networks. The GSM network covers the functionalities required for Voice-type services in circuit mode, the GPRS network provides the first functionalities for implementing Data-type services in packet mode, and UMTS completes these two networks with an offer of additional Voice and Data services in packet mode.

UMTS is thus an extension of GPRS and also operates in packet mode. The transmission speed offered by UMTS networks reaches 2 Mb/s. The UMTS infrastructure allows the extension of frequencies and the modification of data coding. Nevertheless, the investments in network architecture are substantial since the mode of communication between the 3G

terminals, and the BTS (called Node B) is different. Hardware changes are significant (TAYAL 2005)

1.7. The fourth-generation of mobile phone, 4G (LTE)

4G is the fourth generation of mobile networks. It is the successor standard to 3G. To summarize, 4G is the mobile telephony standard, allowing speeds up to 50 times larger than the first standard (PEREIRA 2004).

1.7.1. Definition of LTE networks

One of the particularities of LTE (Long Term Evolution) or 4G technology is to have a "core network" based on IP and to no more extended offer switched mode (establishment of a circuit to transmit a 'voice' call), which means that 4G relies on an IP packet-switched transport network. It has not provided a routing mode for a voice other than VoIP, unlike 3G, which carries voice in circuit mode.

LTE uses Hertzian frequency bands with a width varying from 1.4 MHz to 20 MHz, thus making it possible to obtain (for a 20 MHz band) a theoretical bit rate of up to 300 Mbit/s in "downlink," while "4G" offers downlink speeds of up to 1 Gbit/s.

LTE technology is based on a combination of sophisticated technologies capable of significantly raising the level of performance (very high speed and latency) compared to existing 3G networks. OFDMA (Orthogonal Frequency Division Multiple Access) multiplexing optimizes frequencies by minimizing interference. The use of multiple antenna techniques (already used for Wi-Fi or WiMax) makes it possible to multiply the parallel communication channels, which increases the total speed and range (YELOME 2015).

1.7.2. 4G LTE network architecture

LTE networks are cellular networks made up of thousands of radio cells that use the same radio frequencies, including in adjoining radio cells, thanks to OFDMA (Orthogonal Frequency Division Multiple Access) and SC-FDMA (Single Carrier – Frequency Division Multiple Access) radio coding. Figure I.4. presents the architecture of the 4G LTE network (REMY 2014).
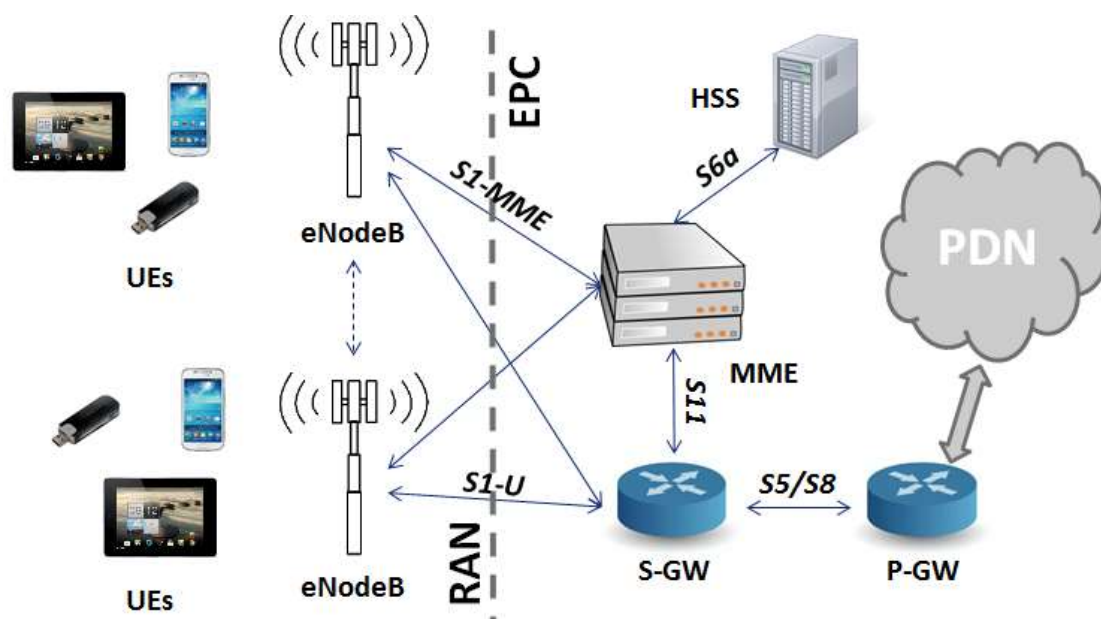
Figure 1. 4. 4G LTE network architecture (REMY 2014).

The new blocks specified for the architecture, also known as EPS (Evolved Packet System), are EPC (Packet Core Evolved) and E-UTRAN (Evolved UTRAN).

EPC: Evolved Packet Core

The core network called "EPC" (Evolved Packet Core) uses "full IP" technologies, i.e., based on Internet protocols for signaling, which allows reduced latency times, voice transport, and data. This core network allows interconnection via routers with other remote ENodeBs, the networks of other mobile operators, fixed telephone networks, and the Internet network. EPC Simplifies all-IP network architecture, as it provides mobility between 3GPP-based and non-3GPP-based systems, e.g., WIMAX and CDMA2000 (FORCONI 2013).

The E-UTRAN radio part

The radio part of the network, called "E-UTRAN," is simplified compared to those of the 2G (BSS) and 3G (UTRAN) networks by integration into the "eNodeB" base stations with fiber-optic links and IP linking the eNodeBs together (X2 links) as well as control functions that were previously implemented in the RNCs (Radio Network Controller) of 3G UMTS networks. This part manages radio resources, carrier, compression, security, and connectivity to the evolved Core network (TINGNAN 2013).

E-Node B.

The eNodeB is the equivalent of the BTS in the GSM network and NodeB in the UMTS. The handover functionality is more robust in LTE. These antennas connect the UEs with the LTE core network via the RF (Radio Frequency) air interface. As they provided the

functionality of the radio controller resides in eNodeB, the result is more efficient, and the network is less latent; for example, mobility is determined by eNodeB instead of BSC or RNC of GSM and UMTS networks (TINGNAN 2013).

1.8. The fifth generation of mobile phones (5G).

The 5G network encompasses a set of technologies corresponding to the fifth generation of the standard for mobile telephony. It is validated by the ITU, the International Telecommunication Union, and the 3GPP consortium (3rd Generation Partnership Project). It officially came into force in 2020 (NAVARRO-ORTIZ 2020).

Each network generation has a lifespan of approximately 20 years. Work on 4G began in 2003 for a launch in 2010 and until 2030. For its part, 5G has been under consideration since 2012 for a commercial launch in 2020.

The main objective is to develop the network to meet various additional needs: to increase the speed of current use of mobile telephony, to support low energy consumption and remote communication of connected objects, and local communication. At the same time, it targets particular uses, such as networking and autonomous vehicles, health, and connected objects. 5G is the internet of the future. This technology will include a radio access network and a convergent core network combining fixed and mobile access. In particular, this involves increasing network speeds and capacity and preparing for the "Internet of Things" event .

From main objectives:

Here are the objectives to be achieved according to the recommendations in IMT-2020 defined on 8KPI (Key Performance Indicator).

- Its bandwidth is at least 100MHz. Bandwidth up to 1GHz is required for high frequencies (>6GHz).
- Connectivity density of 1 million devices/Km2.
- Theoretical throughput of 20Gbit/s in the downlink and 10Gbit/s in the uplink.
- The rate received by the user of 100Mbit/s in the downlink and 50Mbit/s in the uplink.
- Latency of less than 1ms.
- Mobility of 500km/h.
- 99.999% availability and 100% network coverage.
- 90% reduction in energy consumption.

1.8.1. 5G network architecture

A 5G network comprises a 5G access network (AN) and a 5G core network. The access network itself consists of the new generation radio access network (NGRAN), which uses the new 5G(NR) radio interface, and a non-3GPP AN connected to the

5G core network. The various network entities are connected by an underlying TCP/IP transport network, which supports QOS files (BROWN 2017).
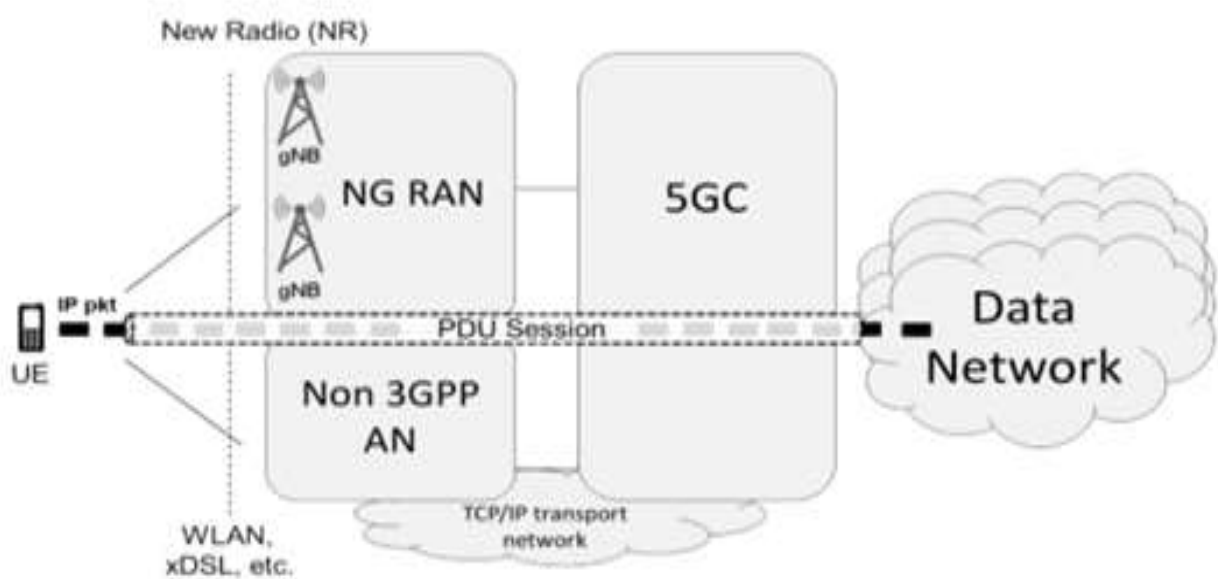
Figure 1. 5. 5G network architecture (NAVARRO-ORTIZ 2020).

Figure [1.5] shows that the 5G network connects the user equipment (UE) to external data networks. The PDU session represents the 5G connectivity service and constitutes a sequence of NG tunnels in the 5GC plus one or more carriers' radios on the radio interface. This set of "pipes" finely connects the UE to its control functions and the external data network for user traffic exchange.

A PDU session is similar to an EPS carrier over LTE, except for the QoS model and supported user data units. Indeed, a PDU session can carry not only the user's IP packets but also the ETHERNET or non-occurring frames, thus enabling Layer-2 communication between groups of UEs. The 5G model is based on the new QOS flow concept, where flow is the most considerable granularity of QoS differentiation (DETTI 2018). The different QoS flows can belong to a single PDU session.

1.8.2. New Generation Radio Access Network (NG-RAN)

The NG-RAN is a set of 5G base stations, called GNBs, connected to the 5GC through logical interfaces. The gNBs can be interconnected through the Xn interface to improve mobility (handover) and management (coordination of intercellular interference) functions.

The functioning of the gNB is sometimes distributed. In this case, the resulting architecture is formed by a central unit (gNB-CU) which requires one or more distributed units (gNB-DU) and connects to a remote radio board (RRH). The central unit is further divided into two parts, one for the control plane functions (gNB-CU-CP) and the other for the user plane functions (gNB-CU-UP).

5G Core Network (5GC)

The decomposition of previous generations' functions performed by network nodes has led to a 5G architecture wholly defined in terms of network functions exposed as services (BERTENYI 2018).

As in the NG-RAN, there is a separation between the control and user planes. In the user plane, one or more UP functions (UPFs) mainly perform packet forwarding between the different NG-U tunnels that form the session PDU. All other network functions belong to the control plane.

Another drastic change from previous generations is interface modelling, which has been changed from "bit-oriented point-to-point" to "web-oriented service-based. «Indeed, 5GC has a service-based architecture applicable to all. The procedures are defined as services so that it is possible to reuse them.

There is a standardized point-to-point interface, either factual or logical, between any pair of interacting 2G, 3G, and 4G network entities. This interface uses a particular bit-oriented protocol. In the 5G core, the interactions between the entities of the control plane use Service-based interfaces supported by web tools such as HTTP/2, REST, and JSON (BERTENYI 2018).

1.9. Comparison between different generations

With 6G on the way, looking at the differences it has over 5G that will make a significant difference in the world of technology, it will be able to provide:

- An increase in energy efficiency.
- A stable connection even on the move.
- A high-performance network capable of operating in real-time, with high requirements in terms of reliability.

The table below summarizes the characteristics of the mobile networks that are currently available:

Table.1. 1. Comparison between the five technologies

Features	1G	2G	3G	4G	5G
Maximum flow	171.2 Kbit/s	9.6Kbit/s	1.9 Mbit/s	1 Gbit /s	20 Gbit /s
Speed (km/h)	/	350	500		
Latency (ms)	/	150	10	1	
Efficiency energy of network	/	/	/	1X	100X
Flow on an area	/	/	/	0,1(Mbit/s/m²)	10(Mbit/s/ m²)
Bandwidth of data	2Kbps	14.4-64Kbps	2Mbps	2Mbps to 1Gbps	1Gbps and more as needed
The band of frequency	150Mhz	1.8Ghz	2Ghz	2 to 8 GHz	3 to 300 GHz
Multiple access	FDMA	TDMA, CDMA	CDMA	CDMA	CDMA, BDMA
Services	Mobile telephony (voice)	Digital voice, higher packet capacity, short messaging	High-quality embedded audio, video, and data	Dynamic access to information on portable devices, HD streaming, global roaming	Dynamic access to information on portable devices, HD streaming, and any user request

1.10. Cell system

In a cellular system, the region covered is divided into cells, as shown in Figure I.6. A cell is circular. However, it depends on the region's topography served by the cell's antenna. For clarity, they can be illustrated with hexagons. At the center of a cell, one or a set of transceivers corresponds to a frequency band (LEE 1998).

Theoretically, cells can take different shapes without necessarily being uniformly distributed. However, a regular pattern can maintain consistency with the rapid development of the coverage point of view and capacity point of view system. The circular shape can ideally represent a covered area, but problems of intercellular overlap are possible (LEE 1998).

However, the hexagonal shape, on the other hand, overcomes these problems while simplifying the process of planning the cellular network. In the same way, this form is imaginary; in practice, one cannot carry out this type of reason considering the propagation conditions of the radio waves in space.
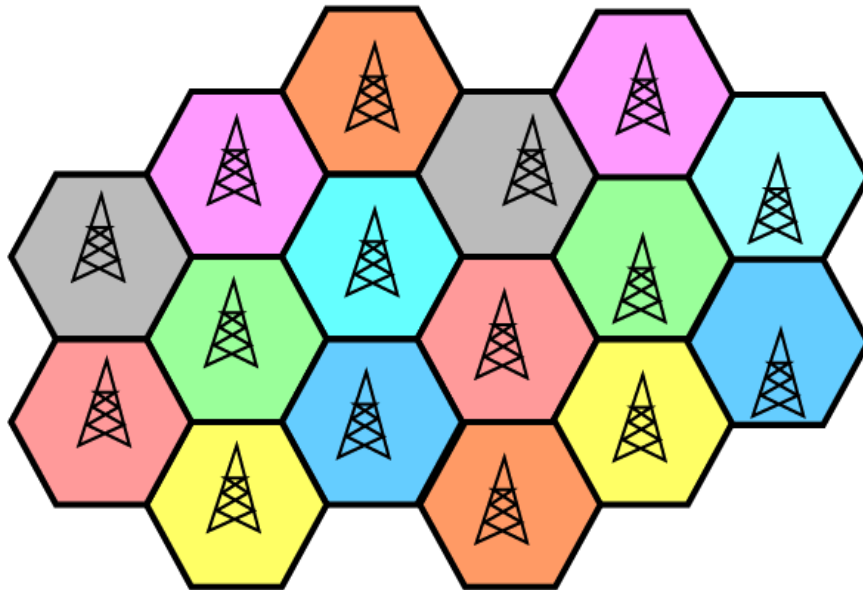
Figure 1. 6. Cell system (LEE 1998).

The size of a cell varies according to a set of constraints, among which we find: the relief of the territory (plain, mountain), the location (urban, rural, suburbs), the density of subscribers, the nature of the constructions (houses, pavilions, towers), Etc.

We can thus distinguish several types of cells:

- Macrocells: Large cells of up to 35 km, suitable for sparsely populated rural areas. Given their size, transmitters must provide very high powers;

- Microcells adapted to dense urban areas are cells of tiny beings of a few hundred meters in radius. They allow the flow of significant traffic per unit area;

- Pico cells: with a few meters' radius and suitable for propagation inside buildings.

In the design of a cellular network, the following aspects must be considered:

- Topography (buildings, hills, mountains, Etc).

- Population (or communications) density to establish cell size.

- To avoid interference, two adjacent cells cannot use the same frequency band (figure I.7). The distance between two cells having the same band should be 2 to 3 times the diameter of a cell. Cell size can vary between 0.5 and 35 km and depends on user density and topography. Cells are grouped into a block (called a pattern or cluster). The number of cells in a block must be determined so that the block can be reproduced continuously over the territory to be covered. Typically, the number of cells per block is 4, 7, 12, or 21. The shape and size of the blocks and the number of cells vary depending on the number of frequencies (channels) available (KNOPP 2000).
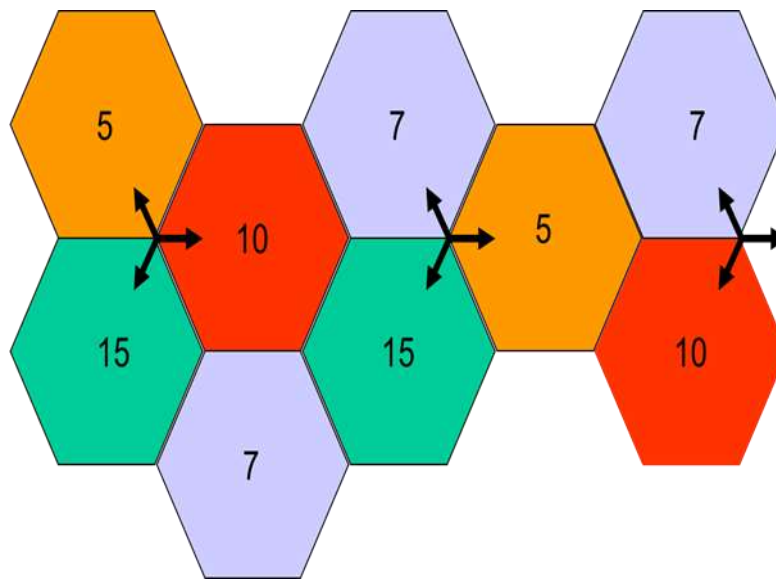
Figure 1. 7. Frequency reuse (KNOPP 2000).

The purpose of cell division is:

- Guarantee roaming: the GSM network must always recognize the subscriber's location. This is called: roaming management or roaming. The terminal number becomes, from the fixed network point of view, corresponds to a physical address that varies.

- Guarantee mobility: by automatic procedures known as transfer or handover, communication must be maintained while the mobile is moving.

1.11. Conclusion

After GSM, the GPRS network was finally a step toward the UMTS network. Technically, the three GSM, GPRS, and UMTS networks' architectures are complementary and interconnected to optimize the quality of service provided to the subscriber. This chapter presents the different elements of the three networks and shows how the telecom architectures of the GSM, GPRS, and UMTS networks are complementary. This chapter also shows that setting up GPRS and UMTS networks is costly beyond the investments linked to the purchase of licenses. Therefore, this part aims to demonstrate to the reader that the marketing of new services must accompany the commissioning of GPRS and UMTS networks to make the investments profitable. It is clear that the GSM, GPRS, and UMTS networks are complementary and that they constitute an evolution of the service offers of the telecom operator, from simple "Voice" type services to advanced "Data" type services.

Chapter 2 :
Radio Waves propagation models

2.1. Introduction

Propagation models are used when designing a radio interface to optimize performance and when deploying systems in the field to determine radio coverage.

The models are implemented in engineering tools to predict different valuable quantities for the deployment of radio telecommunication systems and the study of radio coverage (choice of sites, allocation of frequencies, definition of powers) and the definition of jamming. The models are very dependent on geographical databases containing elements relating to topography and types of land use. This is because how ultra-high frequency (UHF) radio waves will propagate in a given space is closely linked to the obstacles (buildings, tree trunks, mountainsides, Etc.) encountered along the propagation channel (RASID 2005). Therefore, the modeling of geographic objects is essential in any UHF wave propagation model (Saidi 2020).

The propagation models are then used for the mathematical prediction of the propagation of radio waves between the source and the target service area, and they thus give an idea close to reality to allow a receiver of systems to establish in advance that the proposed radiocommunication system will serve the intended service area well (Alnatoor 2020).

2.2. Classification of prediction models

In mobile radio communications, there are two fundamental approaches for predicting the behavior of a transmission channel. The first approach is to model the channel statistically. The second method is an analytical resolution of the propagation equations or simulates paths of the signal in the propagation medium (HROVAT 2013).

The type of model chosen will depend on the level of estimation desired: approximate or precise estimation. In addition, available field data plays an important role. After the prediction estimation, field measurements must be performed to validate the model. This step generally requires the readjustment of the parameters.

The two main types of models resulting from these approaches are theoretical models, based on theoretical modelling, and empirical models. Semi-empirical models using the previous approaches are also defined. They take into account the theoretical propagation equations and are parameterized using the results of actual measurements.

Deterministic models give much more precise results but require much information on the area where they will be applied. Moreover, they require a long calculation time. They are generally reserved for places where other models cannot be used. They are based on geometric optics calculations (reflection, diffraction, Etc.). This method is called the ray method (HROVAT 2013).

2.3. Empirical models

This model describes mathematically (most often using statistics) a set of measurements collected in the field or experimental data; they are models of representation of reality. Most propagation models belong to this type of model (POPOOLA 2018).

If the empirical model is well constructed, with the rigor required by statistical analysis, it will correctly represent the data used to establish it. Because, in general, it is relatively simple and easy to implement (in terms of mathematical development and computer programming), the telecommunications system designer will prefer it to any other.
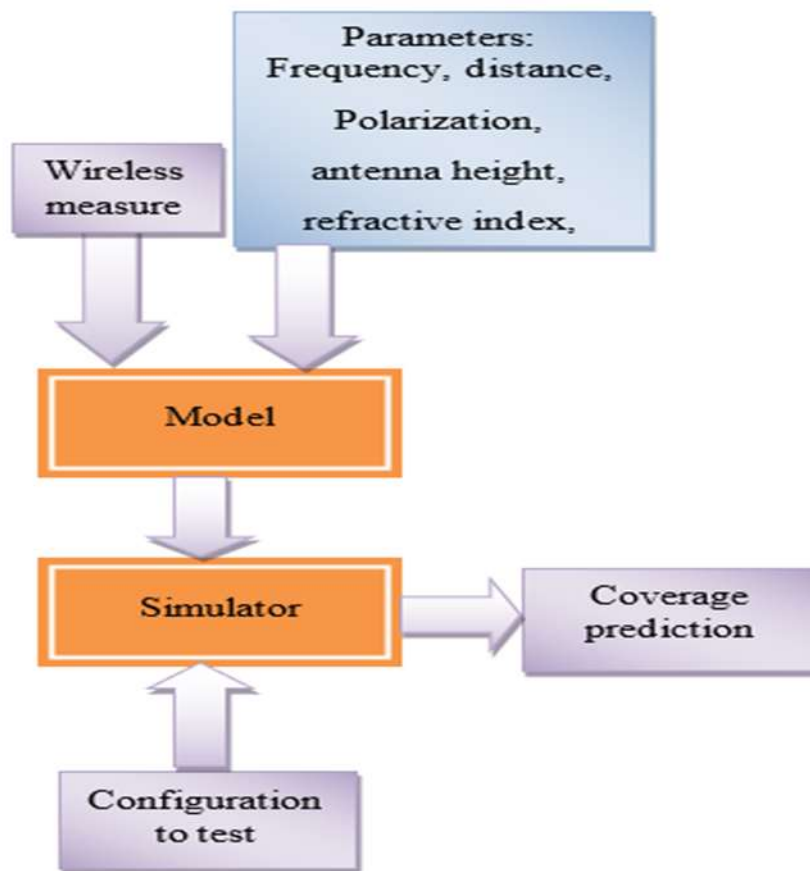
Figure 2. 1 *.* Empirical models work plan.

2.3.1 Okumara-hata model

This is the most commonly used model; it appeared in 1980 and is based on Okumura measurements. It considers the frequency, the radiosity, the distance between the transmitter and the receiver, and the height of the base station and the mobile (MEDEISIS 2000).

It also considers the nature of the environment by qualifying its degree of urbanization (dense urban, weak urban, or rural).

The conditions of validity of this model are summarized below (RANI 2014):

Table 2. 1. Condition of validity of the Okumura-Hata model.

Frequencies	150 MHz < f < 1.5 Ghz
Transmit antenna height	30m <h_b< 200m
Mobile antenna height	1m <h_m< 10m
Distance between mobile and base station	1km < d < 20km
Type of environment	▪ Urban (big city) ▪ Urban (medium city) ▪ Suburban ▪ Rural

For an urban environment, the attenuation is (SHAHAJAHAN 2009):

$$L_0 = 69.55 + 26.16 \log(f) - 13.82 \log(h_b) + (44.9 - 6.55 \log(h_b)) \log d \quad (2.1)$$
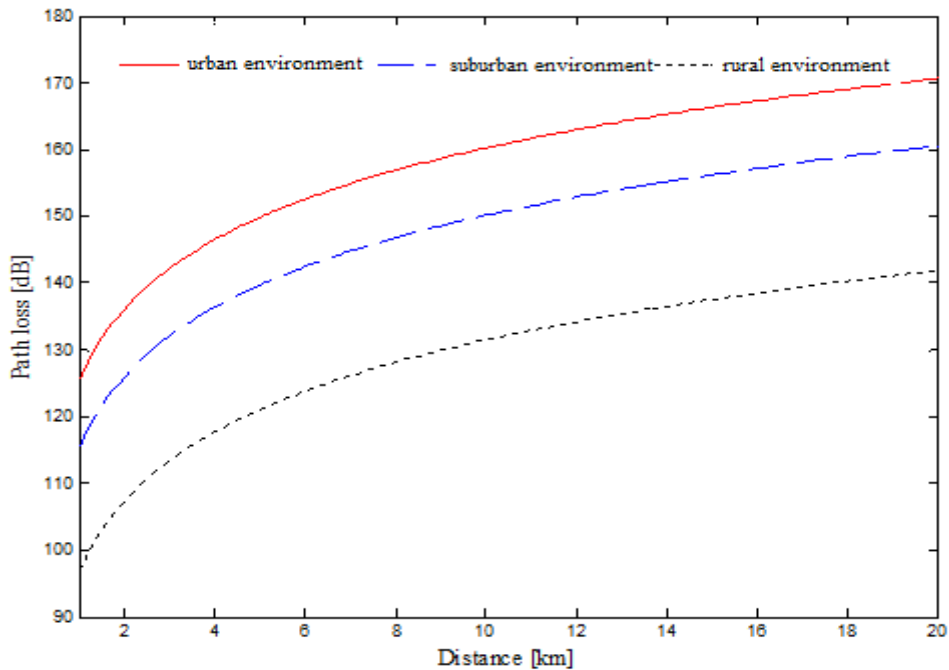
Figure 2. 2. Attenuation for Different Environments (Okumura-Hata Model),

$$f_r = 957.4 MHz, h_m = 1.5m, h_b = 38m.$$

For an average city, the equation is given by (SHAHAJAHAN 2009):

$$L_{urban} = L_0 - a(h_m) \quad\quad\quad\quad (2.2)$$

With: $a(h_m) = (1.1 \log(f) - 07)h_m - 1.56 \log(f) + 0.8$

For a large city, the equation of the attenuation is given by:

$$L_{urban} = L_0 - a(h_m) \tag{2.3}$$

With :

$$a(h_m) = 8.29[\log(1.54h_m)]^2 - 1.1 : \quad f \leq 200Mhz$$

$$a(h_m) = 8.29[\log(1.54h_m)]^2 - 4.97 : f \geq 200Mhz$$

For a suburban environment, the equation of the attenuation is given by:

$$L_{Suburban} = L_0 - \left[\log\left(\frac{f}{28}\right)\right]^2 - 5.4 \tag{2.4}$$

For a clear rural environment, the equation of the attenuation is given by (SHAHAJAHAN 2009):

$$L_{rural} = L_0 - 4.78([\log(f)]^2 + 1.833\log(f) - 40.49) \tag{2.5}$$

2.3.2. Elgi's model

One of the best-known statistical models for predicting propagation loss in urban or rural areas is due to Egli (KAMARUDIN 2010). As in the Okumura-Hata case, it does not include diffraction losses caused by propagation over uneven terrain; However, Okumura implicitly takes into account the effect of buildings, which is not the case for Egli. A first comparison between the two models can be made for open spaces (rural), where both models neglect diffraction.

According to Egli, propagation losses are expressed as:

$$L = 139.1 - 20\log(h_b) + \log(d) \tag{2.6}$$

- h_b: Height of base station antenna.

- d: Distance between base station antenna and mobile station antenna.

It is a model for systematically interpreting measurements made in the 90-1000 MHz band. This model's disadvantage is that it considers diffraction an essential phenomenon in radio propagation.

2.3.3. Model COST 231-Hata

The members of the European COST 231 project have proposed extending the Hata model to higher frequencies (DALELA 2012), in particular, because of the deployment of the GSM 1800 (Europe) and GSM 1900 (USA) networks. The following formula was proposed:

$$L_u = 46.33 + 33.9\, log(f) - 13.82\, log(h_b) - a(h_m) + [44.9 - 6.55(log(h_b)]\, log(d) + C_m \quad (2.7)$$

- $a(h_m) = [\,1.1\log(f) - 0.7\,]h_m - [\,1.56\log(f) - 0.8\,]$ for a medium-sized city.

- $C_m = 0$ dB for suburbs.

- $C_m = 3$ dB for large metropolitan centers.
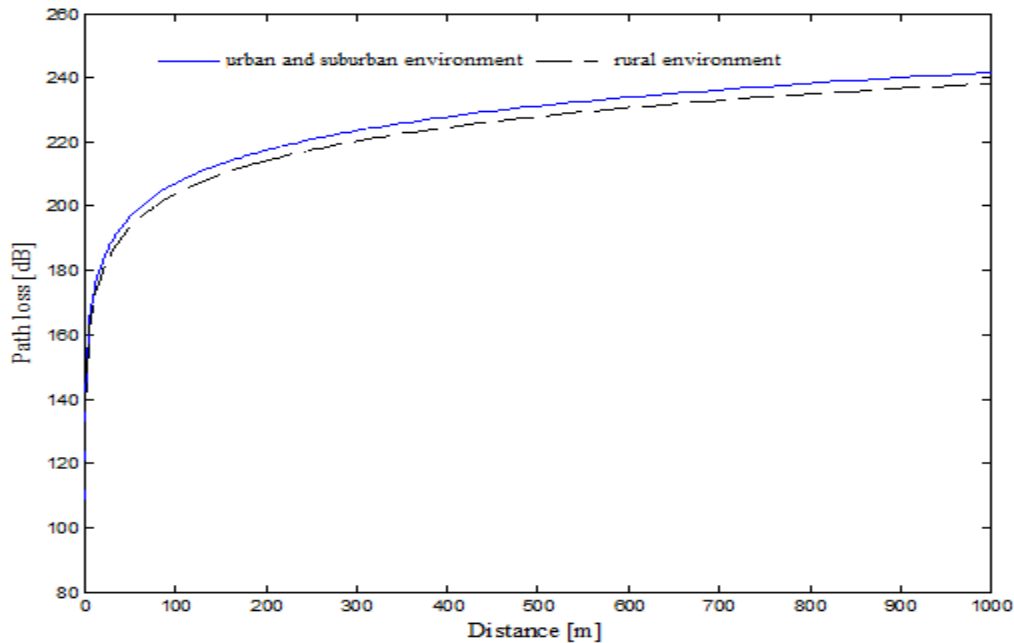
Figure 2. 3. Attenuation For medium-sized cities and large metropolitan centers (COST Model 231-Hata), $f_r = 1800 MHz, h_m = 1.5m, h_b = 38m.$

2.3.4. Long-distance loss model

Several studies have shown that the attenuation in an indoor environment increases with the distance between the transmitter and the receiver (KOPPELMAN 2005):

$$L(d) \propto \left(\frac{d}{d_0}\right)^n \qquad\qquad\qquad (2.8)$$

With:

- L is the average attenuation.

- *n* is the attenuation factor which indicates how the loss varies with distance. The value of n depends on the propagation environment.

- d_0 is the reference distance, generally equal to 1m.

- *d* is the distance between the transmitter and the receiver.

The following table summarizes the values of n for different environments (KOPPELMAN 2005):

Table 2. 2. The values of n for different environments (GIANNATTASIO 2009).

Environment	Attenuation factor (*n*)
Free space	2
Urban environment	2.7- 3.5
Masked urban area	3 - 5
In buildings with LOS	1.6 - 2.5
In Buildings (NLOS)	4 - 6

The attenuation in dB is defined by (GIANNATTASIO 2009):

$$L(d) = L(d_0) + 10n \log \left(\frac{d}{d_0}\right)$$
(2.9)

- $L(d_0)$ Typically, is calculated with the assumption of space or by measurements. For 1m. It is usually equal to the free space loss if the loss is equal to the gain of the antennas.

Equation II.9 predicts the received power when a distance d separates the transmitter and the receiver. The practice has shown that the attenuation follows common law, hence the following expression (GIANNATTASIO 2009):

$$L(d) = L(d_0) + 10n \log \left(\frac{d}{d_0}\right) + X_\sigma$$
(2.10)

σ and *n* are calculated from the measurements using linear regression by minimizing the difference between the measured attenuation values and the estimated values.

2.3.5. SEIDEL model

In a multistage environment, the attenuation can also be described by the Seidel model (SEIDEL 1992):

$$L(d) = L(d_0) + 10n_{SF} \log\left(\frac{d}{d_0}\right) + FAF \tag{2.11}$$

n_{SF} represents the attenuation factor for measurements made on the same floor. Thus, if n_{SF} is well estimated on one floor, the attenuation on a different floor can be predicted while adding an appropriate value of the floor attenuation factor (FAF).

The main advantage of empirical models is that one does not need a precise presentation of the area to be covered. They also allow quick calculations. They can be used to deploy networks with reduced costs and delays. They used to obtain an overview of the deployment. However, they do not give accurate results because they do not consider the actual topology of the area to be covered.
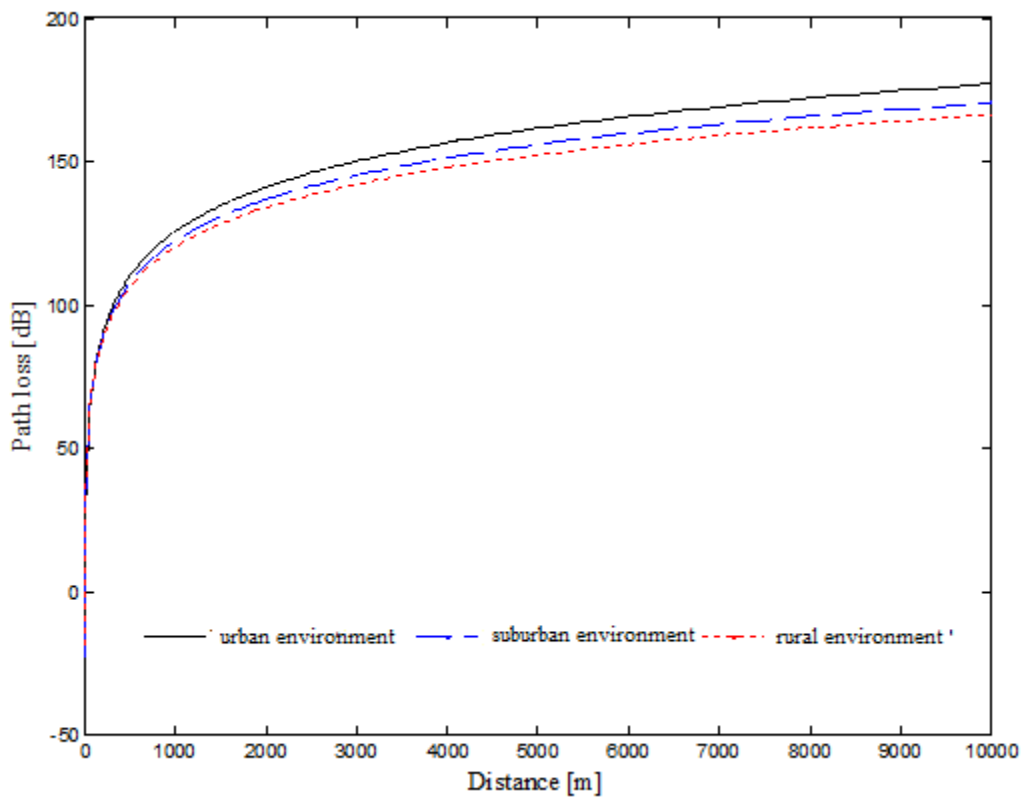
Figure 2. 4. Attenuation for different environments (Seidel model).

2.3.6. Free Space Path Loss (FSPL) model

A path loss is considered in this model. The FSPL number represents the amount of signal strength lost during transmission. The frequency f [MHz] and the distance d [m] between the transmitter and receiver affect the FSPL. In the computation, the corresponding path loss is obtained as follows (ALSAYYARI 2014):

$$PL_{FSPL} = 32.45 + 20log_{10}(d) + 20log_{10}(f) \tag{2.12}$$

Where power attenuation is usually expressed in decibels (dBm).

2.4. Semi-empirical models

These models are a combination of both approaches. These models whose input and output variables have been chosen according to a physical analysis of the phenomenon. If this analysis is pushed far enough, it may be possible to determine the a priori form of the relations between the variables.

The empirical part lies in estimating the numerical values of the model's coefficients from the experimental results.

This approach is better than the previous one because it avoids modelling errors due to linked variables. This is why we will permanently attach more confidence to the generalizations of this type of model than to those coming from purely empirical models.
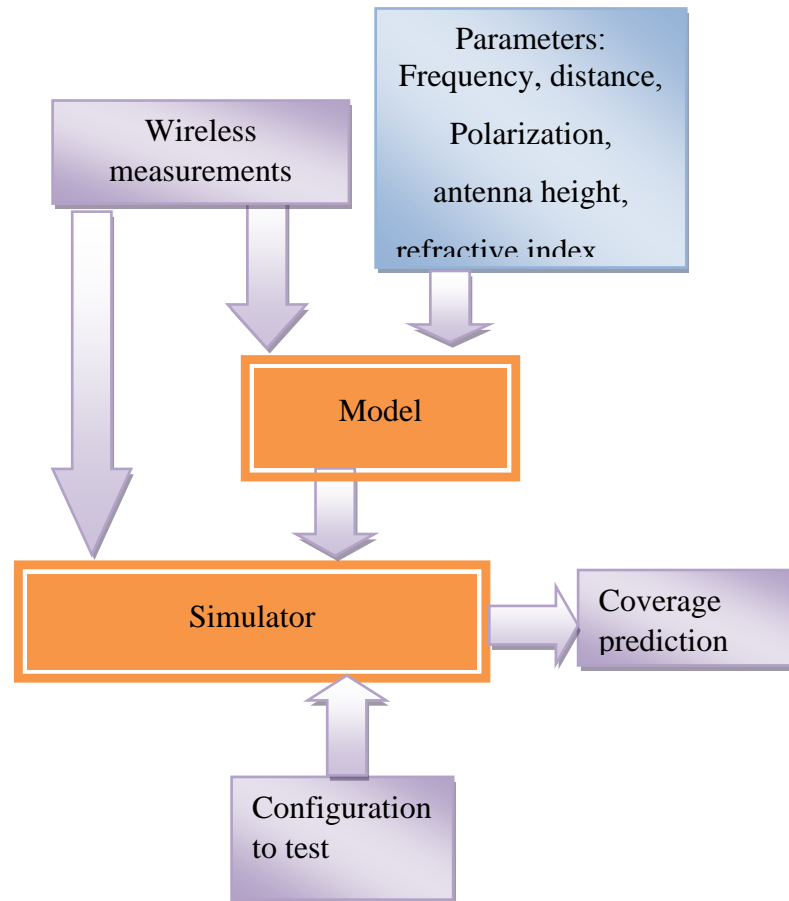
Figure 2. 5. Work plan of semi-empirical models.

2.4.1. Walfisch-Ikegami (WI) model

When the antenna is positioned on a rooftop but surrounded by taller structures, this model has been used for distances more than 20 m in cells less than 1 km. This model allows for the calculation of attenuation as a function of various variables, including the city's topography. In COST 231, the Walfisch and Ikegami (HAR 1999) models were integrated. The model improves the calculation of trip losses by analysing additional data to describe the features of the urban environment, summarized in the table below:

Table 2. 3. Validity of the Walfisch-Ikegami (WI) model.

Frequencies	800 MHz $< f <$ 2000 MHz
base station antenna height	4m $< h_b <$ 50m
antenna height of the mobile station	1m $< h_m <$ 3m
The distance between the mobile and base station (MS and BS)	0.02km $< d <$ 5km
average height (m) of buildings	$h_{Roof} \geq h_{RX}$
the width of the road (m) where the mobile is placed	b/2 if there is no indication
distance (m) between building centers	between 20 and 50 if there is no indication

Angle	in degrees

- LOS (Line of Sight) line of sight case:

$$L_p = 42.64 + 26\log(d) + 20\log(f) \qquad (2.13)$$

- The attenuation in free space is given by:

$$L_{fs} = 32.45 + 20\log(d) + 20\log(f) \qquad (2.14)$$

- The attenuation in case of visibility is written:

$$L_p = L_{fs} + 10.19 + 6\log(d) = L_{fs} + 6\log(50d) \qquad (2.15)$$

- Cases of non-direct visibility NLOS (Non-Line of Sight):

$$L_p = \begin{cases} L_{fs} + L_{rts} + L_{msd} & L_{rts} + L_{msd} > 0 \\ L_{fs} & L_{rts} + L_{msd} \leq 0 \end{cases} \qquad (2.16)$$

With:

L_{rts} : Attenuation due to diffraction on the roofs of buildings.

L_{msd} : Attenuation due to multiple diffractions.

$$L_{rts} = -16.9 - 10\log(w) + 10\log(f) + 20\log(\Delta h_{RX}) + L_{ori} \qquad (2.17)$$

L_{ori} is a term that depends on the orientation of the road relative to the transmitter.
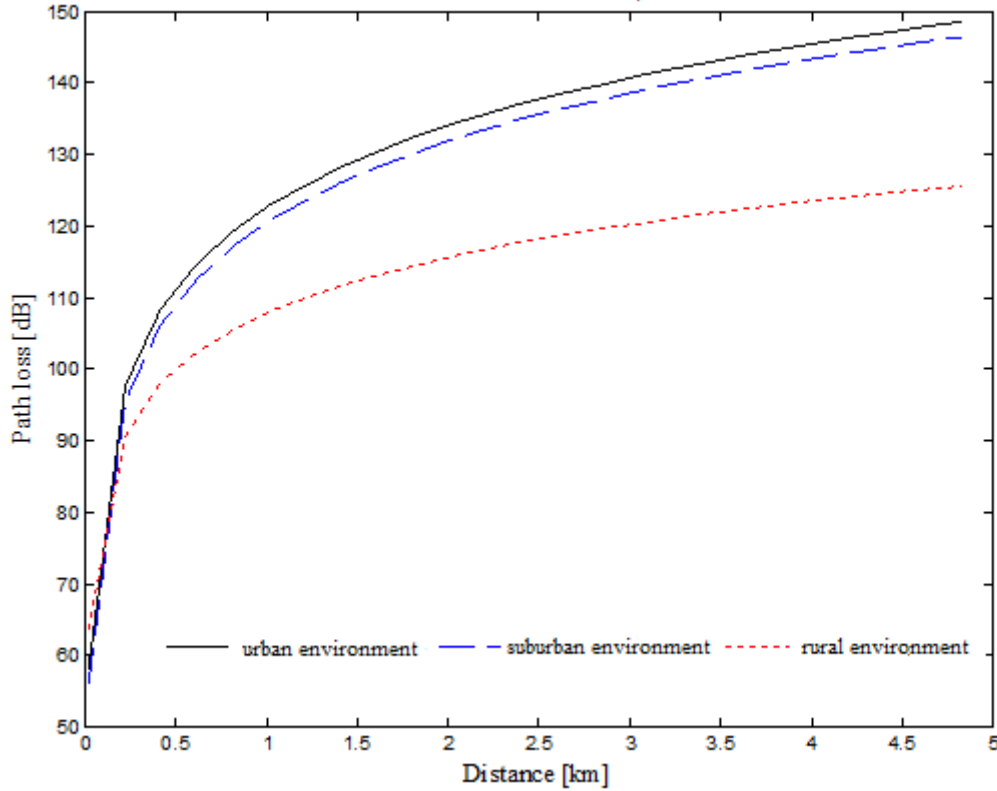
Figure 2. 6. Visibility loss (Walfisch-Ikegami model).

$$L_{ori} = \begin{cases} -10 + 0.354\,\alpha & 0 < \alpha < 35 \\ 2.5 + 0.075(\alpha - 35) & 35 < \alpha < 55 \\ 4.0 + 0.114(\alpha - 55) & 55 < \alpha < 90 \end{cases} \qquad (2.18)$$

The loss of orientation is an empirical correction term obtained after calibration.

The disadvantage of this model is that it requires knowledge of many parameters of the area to be studied, although it can be used for default values. Likewise, it neglects multipath waveguide effects.

2.4.2. Stanford University Interim (SUI) model

The IEEE 802.16 Broadband Wireless Access Working Group suggested the SUI model for the frequency range below 11 GHz (HASHIBSIDDIQUE 2013), (JENG 2010). The Stanford University channel model incorporates it. This prediction model was created using a Hata model with a frequency over 1900 MHz. This model may be extended to the 3.5 GHz range using the correction param. This kind is intended for use in the United States Multipoint Microwave Distribution System (MMDS) in the 2.5 to 2.7 GHz frequency band (HASHIBSIDDIQUE 2013). The SUI model's base station antenna height varies between 10 and 80 meters. The receiver's antenna height changes between 2 and 10 meters. The cell radius ranges from 0.1 to

8 kilometers (JENG 2010). The SUI model distinguishes three types of terrain: Terrain A, Terrain B, and Terrain C. There is no mention of a particular environment. Terrain A is best suited to mountainous terrain with light to dense vegetation. The terrain with the most path losses is this one.

2.4.3. Ericsson model

This model is based on an updated Okumura-Hata (HOOMOD 2018), which allows for parameter changes based on the propagation environment.

The path loss is calculated as follows:

$$PL = a_0 + a_1.(d) + a_2.(h_b) + a_3.(h_b).(d) - 3.2((11.75.h_r)^2) + (f) \qquad (2.19)$$

$g(f)$ is described by the following equation (HOOMOD 2018):
$$g(f) = 44.49log_{10}(f) - 4.78(log_{10}(f))^2 \qquad (2.20)$$
Where:
h_b: Transmission antenna height [m]
h_r: Receiver antenna height [m]

Table 2. 4. Parameter values for the Ericsson model (HOOMOD 2018).

Environment	a_0	a_1	a_2	a_3
Urban	36.2	30.2	12	0.1
Suburban	43.2*	68.93*	12	0.1
Rural	45.95*	100.6*	12	0.1

2.4.4. The cons of empirical and semi-empirical models

In general, the previous models, whether empirical or semi-empirical, help give orders of magnitude, but their lack of precision often makes them unsuitable for setting up satisfactory engineering. In addition, such models are established starting from a grid of parameters. One can extend it only with difficulty to a new range of use. Because It does not have the mark of the laws of electromagnetism to assess the change this can bring to precision results. In addition, comparing the results provided by these models with reality has made it possible to conclude that this category of models. However, it undergoes a calibration and refinement operation and presents precision defects, especially in places with a high density of buildings. The second category of models appeared to remedy this drawback and have a reliable situation. These are the exact models.

2.5. Deterministic models

This model describes mathematically (often using statistics) a set of measurements collected in the field or experimental data. They are models of representation of reality. The majority of propagation models belong to this type of model.

If the empirical model is well constructed, with the rigor required by statistical analysis, it will correctly represent the data used to establish it. Because, in general, it is relatively simple and easy to implement (in terms of mathematical development and computer programming), the telecommunications system designer will prefer it to any other.
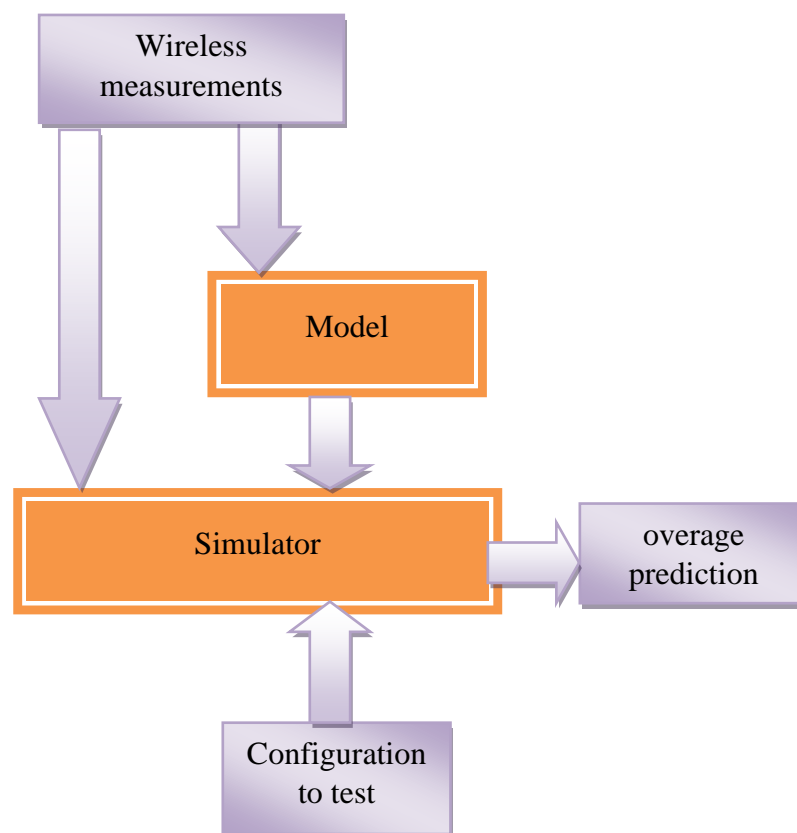
Figure 2. 7. Work plan of deterministic models.

2.6. Conclusion

We are interested in deterministic, empirical, and semi-empirical propagation prediction models in this chapter. We have shown that these propagation models are only mathematical formulas obtained from statistics on many measurements. These models allow fast calculations and do not consider the topology of the terrain, such as flat or rigorous terrain

Chapter 3:
Related works

3.1. Introduction

Many experiments have been done by global companies in the field of mobile networks to reach near-zero access delays in wireless communication. However, there is still a problem in propagation because there are absent frequency bands in the channel of modeling .in the field of telecommunication, propagation is divided into three types indoor, outdoor, and emerging signal propagation. Wireless connections have been used widely in the last decade. Most wireless connections use indoor propagation. Wireless Local Area Networks (WLANs) are used for indoor mobile internet access and as a dependable offloading mechanism for macrocell connections in interior situations (Plets 2016). The majority of internet activities need constant data transfer with negligible latency. The route loss between the transmitter (access point AP) and the receiver determines the dependability of wireless communications (receiving mobile). Time-consuming ray-tracing methods have attempted to describe the channel entirely by considering the signal's reflection, refraction, and wall absorption effects. At a high level, we have outlined various distinct Indoor propagation models. In this chapter, we will summarize some related work on the propagation channel for LOS (line of sight) and NLOS (non-line of sight) in the microwave and mm-Wave bands at various frequencies (COLD PREY 2012).

3.2. Measurement of the Path Loss Exponent for Uniformly Attenuated Indoor Radio Channels with Efficient Experimental Path Loss Exponent Measurement

This experiment uses route loss measurements for similar indoor radio channels to develop a prediction model. In the previous studies, the path loss in signal propagation was the pivot, and it took much work to measure and analyze the data in all rooms, especially if they had a large building. That makes creating a path loss model with good accuracy challenging. They utilized the Seidel site-specific log-normal channel model, a basic model for indoor wave propagation, as their computer-based theoretical model. The experiment occurred at the University of North Carolina's Woodward Hall. "uniformly attenuated buildings" (UAB) refers to attenuation induced by equal walls. Any UAB will have the same large-scale channel model if two TX (transmitter) sites with the same covered distance have the same RSS (receiver signal strength) data. If two TX locations with the same covered distance have similar RSS statistics, their large-scale channel model will be similar. If two TX locations with relatively covered distances have similar RSS data, they will have a large-scale channel model that is virtually identical. The second half of the experiment was separated into five places to find similar RSS mean and standard deviation values. Then, using the specified levels, they choose RSS standard deviation values to determine the optimum levels that minimize the error between the RSS

standard deviation and flat-top construction. The average route loss exponent is calculated by measuring the received signal intensity and distance at several locations across the floor plan for each specified TX position. They arrive at the final formula (ALASTI 2009), which computes the average path loss exponent (ALASTI 2009).

3.3. Effects of Singularity on Wireless Network Performance in Unbounded Path-Loss Models

This model is great when we have signal propagation at a significant distance, but it is not that effective when the value of the distance is small. For studying this model mathematically, it should be a formula that connects the transmitter with the receiver. The power gain of the wireless channel was modeled using the equation $G(d)= d^{-\alpha}$, where d is the distance between two terminals and α is the exponent of path loss. The singularity at 0 is a fundamental feature of this paradigm. When the transmitter and receiver are close to one another, the efficacy of this function improves. The implications of the unbounded path-loss model's singularity at 0 on network performance were investigated by comparing it to a limited path-loss model in which nodes are evenly distributed over the network domain and acquire channel access using an Aloha style medium access control (MAC) protocol. Previous research on a similar topic, the signal-to-interference ratio for wireless ad hoc networks, used randomly dispersed nodes to derive distribution limits. Laplace will be valid for estimating the decay rate of the network interference PDF (probability density function of signal). The transmitters are evenly dispersed over the network's disk shape area. The network's nodes are supposed to employ binary phase-shift keying (BPSK)to simplify the mathematical presentation. Bounded (BPM) and unbounded (UBM) route loss models have been identified (UBPM). The sum of demodulated residual signals from all interfering transmitters in the network has been considered the overall network multiple-access interference. The Interference Behavior for $\alpha \leq 4$ has shown that the interference signal strength does not converge in distribution to a real-valued random variable for either of the path-loss models. The implications of singularity on network performance in unbounded path-loss models have been investigated. The consequences of the UPM singularity on more tangible performance measures, including bit error rate, packet success probability, and wireless channel capacity, have been studied. When the UPM is used, it produces substantial variances from more realistic performance values found with the BPM. These findings imply that the traditional unbounded path-loss model should be done with caution. In many cases, the implications of the UPM singularity on network performance cannot be overlooked (INALTEKIN 2009).

3.4. Path Loss and Delay Spread in Indoor Optical Wireless Systems: A Modified Ceiling Bounce Model

This model is based on Carruthers' (Ceiling Bounce Model) method, which assumes an indefinitely ample space and only considers a single reflection from the transmitter to the receiver via the room's ceiling, ignoring higher-order reflections from the walls and ceiling. Other elements that impact propagation should be considered to achieve a better prediction. Calculation of RMS Delay Spread This number is utilized to determine the actual impulse response by determining the distance between the transmitter and receiver and the angle of reflection between them. Furthermore, to determine the exact impulse reaction, examining the impacts of multipath dispersion and calculating the power distribution profile is necessary. Two experiments were conducted in the same room to investigate the factor of transmitter-receiver position. In the first experiment, the transmitter was placed in the corner of the room, and the receiver moved around the room. The second transmitter is in the middle of the room, and the receiver moves around the room, with the length being x, the width being y, and the height being z. When we compared the two situations, we found that the RMS delay spread value in the first case was more significant than in the second case for the identical receiver position (SMITHA 2009).

3.5. Analysis of path loss models of 4g femtocells

FEMTOCELL (from FEMTO - prefix emphasizing the minimal size -, and cell), also called "HNB" (Home Node B) or "HENB" (Home ENODE B) in 3GPP standards, is an essential element of a low-power cellular mobile telephone network, designed to offer limited radio coverage and often intended for residential or business use. It connects to the mobile telephone operator's network via a high-speed Internet connection (by a cable, xDSL, or optical fiber router, Etc.). Depending on the model, it can support 4 to 8 simultaneous communications or Internet access. (Voice and data).

FEMTOCELLS need to provide a good network connection; however, interfering with base stations on the same frequency concerns this type of network. Different factors, such as macrocell size, Femto and macro base station transmission power, and FEMTO cell locations, can be used as input to the chosen model. The femtocell simulation model dynamically evaluates interference distribution for the serving and interfering base stations. The experience was in a building with six floors and ten walls at KL university in India.

The results of the comparison between FEMTO cells and macrocells show:

- The interfering and noise ratio in Femto BS link is high, while in the macro Bs link is low

- . The throughput in the Femto BS link is low, while the macro Bs link is high.

- The path loss in the Femto BS link is high, while the macro Bs link is low.

So that shows us that the macro Bs link is better to use than the FEMTO Bs link (VARDHAN 2014).

3.6. Mobile WiMAX performance assessment and route loss model selection for UGV

WiMAX is a high-speed internet technology based on IEEE 802.16e-2005 that provides broadband wireless access. A Mobile WiMAX communication system running in the 1 GHz frequency range with 512 FFT for 3.5 MHz bandwidth was used in the test. The field testing for UGVs was conducted using the Mobile WiMAX communication technology (unmanned ground vehicle). On high ground and horizon line areas, the connection quality and throughput for cell coverage and an ideal route loss were tested at various places. The two-ray ground has used a reflection model for computing RSSI from data. The performance of a mobile WiMAX base station in the field has been demonstrated using the route loss model, which has been measured experimentally and theoretically (Appelqvist 2007).

3.7. In mango greenhouses, a new empirical route loss model for wireless sensor networks has been developed.

An effort to build an improved path loss model for wireless sensor networks is presented (WSNS). This technology is interesting because it is cheap, with little energy usage and a few hundred meters of communication range. The model is based on the empirical models (COST35, ITUR) to create the new model by considering the factors that affected signal propagation like diffraction, reflection, and scattering, not to mention the distance between the transmitter and receiver, as well as the effect of vegetation.

The readings were conducted in a mango greenhouse in Malaysia's northwestern region. The greenhouse diameters are 50 m in length, 10 m in width, and 5 m in height with 13 trees of mango. Seven wireless nodes have taken the measurements with parameters: range of frequency 2.245 GHz, data rate 250bps with receiver sensitivity -95dbm. The height of the transmitters was (0.5 m, 1.0 m, 1.5 m, 2 m, 2.5 m, 3 m, and 3.5 m) and the receivers were positioned at each tree at the same height as the transmitters. The comparison between the prediction models and the actual measurement showed the most significant difference between the objective

measurements and the predictions in the transmitter with 1.5 m, which shows that the empirical models do not consider the foliage effects.

Furthermore, the MAPE values (the relation between the measured and the predicted data) have a very significant value. On the other hand, the new models have a low MAPE value (2.75 percent). According to the MAPE, the novel suggested model is a good route loss prediction tool in the mango greenhouse and outperforms the previous foliage models (RAHEEMAH 2016)

3.8. Path-Loss Models and Network Planning Optimization

The Wicca Heuristic Indoor Propagation Prediction (WHIPP) tool is at the heart of the system. The Wireless & Cable group developed the WHIPP tool, a wireless indoor network planning toolkit. This network prediction tool takes into account both interior and outdoor propagation. The original utility is built as a web service that communicates with a backend server. The lowest available Android version (Android 2.2 Froyo) was chosen to increase the number of devices compatible with the mobile application. The android made it possible to make changes to the original WHIPP tool. The device's mobile nature and inbuilt antenna make receiving signal strength indication (RSSI) readings rapid and straightforward. A route loss model utilizing an unobstructed free space environment is known as free space loss (FSL).

$$\text{FSL} = 20 \cdot \log 10(d) + 20 \cdot \log 10(f) + 32.45 \tag{3.1}$$

While d is measured in kilometres and f is measured in (MHZ) The IEEE 802.11 and TGn model (TGN) is a two-path loss model used in office contexts to estimate path loss.

$$\text{TGNL} = PL_0 + 10 \cdot n_1 \cdot \log 10(d)\ (d < d_{br}) \tag{3.2}$$

$$\text{T GNL} = PL_0 + 10 \cdot n_2 \cdot \log 10(d) - 32\ (d > d_{br}) \tag{3.3}$$

The multiwall model (MWM) is a two-part model with a distance-dependent portion and a wall-dependent part that adds a wall-specific loss for each wall that the direct ray between transmitter and receiver passes through. The technology was tested in three distinct indoor settings. Because of the built-in antenna of mobile devices and the ability to designate measurement places on a tablet, the program is elementary to use. It has been demonstrated that simply a few more mobile observations are frequently sufficient to enhance the route loss model in a given environment (D. R. Plets 2016).

3.9. Propagation Loss Prediction Models for Land Mobile Communications

By defining important system characteristics like transmission power and frequency reuse, it is possible to build Propagation Loss and Prediction Models. Many prediction models for cellular mobile radio systems operating in the microwave spectrum have been developed. Information regarding buildings and roads is essential, and geometrical routes between transmitter and receiver should be included for reliable prediction, according to the history of propagation loss prediction models. The ray-tracing method was developed more precisely for small regions such as indoor picocells. To meet rising demand, the cell size of today's cellular systems in urban areas is shrinking. The ray-tracing approach may now be used to construct microcells and indoor Pico cells. For microcells that are bigger than street microcells, the Walfisch-Bertoni model is also helpful. However, for suburban and rural regions to benefit from cost-effective systems, macrocells with a cell radius more significant than 1 km are still required. Given its simplicity, the Okumura-Hata model with Akiyama and terrain correction is beneficial in several application areas. As a result, selecting the proper prediction model for the planned cell size is critical in designing cellular mobile radio systems. The IMT-2000 third-generation mobile communication system will operate in the two-GHz range and enable user bit rates of up to 2 Mbiffs. Microwave and millimetre-wave frequency bands are necessary to handle greater bandwidth in the fourth-generation system to provide higher-rate multimedia services. To combat the growth in route loss and delay spread, space and time equalization technology that combines adaptive equalization and adaptive array antenna will be a breakthrough. The direction of arrival (DOA), the time of arrival (TOA; delay), and, therefore, the power (path loss) of the received signal are all essential factors to consider as this technology develops. Not only can the ray-tracing approach predict route loss, but it can also predict DOA and TOA. As a result, it will play a more significant role in future system design (Hata 1998).

3.10. Adaptive Neuro-Fuzzy Inference System path loss estimates for multi-transmitter radio propagation in VHF bands.

The measurements for this model have been taken by three drive tests in an urban environment for three base stations with frequency (89.3MHZ,103.5MHZ,203.25MHZ) in different routes which do not have the same conditions or terrains. However, the measurement method is almost the same for the three routes, and the data is randomly divided into 75 % for the training system and 25% for to test system.

A comparison has been made between the results of the ANFIS model and the results of 3 empirical models:

The Neuro-Fuzzy (NF) model, a derivation of ANFIS approaches (which are used to handle prediction issues in various disciplines), is used to measure data to train a system to forecast route loss propagation signal. It is made up of fuzzy logic (FL) and artificial neural networks (ANN). The membership function refers to the degree or grade of membership of an element in a fuzzy set, and the model includes five layers to handle the data.

Empirical models include:

1- cost Hata model: an empirical model developed of the Hata model that uses frequency from 150 MHZ to 1500 MHZ. cost Hata model used in a bigger range of frequency up to 20 GHz and distance up to 20 Km.

2- Egli model: empirical model uses frequencies from 90 to 1000 MHZ and distances less than 60 Km.

3- (ECC-33) model: European communication committee developed for European cities uses frequencies from 700 MHZ to 3.5 GHZ in a range of distances from 1 to 10 Km.

The three drive test data for three different routes show that the empirical models can predict the path loss in some points and cannot in others because it is developed based on standard parameters. On the other hand, the ANFIS model can predict almost all the path loss propagation signal in the three routes with a tiny prediction error because it is based on the backpropagation gradient descent algorithms and improve the accuracy of path loss predictions in VHF bands. Good stability and faster convergence were achieved (SURAJUDEEN-BAKINDE 2018).

3.11. path loss model for cellular mobile networks at 800 and 1800 MHz bands

The dataset has been collected from an urban area in the south of India for a distance of 4.6 Km; considering the environment of a building and vegetation shelter around the area, the receiver was placed on a motor vehicle and connected to only one base station. 72 % of the measurement data were used to train the system, and the rest were used to test the system.

The COST 231 Walfisch Ikegami model was utilized in the prediction models. These models are used to represent radio wave propagation channel conditions, and they are simple to build and compute, but their accuracy varies depending on operational frequencies and propagation settings. It solely takes into account signal diffractions from building roofs. Neural networks (artificial intelligence) (ANNs) An artificial model developed from a training system to predict path loss in mobile networks using a Multilayer Perceptron Neural Network (MLP-NN) that consists of an input layer followed by ten hidden layers to process the data and using the parameters of the CWI (Catchment Wetness Index) model, which include a transmitter to

receiver distance (d), transmitting antenna height (ht), receiver height (hr), and a transmitter to receiver distance (d) (PL).

They discovered that the NN model had the lowest MAPE percentage after adopting the two models (0.43 percent for 800 MHz and 0.42 percent for 1800 MHz) The MAE (mean absolute error) is a metric that determines the difference between anticipated and measured route loss values. The MAPE (Mean Absolute % Deviation) percentage is also known as Mean Absolute Percentage Deviation. As a result, the NN model's prediction accuracy was more remarkable than previous route loss models. It was better at predicting nearly all path loss signal propagation in mobile networks (CHEERLA 2018).

3.12. Path Loss Prediction Improvement Using a Semi-Deterministic Hybrid Model

The model is a hybrid model for path loss prediction from merged models (empirical model (cost hata231), semi-empirical (Walfish_Ikegami)) with statistical processing of the empirical measurement in GSM mobile network with 900 MHZ as a frequency in a city in the south of India. The data was collected by a vehicle across a 3 km range. In an urban area with building dimensions of 15mX20m and a height of 10 meters, the base stations are fixed on building rooftops, and the receiver is installed in a vehicle at 1.5m above ground level. The street width is assumed to be 20 meters. The following models were used to assess the model's validity: 1) Walfisch-Bertoni Path Loss Model: this model considers the building's effect in the signal propagation area, but the buildings have to be the same size, and the distance between them is equal.

Moreover, the frequency is between 800 and 2000 MHz 2) COST 231 Walfisch-Ikegami Path Loss Model: This model considers both line of sight (LOS) and non-line of sight (NLOS) and uses factors such as street width, building spacing, building height, angle of incidence, diffraction loss factor, distance factor, and frequency factor. However, such models only examine roof-to-street diffraction and neglect the impact of buildings. as a result, to enhance those models, Ten ray computation of multiple reflection loss. The model has been used to present all the signal propagations and the factors that affect the transmitter to receiver, which is called a hybrid model. When this model was tested on the network, it gave results almost the same as the data measured, and for sure, it is better than the empirical and semi-empirical models (BHUVANESHWARI 2016).

3.13. Large-scale path loss models and temporal dispersion for 5G wireless communications in an outdoor line-of-sight environment.

The outdoor propagation channel for LOS (line of sight) at several frequencies in the microwave and mm-Wave bands spanning from 10 to 40 GHz with a 1 GHz bandwidth signal is being investigated in this model. The measuring contexts are as follows: The settings of measurement were a corridor in an outdoor workplace surrounded by solid walls with windows and doors, and the frequencies were (10.5,15,19,28, and 38GHZ). Other terrain variables were concrete steps and a strong concrete pillar. The measurement is taken when the transmitter is fixed and the receiver is moving, with antenna heights of 1.7 meters for the transmitter and 1.5 meters for the reception and a distance of 1 meter between them. A prediction model known as the fa PL model was suggested, which developed the CIW model with the same parameters as the CIW model but included variables for frequency attenuation. According to the results, the CIW model's route loss decreased as the frequencies rose. The greatest XF attenuation value in the fa PL model is 9.7 dB at 38 GHz, while the smallest XF attenuation value is 2.2 dB at 28 GHz. The propagation properties of mm-Wave 5G channels were studied. For an outdoor setting, the PL and time-dispersion characteristics were calculated at frequencies ranging from 10 to 40 GHz. The collected data was used to build several well-known and freshly proposed route loss models. For all of the observed frequencies, the PLE values for the LOS scenario were reported in the range of 0.2–1.4. The multiple waveguiding events inside the outdoor corridor resulted in these modest values. The frequency dependence path loss model is taken into account in the suggested FA PL model. In the range of frequencies, the FA model's XF [dB] attenuation factor values ranged from 2.2 to 9.7 dB, corresponding to an increase in PL as a log (frequency) function. RMSDS, MN-EX, and MAX-EX were used to describe the time-dispersion parameters. The delay spread has very modest mean values, with all values less than 1 ns (Al-Samman 2016).

3.14. Path Loss Models for 5G Millimeter Wave Propagation Channels in Urban Microcells

Engineers and researchers were motivated to build the next generation of mobile networks by requiring higher communication speeds. The millimeter-wave bands can give a frequency range ranging from 28 to 38 GHz, which is a possible frequency band for a 5G cellular infrastructure. At 28 GHz and 38 GHz, propagation measurements were taken in New York City and Austin, Texas, to give channel model data. Barriers and other random propagation variables caused shadowing, reflecting random variation in the distant-dependent large-scale

route loss model. The equation that expresses the relationship between route loss and transmitted power as

$$PL (d) (dB) = \alpha + \beta \cdot 10 \log 10(d) \tag{4.3}$$

PL(d) denotes route loss in decibels over all distances, the floating intercept, the linear slope, and d is the distance between the two points (TX-RX). The results demonstrate that models created using measured data in New York and Austin produced reduced shadowing than models created with a slope pivot point that was close in. According to the models, the shadow factor is reduced by about 1 dB in New York City and 6 dB in Austin, Texas. The model has enabled the development of a novel millimeter-wave propagation model in urban microcellular settings. According to the model, mobile devices should have antennas with higher gains for millimeter-wave communications to compensate for the increased path loss caused by the frequency shift from low microwave to millimeter-wave regime (MACCARTNEY 2013).

3.15. path loss models for 5G cellular networks in the millimeter-wave frequencies of 28 GHz and 38 GHz

Signal propagation route losses in the millimeter-wave band for fifth-generation cellular network planning. The route loss model is based on measurements taken in the field at 28 and 38 GHz. Millimeter-wave signal propagation is lossier than signal propagation in ultra-high frequency and microwave bands. Because of the massive amount of raw bandwidth available for cellular services, mm-wave will become the future of wireless networks. In cellular planning, route loss for a deployment environment must be taken into account, and cell coverage is estimated using antenna gains at the base station (BS) and mobile station (MS), adequate isotropic radiated power (EIRP), RF bandwidth, and modulation and coding methods. For the 28 and 38 GHz mm-Wave bands, empirical measurement data were utilized in this model for both non-line-of-sight (NLOS) and clear line-of-sight (LOS) situations. The RF coverage for future 5G cellular networks has been modeled using the latest mm-Wave propagation models. A 220 m effective cell radius has been modeled, similar to previous observations made at 28 GHz. In the same coverage region, 5G networks will require around three times the number of deployed stations. However, when comparing existing 2G/3G/4G co-located networks to the best single propagation, just two times more sites will be required. Utilizing the available mmWave spectrum, the capacity for the random pointing case products is over 20 times that of today's cell networks, with an additional boost in capacity when using the single best pointing beams and multibeam fusion (SULYMAN 2014).

3.16. Under cover of vegetation, the 3G/4G mobile communications propagation loss NPL model and network optimization approach

Engineers and researchers generally examine elements like buildings, topography, and characteristics that affect electromagnetic wave transmission but often do not include the absorption of waves by thick leaves on street trees. The leaves of trees have been divided into four categories in this model:

. Leaves are very dense.

2. Leaves are comparatively dense.

3. Leaves are dense.

4. Leaves are rare.

Each category has its model, except the fourth category can be neglected.

Table 3. 1. The test results of the categories.

Kinds of vegetation	900 MHz loss(dB)	2GHz loss(dB)
Rubber tree	8.2	6.3
Poplar	7.3	5.5
Plane tree	7.6	6.8
Pagoda tree	5.5	4.6
Ginkgo tree	4.6	3.8

The results of the tests indicate that the system can solve the problem of motion video stoppage caused by plant absorption of electromagnetic waves and reduce handover failure. Ensure base station coverage overlap if we can adequately manage the distance between base stations and the distance between the base station and vegetation (SHUAI 2011).

3.17. Comparative studies

Despite the antiquity of empirical models, they are still used as references for artificial intelligence models. By comparing the empirical models, we find that the Walfisch-Ikegami model is the best among them because it covers the most significant possible distance with the possibility of covering different values of frequencies and with different lengths of transmitting and receiving antennas. However, each model has its advantages in a particular coverage environment. The indoor models conduct in a specific environment. The wireless network simulations usually propose that the distribution between the nodes is uniform. In general, the path loss is determined by calculating the distance between each pair of nodes and then applying an appropriate path loss model as a function of that distance. The benefit of such models is that they may be used to create a network in an environment with comparable features.

The superiority of outdoor models is in the factors that the models consider. The accuracy and speed of these models are very important to building a good cellular network. The models have allowed proposing new propagation models for wave propagation in microcellular environments. According to the models, in-wave communications require antennas with higher strengths to compensate for the extra path loss caused by the frequency leap.

Most of the current path loss model validation work has been completed, and a better approach has been proposed. The data is collected in a given context, and the model is then shown better describe the data than one or more rival models.

3.18. Conclusion.

For researchers, deciphering the vast and varied terrain of route loss models may take much work. We've created a new taxonomy for thinking about commonalities across these models as a result of our effort. We classified models into three groups based on their practicality and intent: (a) coverage and radio transmission, (b) rough planning, and (c) simulation. Applications that require accurate radio environment maps will benefit from a full-life measurement technique that can reconcile forecasts with directed measurements. When direct measurements of the environment are impossible, an experimenter must accept some (potentially significant) error. Many-ray methods are useful, but their accuracy is dependent on the accuracy of information characterizing the environment and barriers, which is seldom available at a good resolution and can be prohibitively expensive to acquire and update. On another hand, the models based on Artificial intelligence (AI) technologies seem promising models because of the accuracy and speed of predicting the path loss in signal transmission. The problem with this kind of model is that it is effective in a specific environment. We tried our best to summarize and compare the models to find the points of difference and agreement between the models to help the researchers to develop better path loss prediction models. The next generation of models, we think, will be data-driven, gaining knowledge from guided measurements and potentially employing hybridized prediction approaches.

Chapter 4:
Artificial neural networks and our contribution

4.1. Introduction

When a new technique appears, the engineer naturally wonders how this novelty can be helpful to him if it has a name that is more metaphorical than technical, which is the case for neural networks.The answer of McColloch and W. PITTS was yes, and it can be helpful to us in many fields. Among these fields, we find electromagnetism; more precisely, we are interested in applying this technique to model and optimize microstrip antennas of all shapes, sizes, and types of excitement. A neural network can be considered in its simplest form as a black box, equivalent to a function with several accesses and outputs. This black box has an important feature called 'Learning. 'This learning is done using an algorithm and a database.

The outputs of the function are matched to the input. This function is adjusted according to the number of training examples constituting the database and the convergence speed toward an optimal solution. This function adjusts for each example, which implies that the database must be as rich as possible. At the end of this process this box can give outputs for any input, even if it is outside the database, with optimal precision.

4.2. History of neural networks

The concept of the formal neuron was born in 1943 due to the work of McCulloch and PITTS, followed by the publication of ROSENBLATT in 1958, which proposed the first learning algorithm that allows the neuron to adjust these parameters (MCCULLOCH 1943). This concept quickly fell into oblivion. In 1969, MINSKY and PAPERT published the book Perceptron, which demonstrated the limitations of neural networks; because they can only approach simple mathematical problems. This embarrassing problem failed to kill this new technique; practically all the researchers have abandoned this field of research. Fortunately, HOPFIELD did not let go; he proposed 1982 associative neural networks, and interest in neural networks was reborn among scientists (HOPFIELD 1982).

In 1986, RUMELHART, HINTON, and WILLIAMS published their algorithm called back-propagation of the error, which makes it possible to optimize the parameters of a neural network with several layers. From there, the door was wide open to this area in order to explore new applications.

4.3. Biological Neuron and Formal Neuron

Formal neural networks are initially an attempt to model the human brain (PERLOVSKY 2001) mathematically. While to model this biological computer, one must pass the replacement

of these elementary components, the biological neuronal cells (Figure **4**.1), by artificial neurons. McColloch and PITTS realize that they proposed a model that can perform some elementary calculations; what is clear, by connecting several neurons to see a network, the complexity of the calculations that this network can perform increases exponentially.
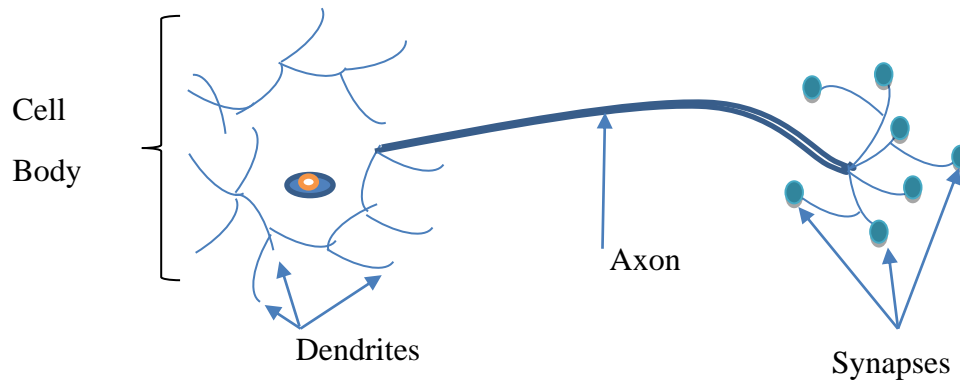

Figure 4. 1. The biological neuron.

Neurons communicate with each other through Dendrites which are inputs. Synapses which are outputs, the information received by the Dendrites will be processed in the nucleus of the cell body. The information to be transmitted will be conveyed along with the distance that separates two cellular bodies by an Axon, which ends in Synapses connected to the Dendrites of the cell receiving the message; this allows information in the electrical form to wait for its destination without deformation and route error (SEUNG 2012).

The neuron output signal depends on the input signals from other cells, and this output signal is not likely to occur if the sum of the input signals does not exceed the activation threshold. The output signal will be either an excitation signal or an inhibit signal. However, a formal neuron and a simple process may be simulated or realized as an integrated circuit. Where the components of the equivalent artificial neuron are as follows (YANG 2020):

Table 4. 1. Biological Neuron Vs. Formal Neuron (MCCULLOCH 1943) .

Biological Neuron	Neuron Formal
Synapses	Connection weight
Dendrite	Input signal
Axon	Output signal
Summation	Activation function

From the analogy table between biological neurons and formal neurons above, we can give a simple diagram of an artificial neuron shown in (Figure 4.2). Where the X_i are the input signals, the W_i is the connection weight, W_0 is the threshold, and we go through the activation function, we obtain the Y, which is the output signal.
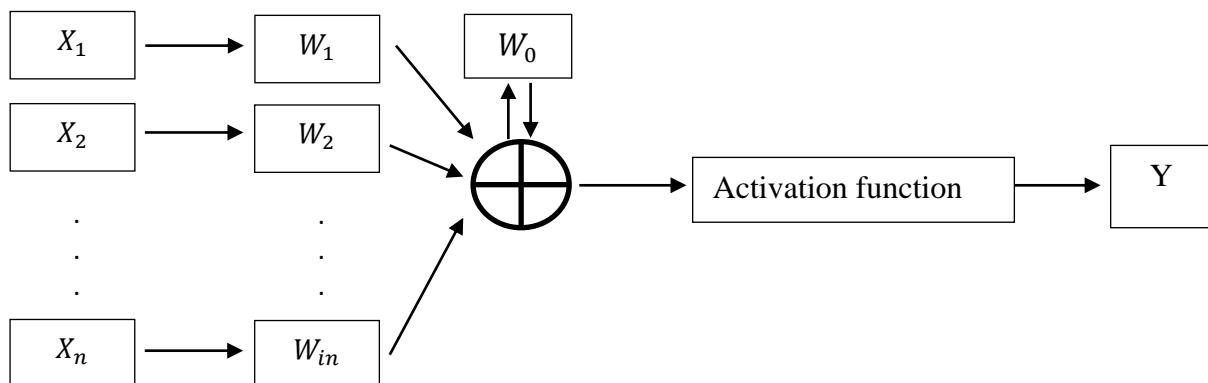
Figure 4. 2. The Artificial neuron.

In turn, the output signal can again be an input signal from one or more upstream neurons in the same network as the originating neuron.

We can see that this neuron is composed of two essential parts, the first part of the neuron inputs until the output of the summation function. This part has the role of calculating the weighted sum of the inputs X_i. If this sum waits for a certain threshold, the second part intervenes to calculate the value of the state of neuron Y by application of the transfer function.

$$Y = f(W_0 + \sum_{i=1}^{n} W_i X_i) \qquad (4.1)$$
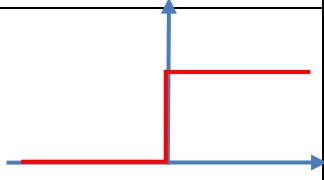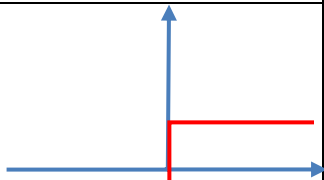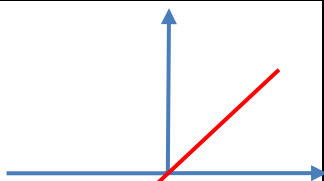
4.4. Activation function

Any differentiable function can be used as an activation function (DING 2018); The activation function is a nonlinear saturation function that limits the amplitude of the neuron's output signal (LIEW 2016). Whose forms are frequently used as activation functions are the linear, threshold, or sigmoid functions (Table 4.2).
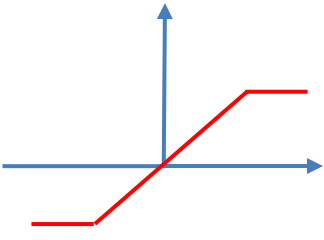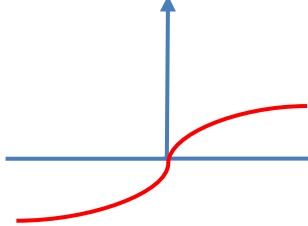
A multi-layer perceptron or MLP (multi-layer perceptron) of a single hidden layer having the sigmoid function as the function of the activation of the neurons of the hidden layer, and the linear function for the activation of the neurons of the output layer can approximate any function as complex as it is provided that the number of neurons and the number of training examples are sufficient (DONGARE 2012).

4.5. Architecture of neural networks

An ANN (Artificial Neural Network) is an association of several formal neurons to create a structure capable of solving mathematical problems of greater complexity than a single neuron can deal with. Neural networks can be subdivided into two large families, unlopped (static) networks and looped (dynamic) networks (CARLEO 2017).

Table 4. 2. Some activation functions

Function	Formula	Shape
Threshold or Heaviside function	$f(x) = 0 \; if \; x < 0$ $f(x) = 1 \; if \; x \geq 0$	
Symmetrical threshold function	$f(x) = -1 \; if \; x < 0$ $f(x) = +1 \; if \; x \geq 0$	
Right	$f(x) = \alpha x + \beta$	

Linear Saturated 'Balanced'	$f(x) = -1 \; if \; x < -1$ $f(x) = \alpha x + \beta \; if -1 \leq x \leq 1$ $f(x) = 1 \; if \; x > 1$	
Sigmoid	$f(x) = \dfrac{1}{1 + e^{-x}}$	

A neural network is designed with an input layer, and one or more hidden layers is an output layer. Each layer is a group of several neurons that performs linear activation functions for the neurons of the output layer and is nonlinear for the other neurons (KARSOLIYA 2012).

4.5.1. Unlopped Neural Networks (Statistics)

An unlopped neural network performs one or more algebraic functions of its inputs by the composition of the functions performed by each of these neurons. This network is represented graphically by a set of neurons connected. In such a network, the flow of information circulates from the inputs to the outputs without backtracking (KARSOLIYA 2012).

Unlopped neural networks are static objects: if the inputs are independent of time, the outputs will be too. They are mainly used to perform nonlinear function approximation, classification, or nonlinear static process modeling tasks (Rabeb 2013)

Single layer network

A monolayer neural network is a structure formed by a layer of input neurons, wholly connected to the neurons of the output layer passing through a hidden layer of a weight W (Figure 4.3) (PLÖCHL 2001).
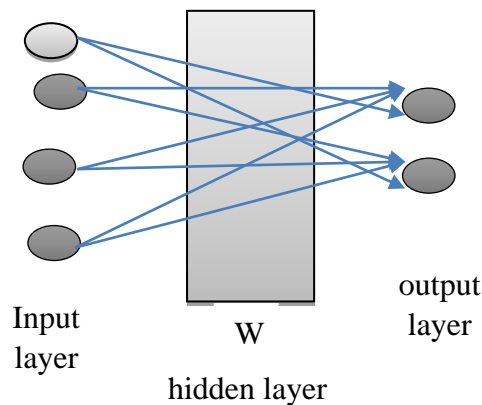
Figure 4. 3. Single layer network.

Multi-layer networks

The neurons are arranged by layer. There is no connection between neurons of the same layer, and the connections are only made with the neurons of downstream layers (Figure 4.4). Usually, each neuron in one layer is connected to all the neurons in the next layer and only this one. This allows us to introduce the notion of the direction of the information path of activation within a network and thus define the concepts of input and output neurons (ZAEEM 2021).

Figure 4. 4. Multi-layer network.

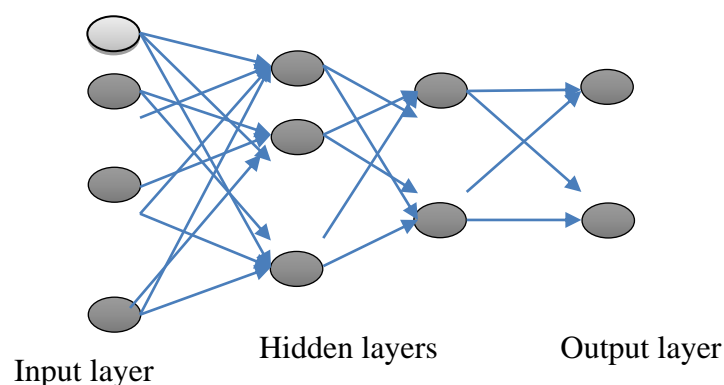### 4.5.2. Looped Neural Networks (Dynamics)

Unlike non-looped neural networks whose connection graph is cyclic, looped neural networks can have any topology of connections, including in particular loops, which bring the value of one or more outputs back to the inputs. A discrete-time looped neural network is therefore governed by one (or more) nonlinear difference equations, resulting from the composition of the functions performed by each neuron and the delays associated with each of the connections (Gadh 1995).

Networks with recurring connection

Recursive connections take information backward from the defined direction of information propagation in a multi-layer network. These connections are most often local (Figure 4.5) (LILLICRAP 2020).
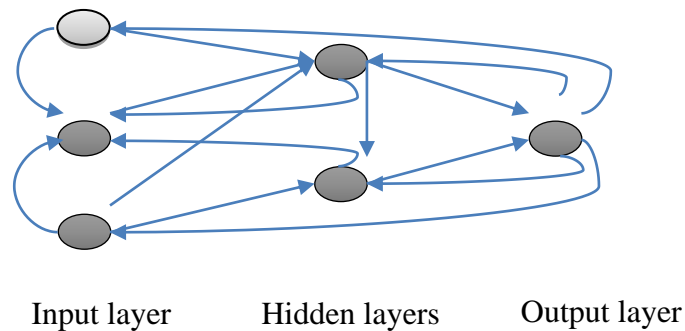

Input layer   Hidden layers   Output layer

Figure 4. 5. Multi-layer network with the recurrent connection.

Full connection network

In a complete connection network, each neuron is connected with all the other neurons in the same network, including in the opposite direction to information propagation (Figure 4.6)
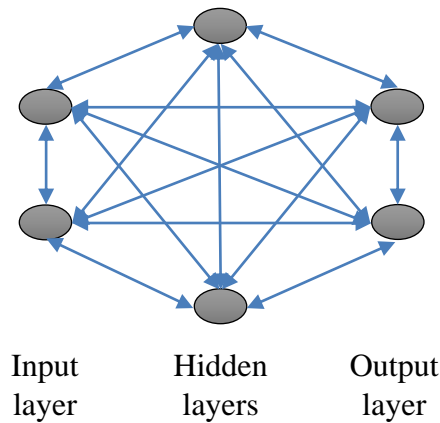

Input   Hidden   Output
layer   layers   layer

Figure 4. 6. Full connection multi-layer network.

4.6. Neural networks learning

Learning is the most exciting property of neural networks. The learning of a neural network is carried out along a phase called learning, during which the behavior of the neural structure adjusts until the desired behavior is obtained. This is accomplished using a learning algorithm and a so-called learning database (VILLAVERDE 2006). Neural networks generally serve the results of analytical methods or measurements as a database for learning.

There are two categories of learning, and one supervised and the other unsupervised:

4.6.1. Unsupervised learning

Learning is called unsupervised when only input values are available. In this case, the examples presented at the input cause the network to self-adapt to produce relative output values in response to similar input values (DONALEK 2011).

The networks must detect points common to the examples presented by modifying the weights to provide the same output for inputs with similar characteristics. Unsupervised learning is well suited to modeling complex data, whose rules governing the system's behavior to be modeled by neural networks are less precise (RIBEIRO 2016).

4.6.2. Supervised learning

For this type of learning, we present to the neural networks the values of the inputs and the outputs we want for these inputs. The network is reconfigured to the input-output function. That is to say, calculate its weights so that its output corresponds to the desired output (DONALEK 2011).

4.7. MLP and RBF networks

4.7.1. The MLP multi-layer perceptron

A multi-layer perceptron is an unlooped neural network with several neural layers hidden between these two input and output layers. To endow the multi-layer perceptron with the property of nonlinearity, it must include at least one hidden layer, and the activation functions of the neurons, which compose it, must be nonlinear (GROSAN 2011)

A single-layer network with suitably chosen weights could exactly reproduce the computations performed by any multi-layer network (GROSAN 2011).

In other words, a perceptron has a hidden layer composed of neurons of generally sigmoid nonlinear activation functions that can approach any result of a mathematical function calculated by any multi-layer network.

MLP Architecture

In the general case, an MLP can have any number of layers. However, to improve the operation of the MLP on one side and minimize the computation time on the other, it must look for an optimal architecture matching the number of layers and number of neurons per layer (Alnatoor 2020).

A back-propagation network is a multi-layered MLP network consisting of at least an input layer, a hidden layer, and an output layer (Figure 4.7). Each layer contains one or more neurons, depending on the data we want the network to learn and the number of outputs we want. There needs to be a more precise method to determine the number of layers and neurons, and it depends on the complicity of the problem to be solved (Alnatoor 2020).

An MLP network with N_0 input, $L - 1$ hidden layers of N_i neurons or $i \in [1, L - 1]$, and an output layer containing N_L neurons, i is the index of the layer, X_{ik} s the output of the

neuron k of layer i, W_{ik} is the weight linking output x_{i-1} to neuron k of layer i, output X_{ik} of neuron (i, k) is :

$$X_{ik} = f(Y_{ik}) \tag{4.2}$$

$$Y_{ik} = \sum_{j=1}^{N(i-1)} W_{ijk} x_{i-1\,j} + b_{ik} \tag{4.3}$$
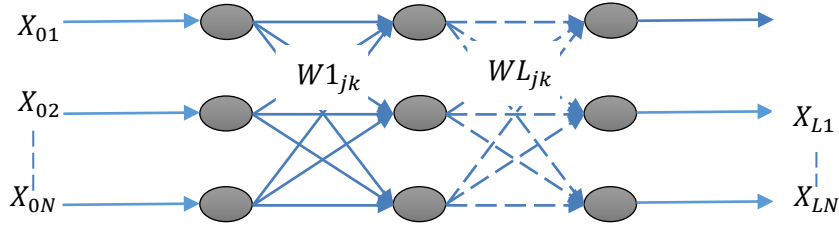

Figure 4 .7. Architecture of an MLP network.

MLP learning

The learning of the MLP is supervised using an algorithm called back-propagation (back-propagation), whose objective of this phase is to adjust the weights and minimize the value of the quadrature error between the network and the desired output. Where It is the decreasing of the error gradient for a minimum is ensured by the back-propagation algorithm (GRUM 2022). The error gradient E(x) is calculated for each weight by:

$$E(x) = \left|\left| d(n) - Y_L(n) \right|\right|^2 \tag{4.4}$$

where d(n) is the desired value, and $Y_L(n)$ is the network output value.

$$\frac{\partial E(n)}{\partial W_{ijk}(n)} = \frac{\partial E(n)}{\partial Y_{ik}} \frac{\partial Y_{ik}}{\partial W_{ijk}} = \frac{\partial E(n)}{\partial Y_{ik}} x_{i-1\,j} \tag{4.5}$$

For the output layer i = L, the output error is denoted δ_{Lk}, and it is calculated as follows:

$$\delta_{Lk} = \frac{\partial E(n)}{\partial Y_{ik}} = 2f'(Y_{Lk})(d_k - x_{Lk}) \tag{4.6}$$

Where f(x) is the activation function.

For the hidden layers, the error δ_{ik} is given by:

$$\delta_{ik} = f'(Y_{ik}) \sum_{j=1}^{N(j+1)} \delta_{i+1\,j} W_{i+1\,kj} \tag{4.7}$$

The modification of the weights W(n) and the biases b(n) is obtained by the following two equations:

$$W_{ijk}(n+1) = W_{ijk}(n) + \eta \delta_{ik} x_{i-1\,j} + \Omega(W_{ijk}(n) - W_{ijk}(n-1) \tag{4.8}$$

$$b_{ik}(n+1) = b_{ik}(n) + \eta \delta_{ik} \tag{4.9}$$

Where η is the learning step that determines the convergence speed, and Ω is the momentum or inertia term that prevents the algorithm from getting stuck. Typically, the minimum value of $\Omega = 0.9$.

4.7.2. The Radial Basis Function Network (RBF)

A radial basis function network is based on an architecture organized into only two layers; a hidden layer and an output layer.

The hidden layer, made up of neurons or nuclei, has a radial basis function that performs a nonlinear transformation of the input space. The output layer calculates a linear combination of the outputs of the hidden layer, but it is possible to use a nonlinear function as the output function.

Each kernel calculates the distance between the input and its centre, passing through a nonlinearity accomplished by a Gaussian activation function—the value of the kernel output closest to its centre. An RBF can approximate any continuous function with sufficient neurons (WU 2015).

RBF Architecture

On the other hand, The RBF does not contain an input layer, and the number of layers does not depend on the complexity of the calculations. The activation function is always a Gaussian (Figure 4.8). The standard deviation of the Gaussian represents the distance between the input and the center of the kernel. When this distance becomes large, the output of the network is given by the following formula:

$$Y_i = \sum_{k=1}^{N_1} W_{kj}\, \varphi_k(\,||x - c_k||\,) \tag{4.10}$$

$$\varphi(\xi) = e^{-(\frac{\xi^2}{2\eta^2})} \tag{4.11}$$

Where x is the input vector, c_k *is* the center of kernel k, N_1 is the number of kernels of the hidden layer, and the W_{ik} are the weights of the output layer, η is a parameter that allows control of the speed of uncrossing of the function φ.
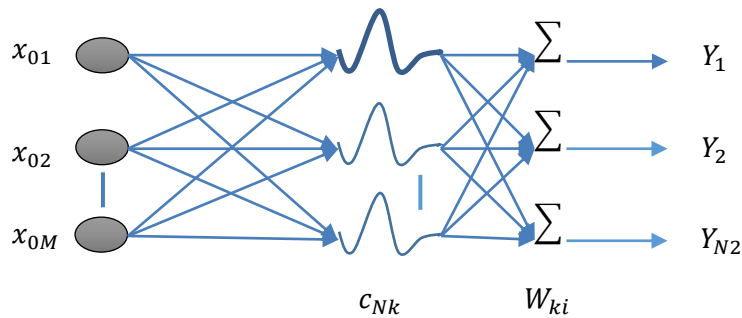

Figure 4. 8. RBF Architecture.

RBF Learning

RBF learning comprises an unsupervised rule for center adaptation and a supervised rule for weight adaptation (WU 2015).

4.8. Applications of AI technologies in mobile networks

Artificial Intelligence (AI) is excellent for problems where existing solutions require much hand-tuning or long lists of rules. For complex problems where there is no good solution at all using traditional methods, for adapting to changing environments, for getting insights about complex problems that use much data, and in general, for noticing patterns that a human might miss. Hard-coded software can be a long list of complicated rules that are hard to keep up with, or it can be a system that automatically learns from past data, finds outliers, predicts what will happen in the future, Etc. AI's ability to learn, along with a large amount of sent data or wireless configuration datasets, can be used to solve these problems. In the table below, we will summarize and compare some previous AI models.

Table 4. 3. A comparison between AI models.

Authors	AI technique	Training model	Model properties	Year
Sotiroudis et al (Sotiroudis 2013).	Supervised learning	Artificial Neural Networks (ANN) and Multi-Layer Perceptron's (MLP).	It is used for modeling and estimating link budget and propagation loss objective functions for wireless networks.	2013
Timoteo et al. (TIMOTEO 2014).	Supervised learning	Support Vector Machines (SVM).	Model for forecasting path loss in urban areas.	2014
Liu et al. (LIU 2015).	Supervised learning	Neural-Network-based approximation.	Channel Learning to deduce channel state information (CSI) that cannot be seen from a channel that can be seen.	2015
Bojovic et al. (Bojović 2016).	Supervised learning	statistical logistic regression techniques and Machine Learning.	It uses for Self-organized LTE high-density tiny cell implementation with dynamic frequency and	2016

			bandwidth distribution.	
Sarigiannidis et al (SARIGIANNIDIS 2017).	Supervised learning	Supervised Machine Learning Frameworks.	Adjust the TDD Uplink-Downlink configuration in XG-PON-LTE Systems to enhance network performance in light of current traffic circumstances in the hybrid optical-wireless network.	2017
Song et al. (SONG 2017).	Unsupervised Learning	K-means clustering, Gaussian Mixture Model (GMM), and Expectation Maximization (EM)	It uses for the selection of relay nodes in vehicular networks.	2017
Parwez et al (PARWEZ 2017).	Unsupervised Learning	Hierarchical Clustering	Wireless network anomalous, defect, and penetration testing	2017

Dilranjan et al (WICKRAMASURIYA 2017).	Supervised learning	Recurrent Neural Network (RNN)	It obtains a remarkable 98% precision.	2017
Zhang et al. (Zhang 2018).	Supervised learning	Conditional random fields (CRFs)	It Obtains a remarkable 90% precision.	2017
Juan et al. (PEREZ 2017).	Reinforcement learning	Q-Learning	aids in maintaining a steady workload	2017
Zappone et al. (ZAPPONE 2018).	Supervised learning	Artificial neural network.	Simplicity gains in computation	2018
Balevi et al. (BALEVI 2017).	Unsupervised Learning	Unsupervised Soft-Clustering Machine Learning Framework.	In heterogeneous cellular networks, latency may be reduced by using fog node clustering to automate the selection of low-power nodes (LPNs) for upgradation to high-power nodes (HPNs).	2018
Wang et al. (WANG 2018).	Unsupervised Learning	Affinity Propagation Clustering.	Resource Allocation in Highly Dense Small Cell	2018

			Networks, Based on Data.	
Balapuwaduge et al (BALAPUWADUGE 2019).	Supervised learning	Hidden Markov Model (HMM)	helps increase channel availability and dependability.	2019
Zhang et al. (ZHANG 2020).	Supervised learning	convolutional neural network (U-Net).	It boosts processing speed and network reliability.	2020

4.9. Our contribution

This work introduces machine learning approaches to efficient path loss prediction to address the issues with empirical and deterministic models in path loss prediction. Considering a multi-transmitter situation, we developed and validated Models for estimating path losses using MLP. The inputs to the machine learning algorithms change from one data set to another. The parameters we used in the outdoor environment were longitude extracted from Payload, latitude extracted from Payload, received signal strength Indicator, signal-to-noise ratio, the frequency used for transmission, spreading factor, sequence of the packet, bandwidth of transmission, the distance between the gateway and the end-device, power received at the gateway. Every parameter of the previous parameters has an affection for signal propagation. For example, the terrain causes attenuation in the signal. We used longitude and latitude to define the nature of the environment to apply the model in a similar terrain environment. The essential indoor parameters were the number of floors and walls between the gateway and the end device. These parameters enable us to test the model in a building similar to the study building. The output layer is the path loss in both environments.

4.9.1. General description of the designed system

In the MLP, neutrons are put in layers that go from the input to the output. The output of each layer node is the weighted sum of its input over a particular activation function. We create three MLPs using path loss as the input layer for the experimental path loss data gathered across fourteen base stations. Figure 2. depicts the network topology of the MLP model with two

hidden layers. We used this kind of network instead of a deep learning network because the aim was to achieve a higher computational speed which is not achieved by a deep learning network.
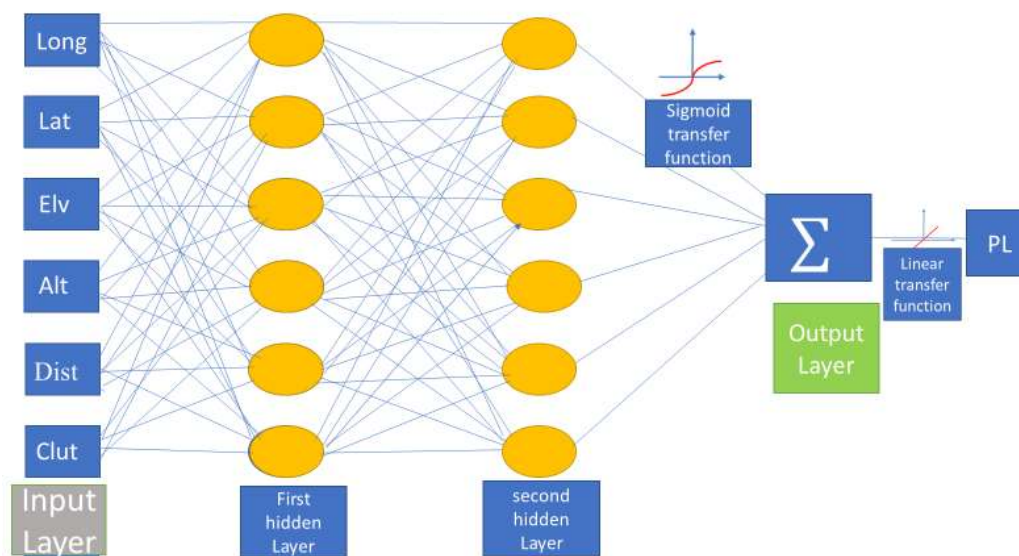

*Figure 4 .9 .*MLP network architecture (with two hidden layers) for dataset 02.

Because it can be used for nonlinear functions and produces a smooth thresholding curve for the MLP, we chose the logistic sigmoid as the activation function for this work. The standard output of the sigmoid function ranges from 0 to 1. When learning is done in an MLP by repeatedly adjusting the weights, the feed-forward approach comes first, followed by the backpropagation algorithm for excellent optimization. By including MLP weights, the training aim is to minimize the loss function. The connections are joined together after the feed-forward operation is finished. The backpropagation optimization approach is one of the essential hyperparameters for the MLP model. It starts by backpropagating to the weights of the first layer, moves on to the next iteration, and stops when the values of the weights reach a certain tolerance threshold.

4.9.2. Our training algorithm

The MLP training was carried out in a supervised manner using a backpropagation algorithm, whose objective is to adjust the weights and minimize the amount of quadrature between the network output and the target result, or the quadrature error is:

$$E(x) = \|d(n) - PL)\|^2 \tag{5.29}$$

Where d (n) is the target value, and PL is the value of the network output, the backpropagation algorithm defines the error gradient to wait for a minimum.

The error gradient E (x) is calculated for each weight as follows:

$$\frac{\partial E(n)}{\partial W_{ijk}(n)} = \frac{\partial E(n)}{\partial PL_{ik}}\frac{\partial PL_{ik}}{\partial W_{ijk}} = \frac{\partial E(n)}{\partial PL_{ik}}x_{i-1\,j} \qquad (5.30)$$

Where: i varies between 1 and 3.

K varies from 1 to 50.

X the number of inputs varies between 6 to 11 according to each dataset.

For the output layer i = L, the output error is denoted. δLket is calculated as follows:

$$\delta_{Lk} = \frac{\partial E(n)}{\partial PL_{ik}} = 2f'(PL_{Lk})(d_k - x_{Lk}) \qquad (5.31)$$

Where f (x) is the activation function.

For hidden layers, the error δ_{Lk} is given by:

$$\delta_{ik} = f'(PL_{ik}) \sum_{j=1}^{N(j+1)} \delta_{i+1\,j}\,W_{i+1\,kj} \qquad (5.32)$$

The modification of the weights W (n) and the biases b (n) is obtained by the following two equations:

$$W_{ijk}(n+1) = W_{ijk}(n) + 0.7\delta_{ik}x_{i-1\,j} + 0.6(W_{ijk}(n) - W_{ijk}(n-1)) \qquad (5.33)$$

$$b_{ik}(n+1) = b_{ik}(n) + 0.7\delta_{ik} \qquad (5.34)$$

0.7 is the learning step determining the convergence speed, and 0.6 is the momentum or inertia term that prevents the algorithm from getting stuck on a local minimum.

Our MLP results compared to Ojo et al. (OJO 2021)were way too better. They designed the model with two hidden layers while we tested three different architectures for the MLP models. However, their Radial basis function (RBF) results were excellent. Isabona et al. (ISABONA 2022)focused on developing the networks in the urban areas while we conducted our models in three different areas. Also, they experienced several training algorithms while we used the same training algorithm in all cases.
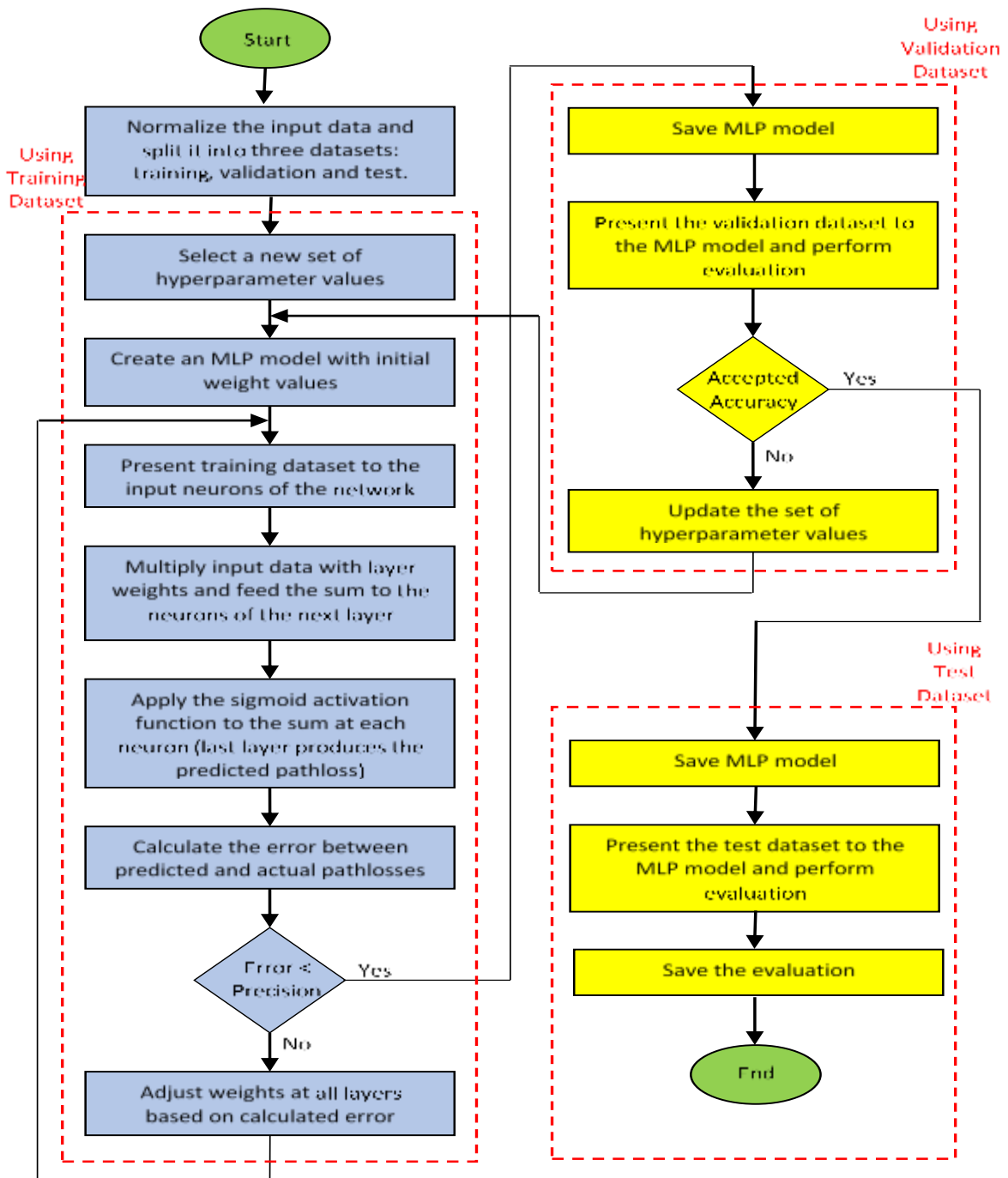
Figure 4 . 10. Flowchart for the execution of Proposed Predictive Modelling with MLP Neural Network.

4.9.3. Formatting of the database used in training and validation sets

Network learning will be done through a parallel learning model. It is necessary to build a learning base to develop network learning. Since the learning is supervised, this base must contain the network input and the desired output. To respond to the neural inputs and make the neural network training more efficient, the databases must go through a preprocessing step (Fig.4.11). Processing is a typical technique to remove spurious discontinuities in the input

function space and reduce the question inputs to manageable data. This is followed by appropriate normalization, taking into account the magnitude of the acceptable network values.
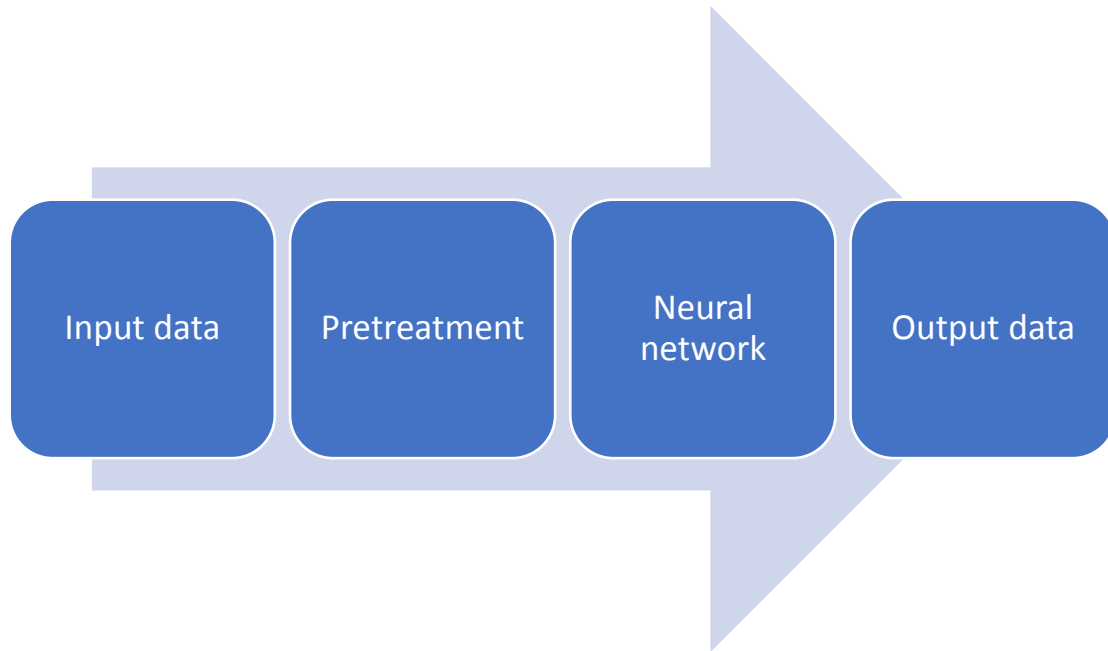
Figure 4 . 11. Database preprocessing phase.

4.9.4. Data collection procedure

Table 4.4. and Table 4.5. summarize the description and parameters of each dataset**.**

Table 4. 4. Description of each dataset

Dataset	Description
1	Smart campus environment within Covenant University, Ota, Ogun State,
2	Nigeria (S. A. POPOOLA 2018)
3	The urban environment in the city of Fortaleza-CE, Brazil (Timoteo 2014)
4	Indoor building in USJ-ESIB Campus in Beirut (ElChall 2019)
5	Outdoor around the USJ campus using three antennas heights (ElChall 2019)
6	Drive tests in Bekaa valley (ElChall 2019)
7	Drive tests in Beirut city (ElChall 2019)
8	ms=1.5 m in Bekaa valley (ElChall 2019)
9	ms=3 m in Bekaa valley (ElChall 2019)
10	ms=20 cm in Bekaa valley (ElChall 2019)
11	ms=1 m in Beirut city (ElChall 2019)
12	ms=1.5 m in Beirut city (ElChall 2019)
13	ms=3 m in Beirut city (ElChall 2019)
14	ms=20 cm in Beirut city (ElChall 2019)

Table 4. 5. Parameters of each dataset

Dataset	Parameters
1	Elv, Alt, Dist, Clut
2	Long, Lat, Elv, Alt, Dist, Clut
3	Long, Lat, Ter Elv, Dist, Hor Ang, Ver Ang, Hor Atn, Ver Atn
4	Long, Lat, RSSI, SNR, Freq, Floor, Wall, Dist, Prx
5-14	Long, Lat, RSSI, SNR, Freq, SF, Seq, BW, Dist, Prx

Definition of parameters:

BW: bandwidth of transmission

Dist: distance between the gateway and the end-device

Floor: number of floors between gateway and end-device

Freq: frequency used for transmission

Lat: latitude extracted from Payload

Long: longitude extracted from Payload

Prx: power received at the gateway

RSSI: received signal strength Indicator

Seq: sequence of the packet

SF: spreading factor

SNR: signal-to-noise ratio

Wall: number of walls between gateway and end-device

4.9.5. MLP Network Learning

Fourteen databases were used to optimize neuronal structures, which are composed of different numbers of samples. These databases are further subdivided into a training set and a test set. The training databases are composed of (60%), the test databases are composed of (20%) items that are reserved for the final performance measurement, and the validation databases of (20%) examples. The test, validation, and training samples must be different and be randomly selected from the original database.

The optimization process (learning, validation, and testing) was performed for N iterations for which error stabilization was obtained. The numbers of neurons in the first, second and third layers were changed, and the associated optimization error was recorded. In this study, the backpropagation algorithm was used. It is important to note that the end of the program can be caused by the following:

- The MSE Mean Squared Error is the average squared difference between the estimated and actual values (ALLEN 1971)and must be less than the minimum error.

- The maximum number of iterations N is reached.

4.10. Conclusion

In this chapter, we started with the history of neural networks and then gave an analogy between formal and biological neurons. The different activation functions and architectures of neural networks were given, and the two types of learning, supervised and unsupervised, were discussed. Moreover, we finished with our scientific contribution the execution of Proposed Predictive Modelling with MLP Neural Network.

Chapter 5 :
Simulations results and discussions

5.1. Introduction

Due to the ability to quickly get radio coverage statistics for network planning, empirical propagation models have been a tool for radio performance analysis in research and industry. Empirical models, unlike deterministic models, do not employ topographical data, which takes more time and resources to process. However, field measurement data must be used to validate the simulation results when employing empirical models to simulate radio wave propagation. Radio waves' propagation may occur in various environments, both complicated and simple, all of which can impact the reception of radio signals. It makes computer simulation and propagation models critical network planning tools for reducing the uncertainties associated with received signal intensity dropping below the minimum acceptable receiver threshold. Empirical propagation models have been used in research (Sizun 2005) to analyze the propagation performance of various wireless communication devices at specific frequencies.

Modeling based on artificial intelligence techniques, which constitutes the bulk of this chapter, does not, in principle, use any simplifying assumptions. So, this modeling makes it possible to provide practical solutions (lower precision and computation time).

In this chapter, we present the applicability of artificial neural networks (ANN) for modeling mobile networks' trajectory losses.

The exciting characteristics of MLP can justify this choice:

- MLP is of the Feed-Forward type; in our study framework, the Feed-Forward type seems the best choice since a layer can only use the outputs of the previous layers.
- Supervised learning: the association of an input configuration with an output configuration, a requirement on which our project is based.

We have divided this chapter into two main parts:

- In the first part, we presented our simulation parameters for empirical propagation models, the obtained results in different environments, and the analysis of the simulation results.

- The second part is organized as follows: Section 1 describes the selected neural network topologies and details of database processing. Section 2 presents the results obtained for loss prediction as a network training function for 14 different datasets with three different architectures for MLP networks. Section 3 compares the different neural network architectures. Finally, Section 4 compares the results of the MLP network and the empirical propagation models.

5.2. Simulations and analysis of empirical propagation models for mobile networks

Using the MATLAB tool, we conducted many simulations at (800MHz,1900MHz,3.5GHz, and 5.8GHz) with three different mobile station antenna heights (3,6, and 10 m). The following table summarizes the parameters and the values of each parameter:

Table 5. 1. Parameter values for the simulations.

Parameters	Values
Base station transmitter power	43 dBm
Mobile transmitter power	30 dBm
Transmitter antenna height	30 m in urban and suburban and 20 m in a rural area
Receiver antenna height	3 m, 6 m, and 10 m
Operating frequency	800 MHz,1900MHz,3.5GHz, and 5.8GHz
Distance between Tx-Rx	0.1km - 4.5 km
Building to building distance	40 m
Average building height	12 m
Street width	25 m
Street orientation angle	30 degrees in urban and 40 degrees in suburban
Correction for shadowing	8.2 dB in suburban and rural and10.6 dB in an urban area

The equations that we used to calculate path loss for each model in the MATLAB simulation in the three environments are as below:

- For Walfisch-Ikegami (WI) model (D. W. HAR 1999) :

$L_{\text{wi model}} = L_{fs} + L_{rts} + L_{msd}$ For an urban and suburban environment

$$L_{msd} = -18\log_{10}(1+H_{base})+54+18\log_{10}(d)+ \\ \left(-4+1.5\left(\left(\frac{f}{925}\right)-1\right)\right)\log_{10}(f)-9\log_{10}(B) \tag{5.1}$$

$$L_{fs} = 32.45+20\log_{10}(d)+20.\log_{10}(f) \tag{5.2}$$

$$L_{rts} = -16.9-10\log_{10}(w)+10\log_{10}(f)+20\log_{10}(H_{mobile})+L_{ori} \tag{5.3}$$

$L_{ori} = -10+0.354\theta$ for the urban environment   (5.4)

$L_{ori} = 2.5+0.075(\theta-35)$ for the suburban environment   (5.5)

we consider the Line of sight equation for a rural environment

$$PL_{\text{wi model}} = 42.6 + 26\log_{10}(d) + 20\log_{10}(f) \quad \text{for a rural environment} \tag{5.6}$$

- For ECC-33 or extended Hata-Okumura model (C. P. DALELA 2012):

$$PL = A_{fs} + A_{bm} - G_b - G_r \qquad \text{for an urban and suburban environment}$$

$$A_{fs} = 92.4 + 20\log_{10}(d) + 20\log_{10}(f) \tag{5.7}$$

$$A_{bm} = 20.41 + 9.83\log_{10}(d) + 7.894\log_{10}(f) + 9.56 \times 2\log_{10}(f) \tag{5.8}$$

$$G_r = x \times y \tag{5.9}$$

$$x = 42.57 + 13.7\log_{10}(f) \tag{5.10}$$

$$y = \log_{10}(h_r) - 0.585 \tag{5.11}$$

$$G_b = c \times (b + a) \tag{5.12}$$

$$a = \begin{bmatrix} 3 & \text{for urban environment} \\ 5.8 \times 2 \times \log_{10}(d) & \text{for suburban environment} \end{bmatrix} \tag{5.13}$$

$$b = \begin{bmatrix} 0.005 & \text{for urban environment} \\ 13.958 & \text{for suburban environment} \end{bmatrix} \tag{5.14}$$

$$c = \begin{bmatrix} 20 & \text{for urban environment} \\ \log_{10}\left(\dfrac{h_b}{200}\right) & \text{for suburban environment} \end{bmatrix} \tag{5.15}$$

ECC-33, or the extended Hata-Okumura model, is not applicable in a rural area

- For the COST 231-Hata model (C. P. DALELA 2012):

$$PL_{\text{costhata model}} = 46.3 + 33.9\log_{10}(f) - 13.82\log_{10}(h_b) - a_{hm}$$
$$+ \left(44.9 - 6.55\log_{10}(h_b)\right)\log_{10}(d) + c_m \tag{5.16}$$

$$a_{hm} = \begin{bmatrix} 3.20 \times (\log_{10}(11.75 \times h_r))^2 - 4.97 \\ (1.11 \times \log_{10}(f) - 0.7) \times h_r - (1.5 \times \log_{10}(f) - 0.8) \end{bmatrix} \tag{5.17}$$

$$c_m = \begin{bmatrix} 3dB & \text{in urban environment} \\ 0dB & \text{in suburban and rural environments} \end{bmatrix} \tag{5.18}$$

- For Stanford University Interim (SUI) model (JENG, Coverage probability analysis of IEEE 802.16 system with smart antenna system over stanford university interim fading channels 2010):

$$PL_{\text{suidelmodel}} = 20\log_{10}(\frac{4 \times \Pi \times d_0}{\lambda}) + (10 \times \gamma \times \log_{10}(\frac{d}{d_0})) +$$
$$6\log_{10}(\frac{f}{2000}) - 20\log_{10}(\frac{h_r}{2000}) + s \tag{5.19}$$

$$\lambda = \frac{3 \times 10^8}{f} \tag{5.20}$$

$$\gamma = a - (b \times h_b) + \frac{c}{h_b} \tag{5.21}$$

$$a = \begin{bmatrix} 3.6 & \text{for urban and rural environments} \\ 4 & \text{for suburban environment} \end{bmatrix} \tag{5.22}$$

$$b = \begin{bmatrix} 0.005 & \text{for urban and rural environments} \\ 0.0065 & \text{for suburban environment} \end{bmatrix} \tag{5.23}$$

$$c = \begin{bmatrix} 20 & \text{for urban and rural environments} \\ 17.1 & \text{for suburban environment} \end{bmatrix} \tag{5.24}$$

$$s = \begin{bmatrix} 10.6 & \text{for urban environment} \\ 8.2 & \text{for suburban and rural environment} \end{bmatrix} \tag{5.25}$$

$$d_0 = 100m \tag{5.26}$$

- For Ericson model (H. K.-M. HOOMOD 2018):

$$PL_{ericson\,model} = 36.2 + 30.2\log_{10}(d) - 12\log_{10}(h_b) + 0.1\log_{10}(h_b)\log_{10}(d)$$
$$-6.4\log_{10}(11.75 \times h_r) + g(f) \quad \text{for the three environments} \tag{5.27}$$

$$g(f) = 44.49\log_{10}(f) - 4.78\left(\log_{10}(f)\right)^2 \tag{5.28}$$

Table 5. 2. Variables of the equations

Parameter	Description
H_{base}, h_b	antenna height of the base station, the height of the roof
H_{mobile}, h_r	height of the roof- antenna height of the mobile station
d	distance between the transmitter and the receiver
f	frequency of signal propagation
B	distance between buildings
W	street width
θ	street orientation angel 30 degree
s	fading standard deviation

5.2.1. Empirical models in the urban areas

In our experiment, we set 3 different antenna heights (i.e., 3 m, 6 m, and 10 m) for the receiver. The distance varies from 100 m to 4.5 km, and the transmitter antenna height is 30 m with frequencies (800MHz,1900MHz,3.5GHz, and 5.8GHz). The numerical results for the six different models in the urban environment are shown in Figure 5.1. - 5.12.
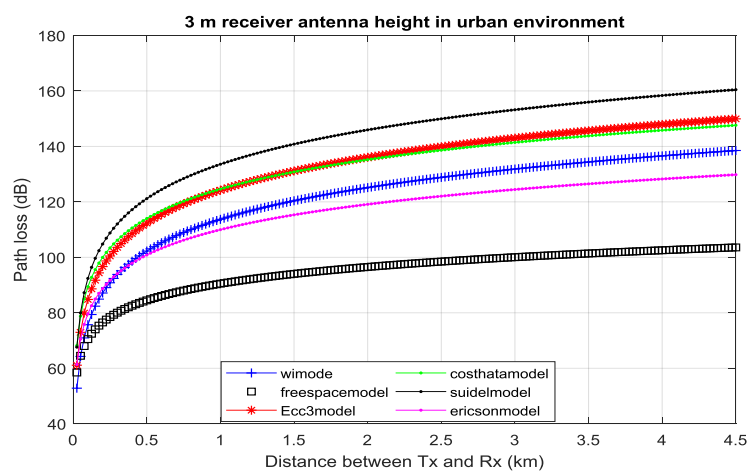
Figure 5. 1. Path loss in an urban environment at hm=3m and 800 MHz
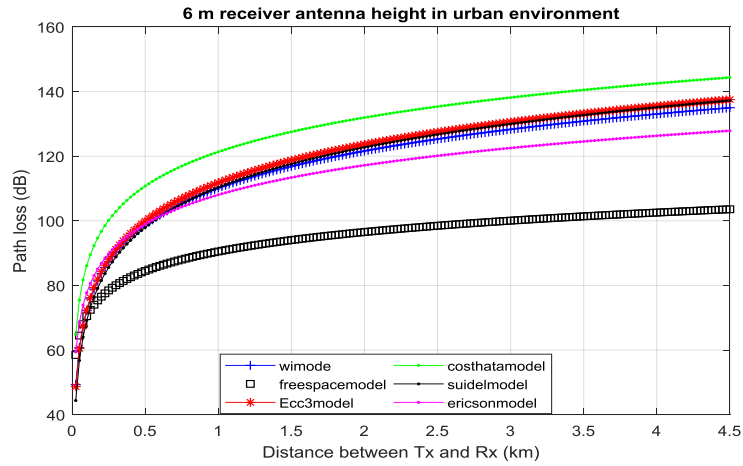
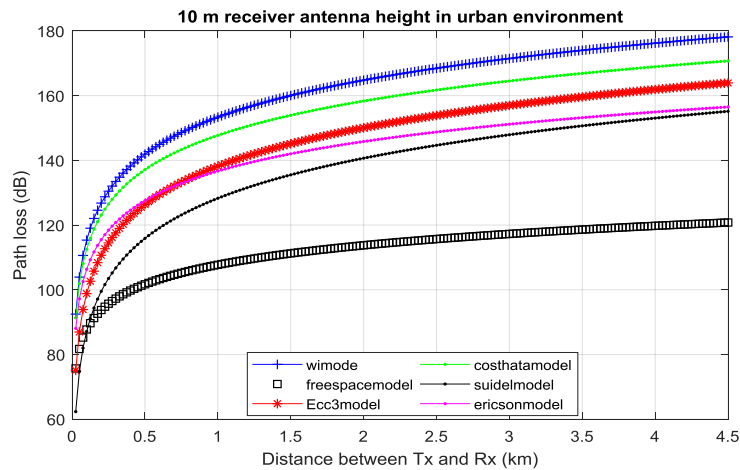**Figure 5. 2.** Path loss in an urban environment at hm=6m and 800 MHz
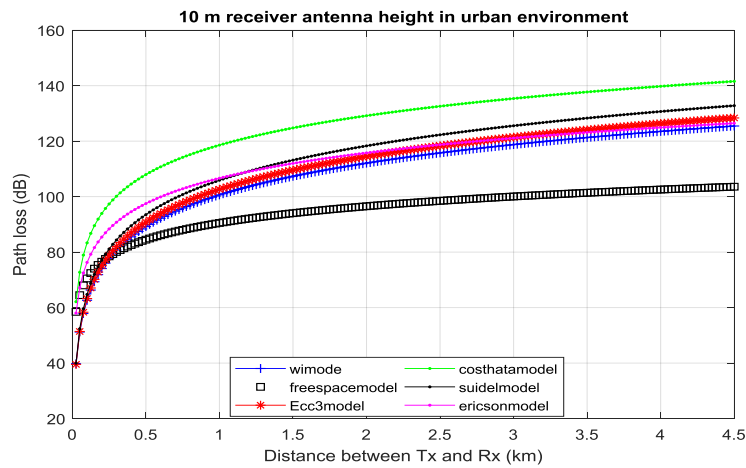
Figure 5. 3. Path loss in an urban environment at hm=10m and 800 MHz
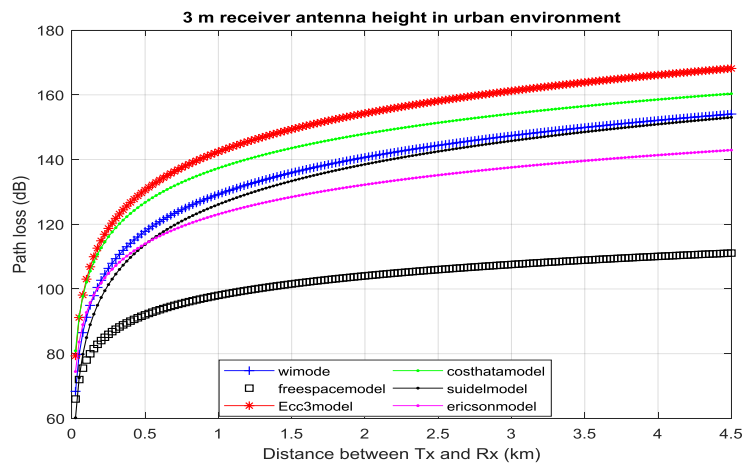
Figure 5. 4. Path loss in an urban environment at hm=3m and 1900 MHz
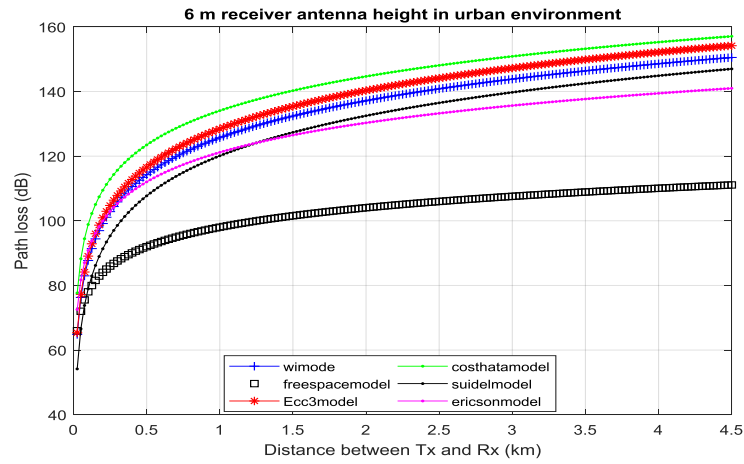
Figure 5. 5. Path loss in an urban environment at hm=6m and 1900 MHz
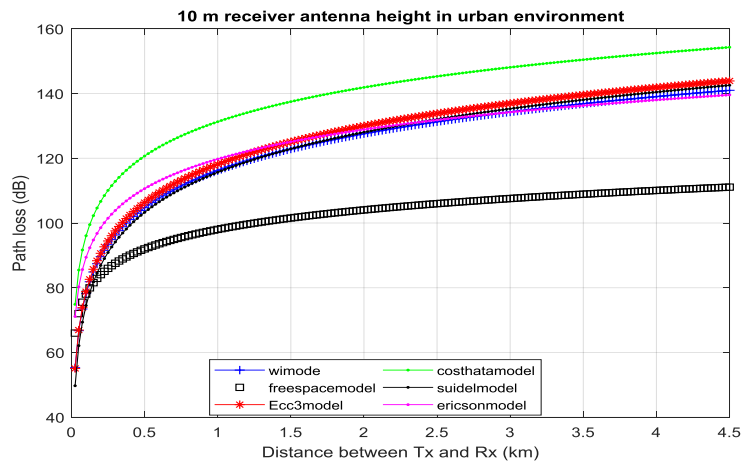
Figure 5. 6. Path loss in an urban environment at hm=10m and 1900 MHz
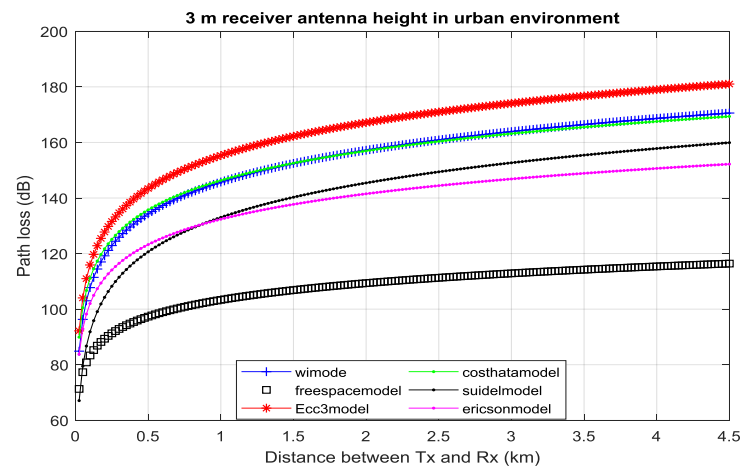
Figure 5. 7. Path loss in an urban environment at hm=3m and 3.5 GHz
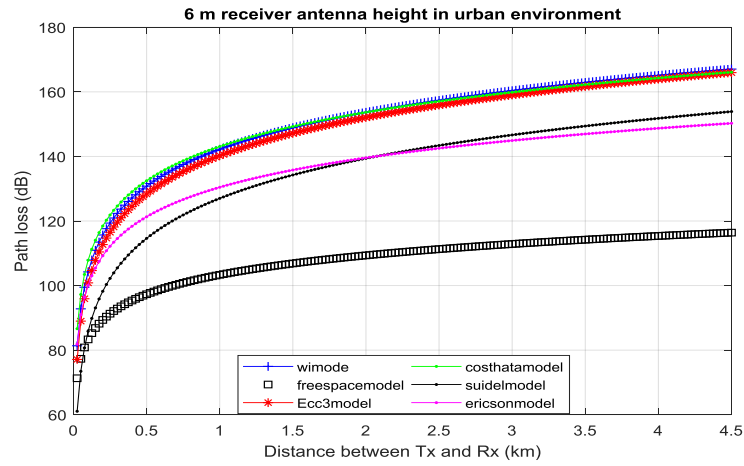
Figure 5. 8. Path loss in an urban environment at hm=6m and 3.5 GHz
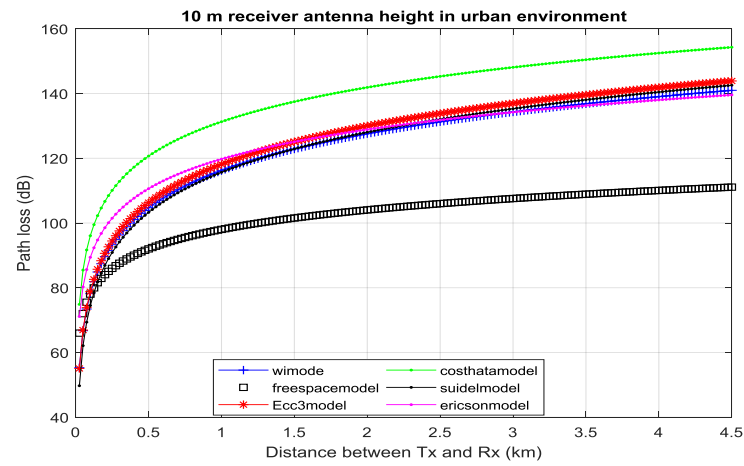
Figure 5. 9. Path loss in an urban environment at hm=10m and 3.5 GHz
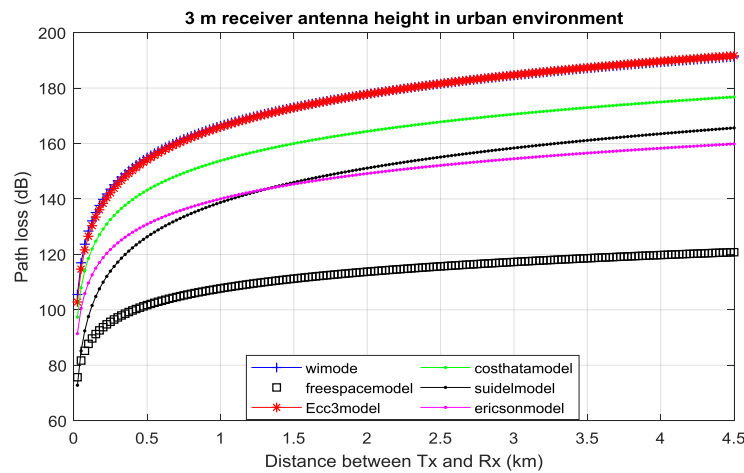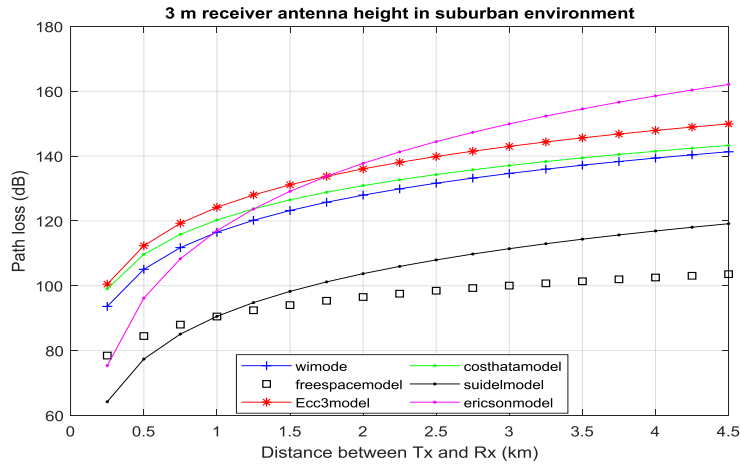

Figure 5. 10. Path loss in an urban environment at hm=3m and 5.8 GHz
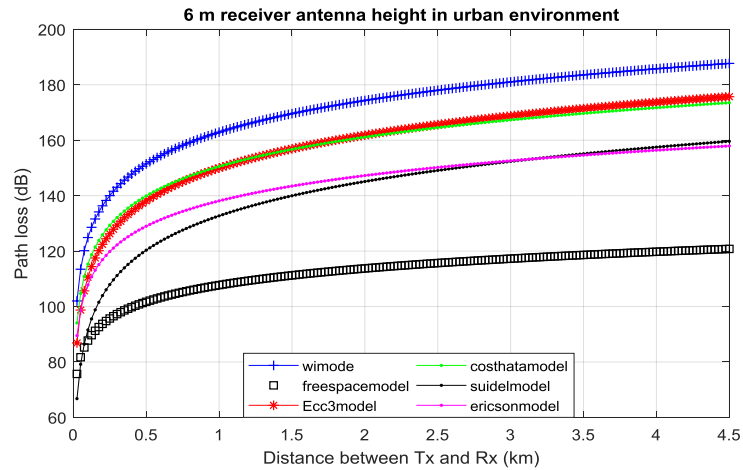
Figure 5. 11. Path loss in an urban environment at hm=6m and 5.8 GHz

Figure 5. 12. Path loss in an urban environment at hm=10m and 5.8 GHz

Table. 5.3. summarized the path loss data in an urban environment. The path loss varies according to the changes in receiver antenna height and frequency value.

Table 5. 3. Path loss estimate in an urban environment

The frequency=800MHz	Path loss min			Path loss max		
Models	h_m=3m	h_m=6m	h_m=10m	h_m=3m	h_m=6m	h_m=10m
Walfish Ikegami model	52.82	49.30	39.75	138.52	135.06	125.45
Free space model	58.47	58.47	58.47	103.57	103.57	103.57
Hata extended model	61.10	48.68	39.53	149.90	137.51	128.36
Cost231 Hata model	68.17	64.90	62.12	147.62	144.34	141.56
Stanford university model	67.61	44.38	39.95	160.45	134.23	132.79
Ericson model	61.35	59.43	58.01	129.80	127.87	126.45
The frequency=1900MHz	Path loss min			Path loss max		
Models	h_m=3m	h_m=6m	h_m=10m	h_m=3m	h_m=6m	h_m=10m
Walfish Ikegami model	68.36	64.83	55.29	154.06	150.54	140.99
Free space model	65.98	65.98	65.98	111.08	111.08	111.08
Hata extended model	79.31	65.35	55.06	168.14	154.18	143.89

Models	h_m=3m	h_m=6m	h_m=10m	h_m=3m	h_m=6m	h_m=10m
Cost231 Hata model	80.91	77.64	74.86	160.35	157.08	154.30
Stanford university model	60.17	54.15	49.71	153.01	146.99	142.56
Ericson model	74.48	72.55	71.13	142.92	140.99	139.57
The frequency=3.5GHz	**Path loss min**			**Path loss max**		
Models	**h_m=3m**	**h_m=6m**	**h_m=10m**	**h_m=3m**	**h_m=6m**	**h_m=10m**
Walfish Ikegami model	84.87	81.35	55.29	170.57	167.05	140.99
Free space model	71.29	71.29	71.29	116.39	116.39	116.39
Hata extended model	92.18	77.12	55.06	181.01	165.95	143.89
Cost231 Hata model	89.90	86.63	74.86	169.34	166.07	154.30
Stanford university model	67.07	61.05	49.71	159.91	153.89	142.56
Ericson model	83.74	81.82	71.13	152.19	150.26	139.57
The frequency=5.8GHz	**Path loss min**			**Path loss max**		
Models	**h_m=3m**	**h_m=6m**	**h_m=10m**	**h_m=3m**	**h_m=6m**	**h_m=10m**
Walfish Ikegami model	105.53	102	92.46	191.23	187.70	178.16
Free space model	75.67	75.67	75.67	120.78	120.78	120.78
Hata extended model	102.82	86.85	75.09	191.65	175.68	163.92
Cost231 Hata model	97.34	94.07	91.29	176.78	173.51	170.73
Stanford university model	72.78	66.75	62.32	165.62	159.59	155.16
Ericson model	91.41	89.48	88.06	159.85	157.92	156.50

We note in Table 5.2. that the path loss increases with the increase of the value of frequency and distance. Moreover, it decreases with the increase in the height of the mobile station antenna. The free space model changes according to the value of frequency, and it does not consider the variation of the mobile station antenna height, and it showed the lowest value of path loss in all frequencies. Hata extended (ECC3) model showed the highest path loss at the frequencies (1900MHz, 3.5 GHz, and 5.8 GHz). Stanford university model showed the highest path loss at the frequency of 800 MHz.

5.2.2. Empirical models in suburban areas

The transmitter and receiver antenna heights are the same as used earlier. The numerical results for different models in a suburban area for different receiver antenna heights are shown in Figures 5.13 – 5.24.

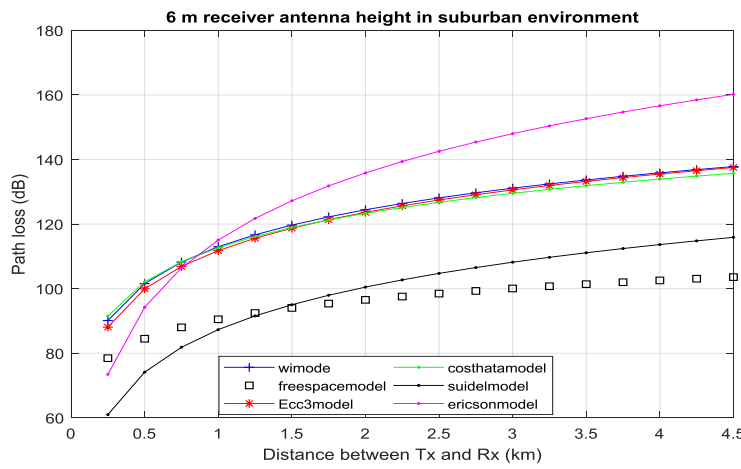**Figure 5. 13.** Path loss in a suburban environment at hm=3m and 800 MHz

Figure 5. 14. Path loss in a suburban environment at hm=6m and 800 MHz
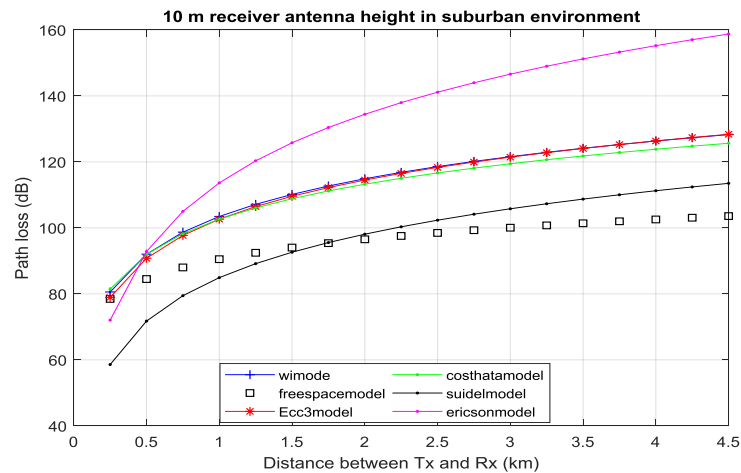

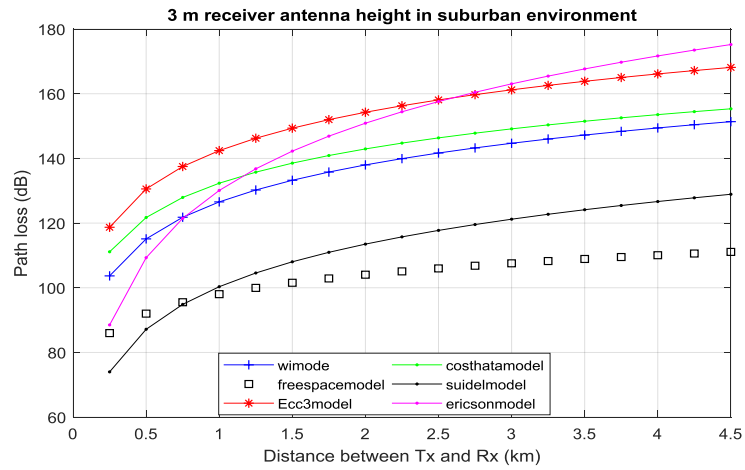**Figure 5. 15.** Path loss in a suburban environment at hm=10m and 800 MHz.

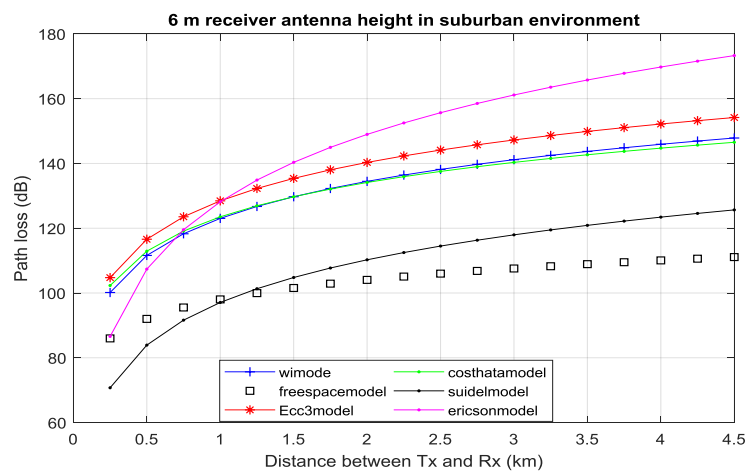**Figure 5. 16.** Path loss in a suburban environment at hm=3m and 1900 MHz.

Figure 5. 17. Path loss in a suburban environment at hm=6m and 1900 MHz.
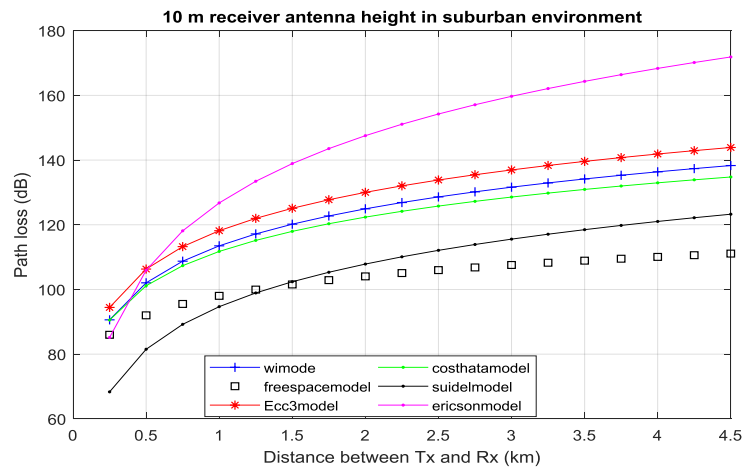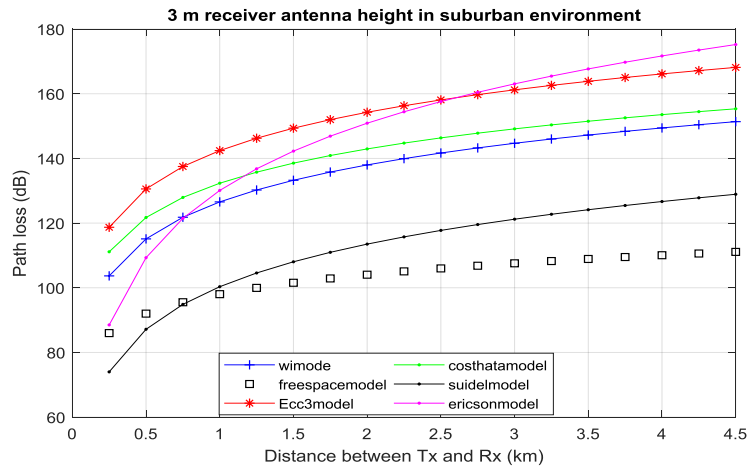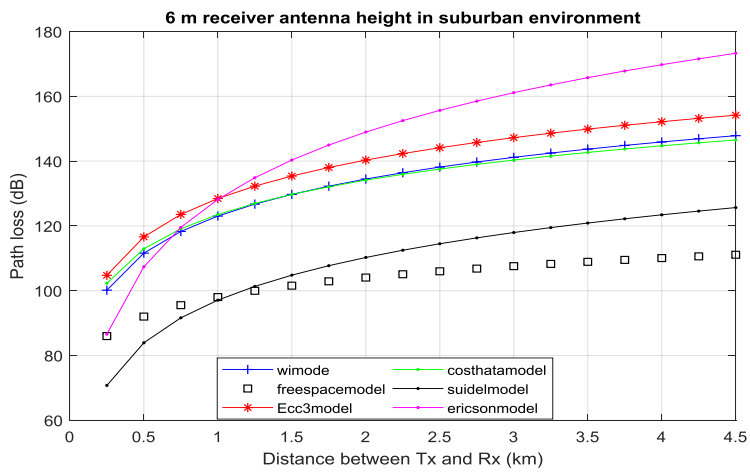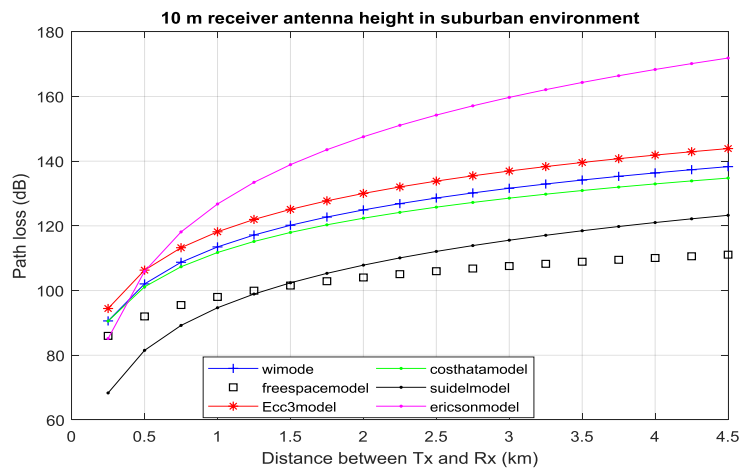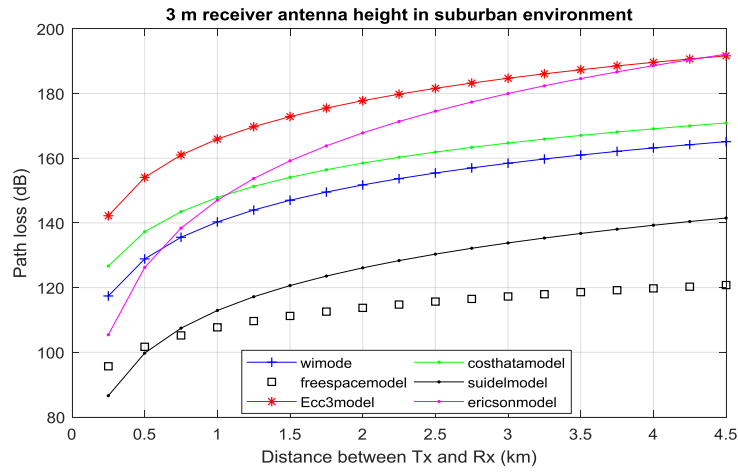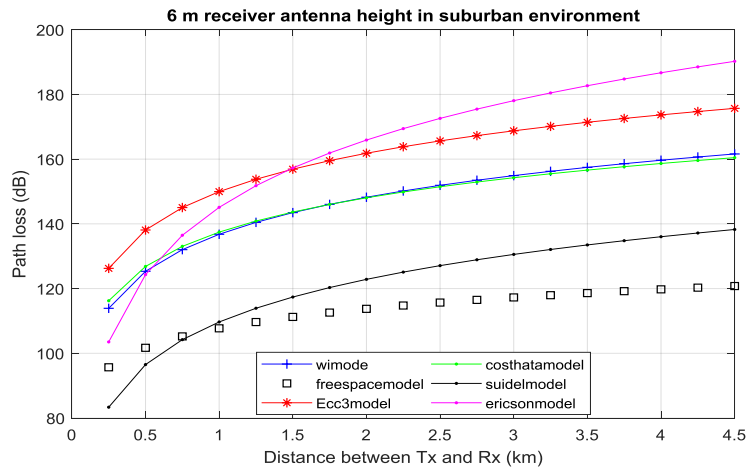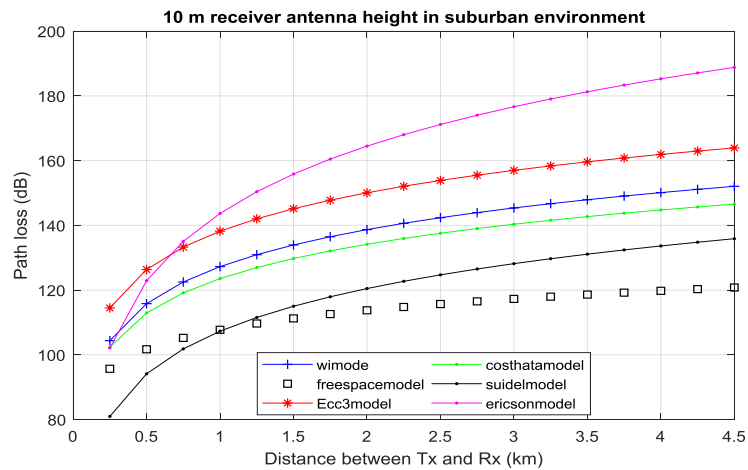

Figure 5. 18. Path loss in a suburban environment at hm=10m and 1900 MHz.

Figure 5. 19. Path loss in a suburban environment at hm=3m and 3.5 GHz.

Figure 5. 20. Path loss in a suburban environment at hm=6m and 3.5 GHz.

Figure 5. 21. Path loss in a suburban environment at hm=10m and 3.5 GHz.

3 m receiver antenna height in suburban environment

Figure 5. 22. Path loss in a suburban environment at hm=3m and 5.8 GHz.

6 m receiver antenna height in suburban environment

Figure 5. 23. Path loss in a suburban environment at hm=6m and 5.8 GHz

10 m receiver antenna height in suburban environment

Figure 5. 24. Path loss in a suburban environment at hm=10m and 5.8 GHz.

Table. 5.4. summarized the path loss data in the suburban environment. The path loss varies according to the changes in receiver antenna height and frequency value.

Table 5. 4. Path loss estimate in a suburban environment

The frequency=800MHz	Path loss min			Path loss max		
Models	h_m=3m	h_m=6m	h_m=10m	h_m=3m	h_m=6m	h_m=10m
Walfish Ikegami model	93.63	90.11	80.57	141.33	187.81	128.27
Free space model	78.47	78.47	78.47	103.57	103.57	103.57
Hata extended model	100.48	88.07	78.92	149.93	137.51	128.36
Cost231 Hata model	99.08	91.51	81.42	143.29	135.73	125.64
Stanford university model	64.22	60.97	58.57	119.14	115.89	113.49
Ericson model	75.38	73.46	72.04	162.01	160.17	158.75
The frequency=1900MHz	Path loss min			Path loss max		
Models	h_m=3m	h_m=6m	h_m=10m	h_m=3m	h_m=6m	h_m=10m
Walfish Ikegami model	103.67	100.15	90.61	151.37	147.85	138.31
Free space model	85.98	85.98	85.98	111.08	111.08	111.08
Hata extended model	118.70	104.74	94.45	168.14	154.18	143.89
Cost231 Hata model	111.12	102.31	90.55	155.34	146.52	134.76
Stanford university model	73.99	70.74	68.34	128.90	125.65	125.26
Ericson model	88.51	86.85	85.16	175.22	173.29	171.87
The frequency=3.5GHz	Path loss min			Path loss max		
Models	h_m=3m	h_m=6m	h_m=10m	h_m=3m	h_m=6m	h_m=10m
Walfish Ikegami model	111.02	107.49	97.95	158.72	155.20	145.65
Free space model	91.29	91.29	91.29	116.39	116.39	116.39
Hata extended model	131.57	116.51	105.41	181.01	165.95	154.81
Cost231 Hata model	119.63	109.93	96.99	163.85	154.15	141.21
Stanford university model	80.88	72.33	75.24	135.80	127.25	130.16
Ericson model	97.77	95.85	94.43	184.84	182.56	181.43

The frequency=5.8GHz	Path loss min			Path loss max		
Models	**h_m=3m**	**h_m=6m**	**h_m=10m**	**h_m=3m**	**h_m=6m**	**h_m=10m**
Walfish Ikegami model	105.41	113.90	104.35	154.85	161.60	152.05
Free space model	95.67	95.67	95.67	120.78	120.78	120.78
Hata extended model	105.41	126.24	114.48	156.65	175.68	163.92
Cost231 Hata model	96.99	116.23	102.33	142.82	160.45	146.54
Stanford university model	75.24	83.34	80.94	132.16	138.25	135.86
Ericson model	94.43	103.51	102.09	184.30	190.22	188.80

Table 5.4 shows that the path loss in the free space model is increasing according to the increase of the frequency value, and it does not consider the variation of the mobile station antenna height. It showed the lowest path loss value at all frequencies in the suburban environment. Table 5.4. shows the highest value at 6m mobile station antenna heights for the six models at frequencies (800 MHz, 1900 MHz, 3.5 GHz, and 5.8 GHz). The highest value of path loss changes according to mobile station antenna height and frequencies. For example, at the frequency 800 MHz, the Ericson model obtained the highest value at a 3m mobile station antenna height, and the Walfish Ikegami model obtained the highest value at a 6m mobile station antenna height.

5.2.3   Empirical models in the rural areas

The mobile station antenna heights are the same as those used earlier. Here we considered 20 m for the base station antenna height. The extended Hata-Okumura (ECC-33) model is not valid in rural areas and the COST 231 W-I model has no specific parameters for rural areas, we consider the LOS equation provided by this model. The numerical results for different models in rural areas are presented in Figures. 5.25-5.36.
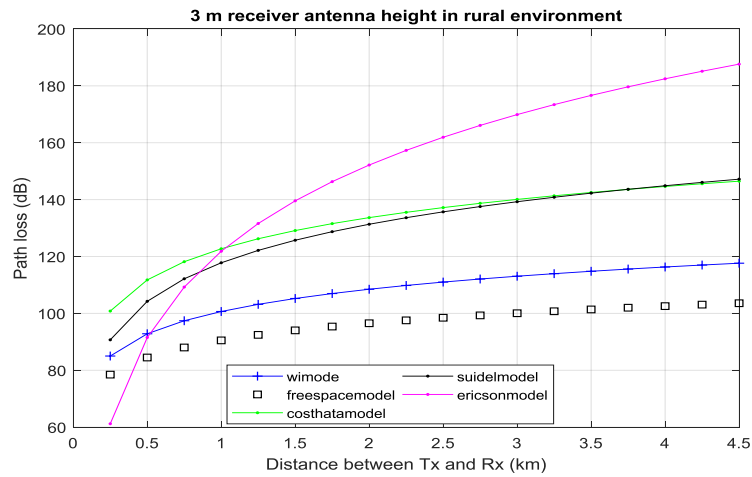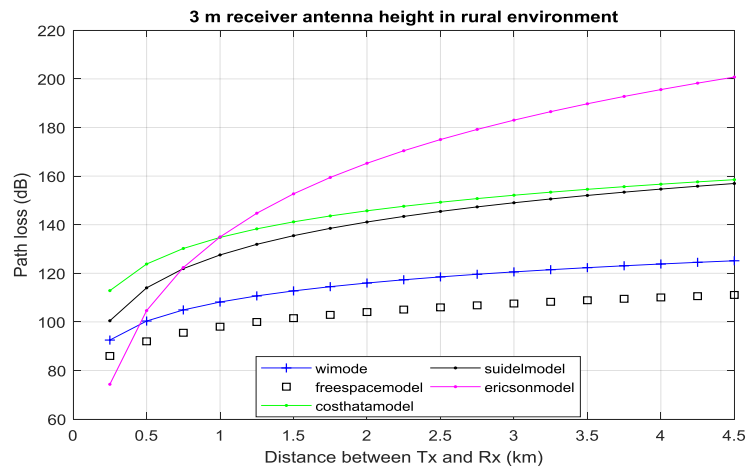
Figure 5. 25. Path loss in a rural environment at hm=3m and 800 MHz
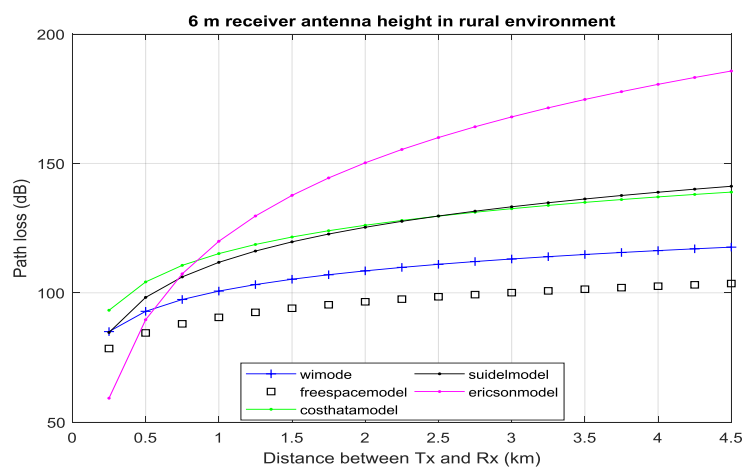
Figure 5. 26. Path loss in a rural environment at hm=6m and 800 MHz
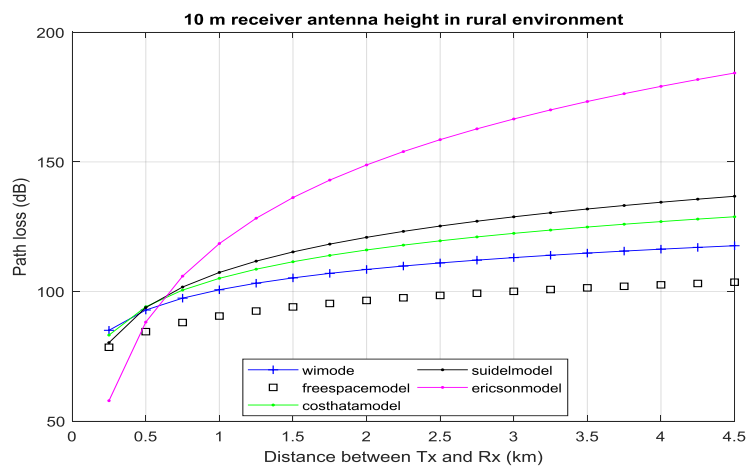
Figure 5. 27. Path loss in a rural environment at hm=10m and 800 MHz

Figure 5. 28. Path loss in a rural environment at hm=3m and 1900 MHz

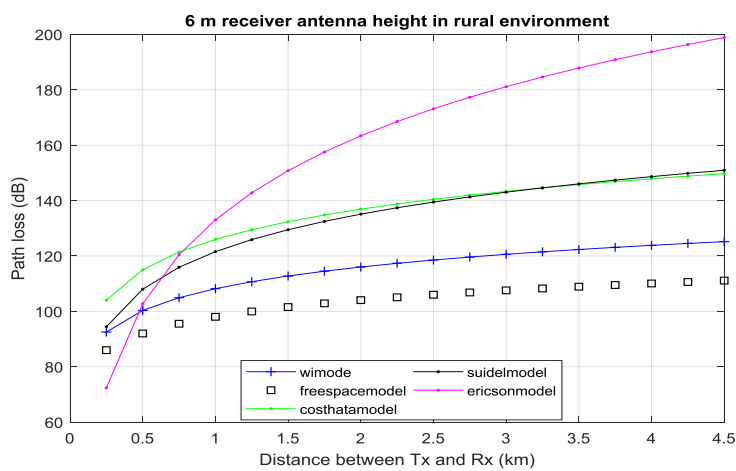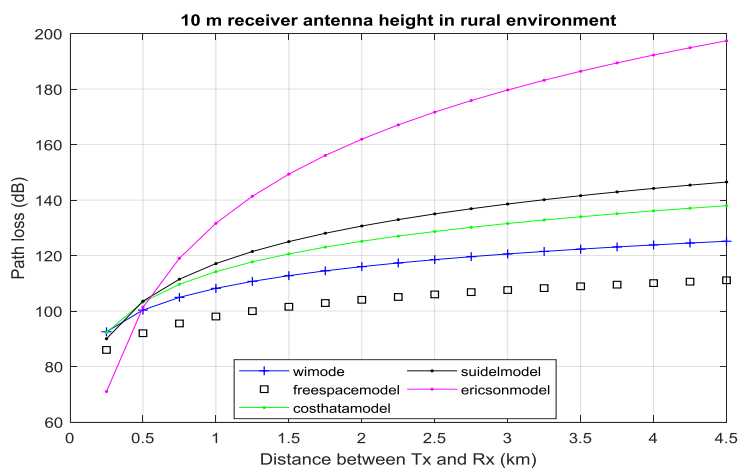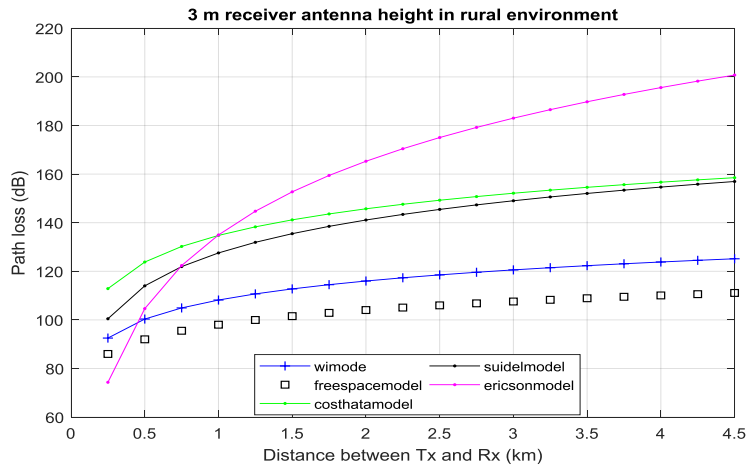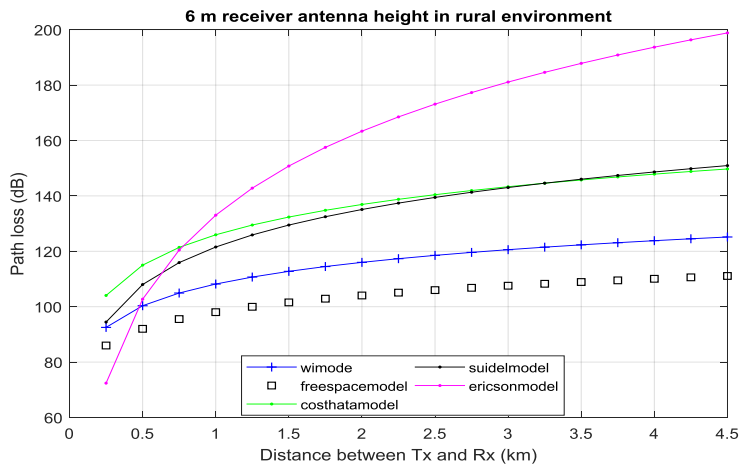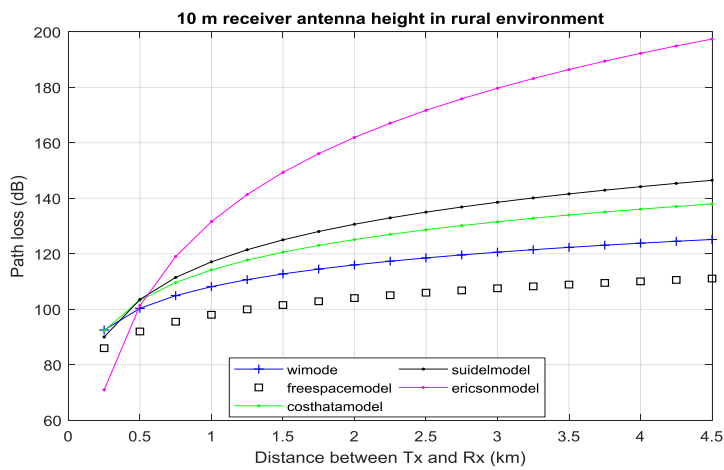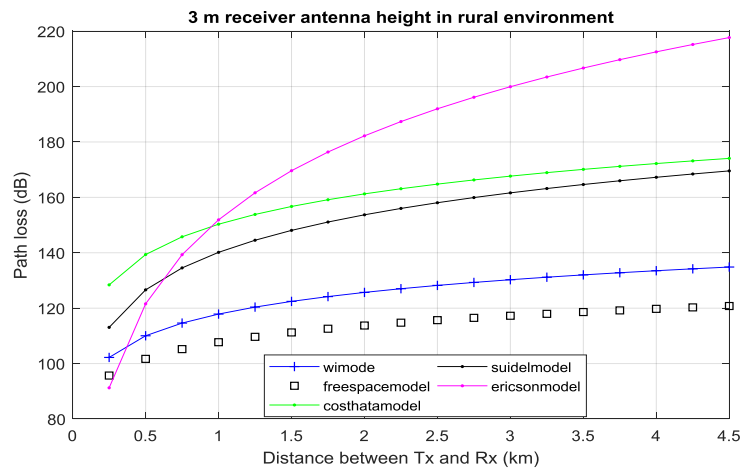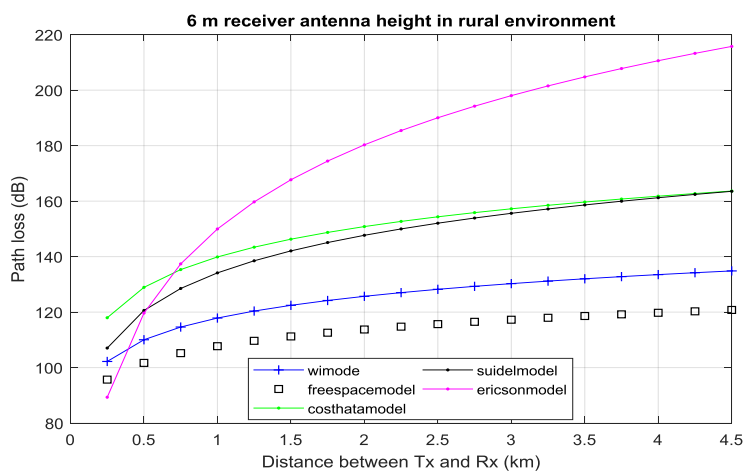**Figure 5. 29.** Path loss in a rural environment at hm=6m and 1900 MHz

Figure 5. 30. Path loss in a rural environment at hm=10m and 1900 MHz

87

Figure 5. 31. Path loss in a rural environment at hm=3m and 3.5 GHz

Figure 5. 32. Path loss in a rural environment at hm=6m and 3.5 GHz

Figure 5. 33. Path loss in a rural environment at hm=10m and 3.5 GHz

Figure 5. 34. Path loss in a rural environment at hm=3m and 5.8 GHz

Figure 5. 35. Path loss in a rural environment at hm=6m and 5.8 GHz
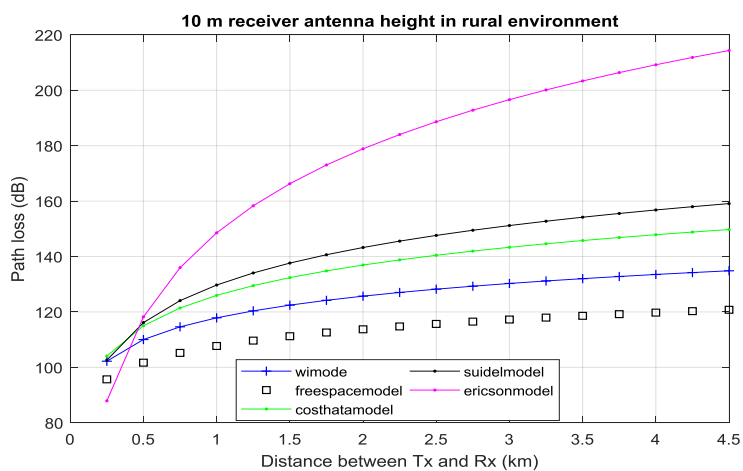
Figure 5. 36. Path loss in a rural environment at hm=10m and 5.8 GHz

Table. 5.5. summarized the path loss data in the rural environment. The path loss varies according to the changes in receiver antenna height and frequency value.

Table 5. 5. Path loss estimate in a rural environment

The frequency=800MHz	Path loss min			Path loss max		
Models	h_m=3 m	h_m=6m	h_m=10m	h_m=3 m	h_m=6m	h_m=10 m
Walfish Ikegami model	85.00	85.00	85.00	117.64	117.64	117.64
Free space model	78.47	78.47	78.47	103.57	103.57	103.57
Cost231 Hata model	100.82	93.25	83.16	146.48	138.91	128.82
Stanford university model	90.70	84.68	80.24	147.18	14.16	136.73
Ericson model	61.19	59.26	57.84	187.63	185.71	184.29
The frequency=1900MHz	Path loss min			Path loss max		
Models	h_m=3 m	h_m=6m	h_m=10m	h_m=3 m	h_m=6m	h_m=10 m
Walfish Ikegami model	92.52	92.52	92.52	125.15	125.15	125.15
Free space model	85.98	85.98	85.98	111.08	111.08	111.08
Cost231 Hata model	112.86	104.04	92.29	158.53	149.71	137.95
Stanford university model	100.46	94.44	90.01	156.95	150.93	146.49
Ericson model	74.31	72.39	70.97	200.76	198.83	197.41
The frequency=3.5GHz	Path loss min			Path loss max		
Models	h_m=3 m	h_m=6m	h_m=10m	h_m=3 m	h_m=6m	h_m=10 m
Walfish Ikegami model	97.82	97.82	97.82	130.46	130.46	130.46
Free space model	91.29	91.29	91.29	116.39	116.39	116.39
Cost231 Hata model	121.37	111.67	98.73	167.04	157.33	144.40
Stanford university model	102.06	96.03	91.60	158.54	152.52	148.09
Ericson model	83.58	81.65	80.23	210.02	208.10	206.68
The frequency=5.8GHz	Path loss min			Path loss max		

Models	h_m=3 m	h_m=6m	h_m=10m	h_m=3 m	h_m=6m	h_m=10 m
Walfish Ikegami model	102.21	102.21	102.21	169.55	134.85	134.85
Free space model	95.67	95.67	95.67	120.78	120.78	120.78
Cost231 Hata model	128.41	117.97	104.06	174.07	163.64	149.73
Stanford university model	113.07	107.04	102.61	134.85	163.53	159.09
Ericson model	91.24	89.32	87.90	217.69	215.76	214.34

Table 5.5 shows that the lowest path loss value has been recorded in rural environments at the free space model. COST 231 W-I model showed flat results in all changes in receiver antenna heights. There are no specific parameters for rural areas. In our simulation, we considered the LOS equation for this environment because we can expect a line-of-sight signal if the area is flat enough with less vegetation. The path loss in the free space model increases according to the frequency increase and shows the lowest value of path loss. Ericson model showed the highest path loss at the frequency of 5.8 GHz and 3m mobile station antenna height.

5.2.4. Simulations analysis for empirical path loss propagation models

The propagation models are then used for the mathematical prediction of the propagation of radio waves between the source and the target service area. They thus give an idea close to reality to allow a receiver of systems to establish in advance if the proposed radio communication system serves the intended service area well.

In most situations, due to the multipath and NLOS environment, all models exhibit more enormous path losses in metropolitan regions than in suburban and rural areas, according to our comparison investigation. Furthermore, we could not locate a single model that could be used in all settings and frequency ranges. In comparison to other models, the free space model had the lowest path loss (103.57 dB in 10 m receiver antenna height) in metropolitan areas. On the other hand, the Stanford university model exhibited the most path loss (160.45 dB in 3 m receiver antenna height). When compared to other models, the free space model demonstrated significantly reduced path loss (103 dB) in suburban regions.

On the other hand, the Ericson model indicated significantly increased route loss for receiver antenna heights of 6 m and 10 m. (i.e.,190 dB and 188.80 dB, respectively). We can pick several models for different viewpoints in rural regions. We may consider LOS computation if the location is sufficiently flat and devoid of vegetation and the likelihood of receiving a LOS signal

is excellent. On the other hand, if there is a lower likelihood of receiving a LOS signal, the COST-Hata model shows less path loss than the Stanford university model and the Ericsson model, especially at a 10 m receiver antenna height. However, when all receiver antenna heights were considered, the Stanford university model had lower path loss (134.85 dB in 3 m and 163.53 dB in 6 m), whereas COST-Hata had higher path loss (174.07 dB in 3m and 163.64 dB in 6 m).

Let us examine the worst-case scenario for deploying a coverage area. We can provide maximum coverage by increasing transmission power, increasing the likelihood of interference with neighboring areas that use the same frequency blocks. However, if we use a lower path loss model to deploy a cellular zone, we may need more to cover the entire area. Some users may lose signal in the operational cell, especially if they move fast. As a result, while selecting a path loss model for initial deployment, we must make a trade-off between transmission power and neighboring frequency block interference.

5.3. Modeling Losses of Mobile Networks using Artificial Intelligence Methods

The optimization method chosen to solve a particular problem depends on the nature of the parameters to be optimized but also on the given problem. Therefore, only some general optimization methods can solve all problems, but many methods are adapted to each case. Therefore, we have applied the experiment to three different architectures (one hidden layer, two hidden layers, and three hidden layers).

As the network design grows, i.e., the number of layers and neurons increases, the network will include more connections, which implies increasingly slow learning and processing. These topologies were chosen using an optimization procedure illustrated in Fig. 5.39. Once the neural network has been trained (after the training), it must be tested on a database that is not the same as the one used for the training. This test allows us to evaluate the neural system's performance and identify the data type that caused the problem. The network architecture will be modified if the performance is not up to par. We used Feedforward MLP as architecture and Backpropagation of errors as a learning algorithm. The transfer function was:

- for input and hidden layers: Log-sigmoid transfer function
- for the output layer: Linear transfer function
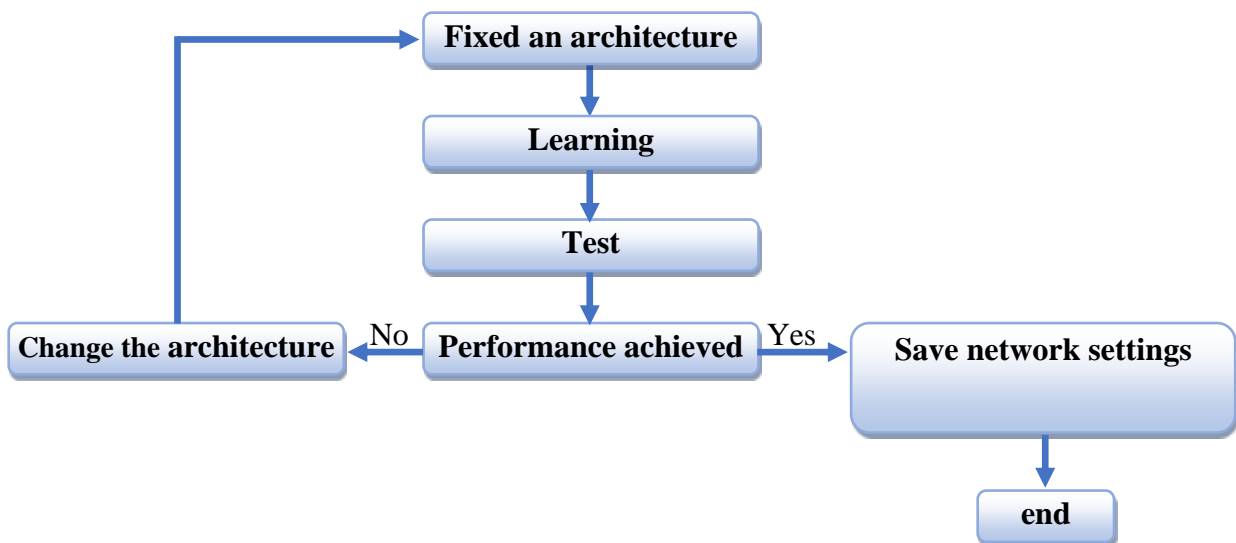
Figure 5. 37. Architecture optimization.

After testing several learning possibilities and measuring performance, we found the following architectures.

5.3.1   Architecture 1 (one hidden layer)

The R-Squared (R2) is a statistical metric that measures the proportion of the variance of a dependent variable in a regression model that is explained by one or more independent variables. In each example, there was a high agreement between the experimental and predicted outcomes (ANS). Therefore, the optimized structure can predict other combinations of input variables. The R-squared of the test set compares the results predicted by the neural model (RNA) at different distances D (m) versus those measured.
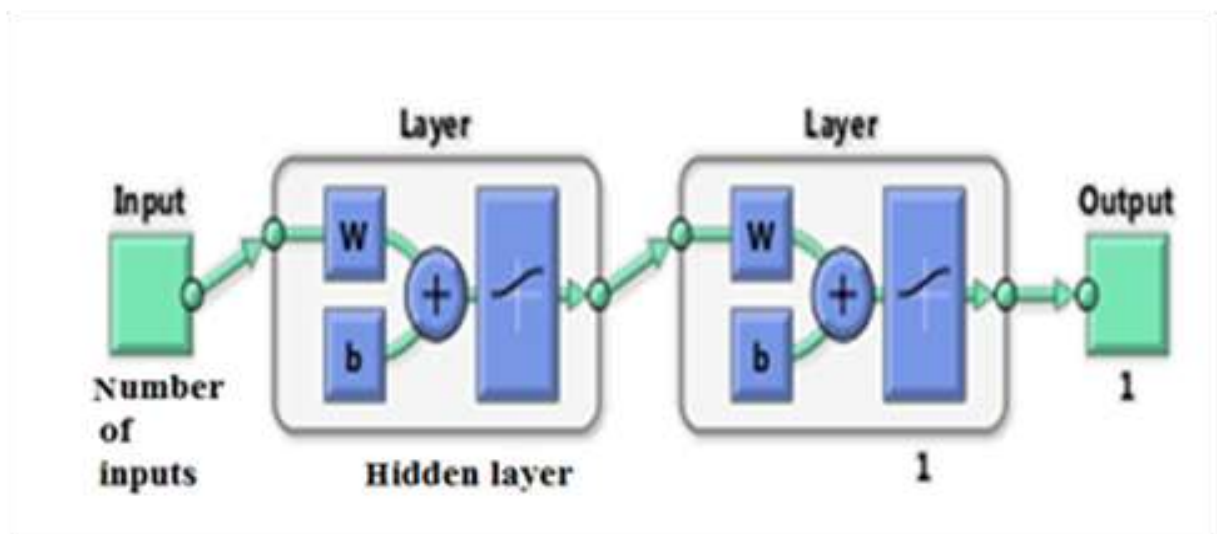
Figure 5. 38. MLP architecture with one Hidden layer.
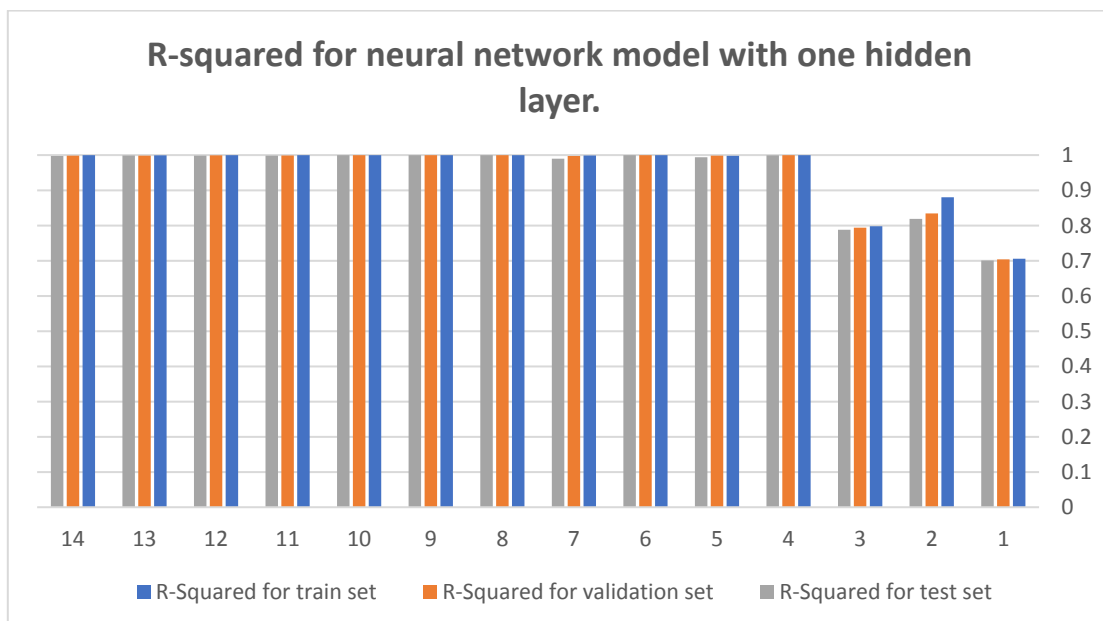
Figure 5. 39. R-squared for the neural network model with one Hidden layer.

There is an agreement between them for all simulations, as illustrated in Fig. 5.39. This last finding demonstrates the usefulness of artificial neural networks in mobile network loss analysis.

5.3.2. Final model 1 (one hidden layer)
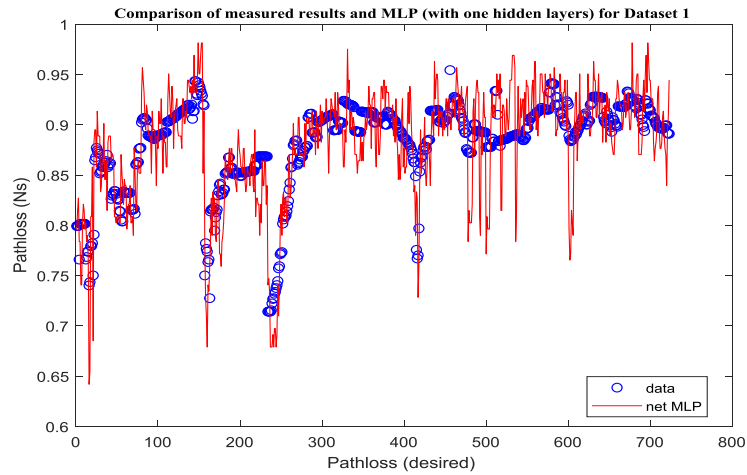
Figure 5. 37. Comparison of measured results and MLP (with one hidden layer) for Dataset 1.
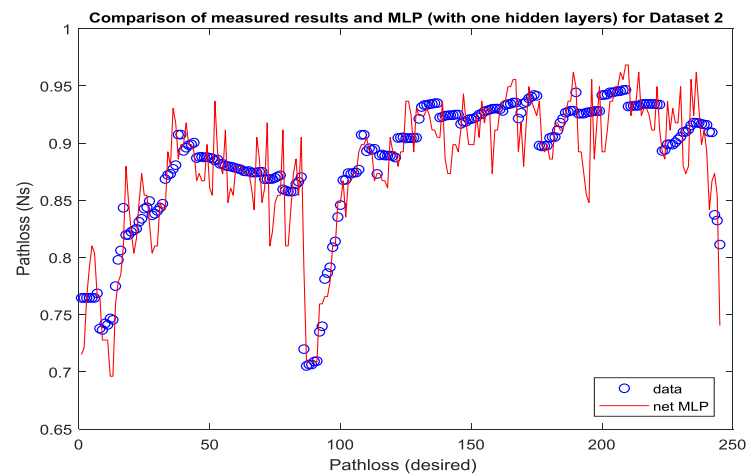
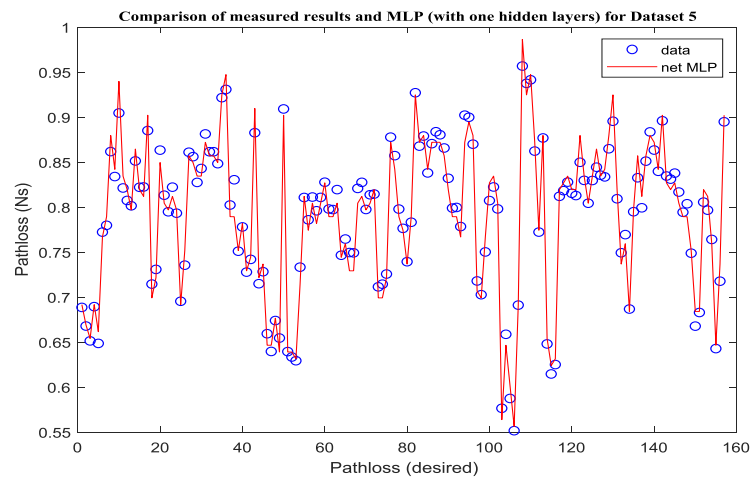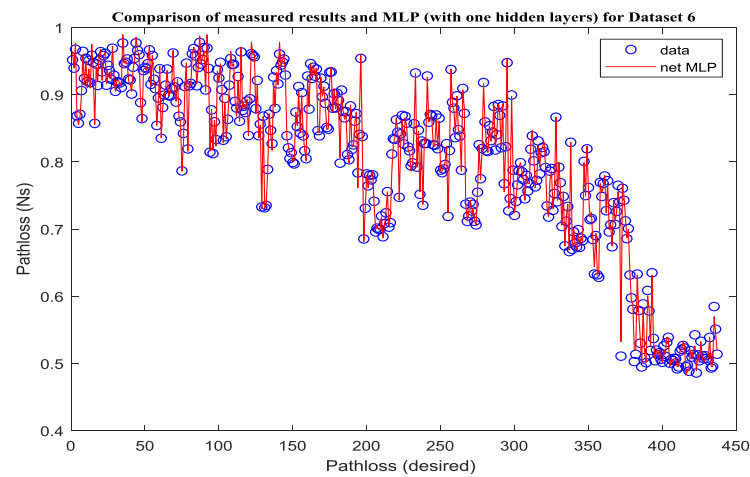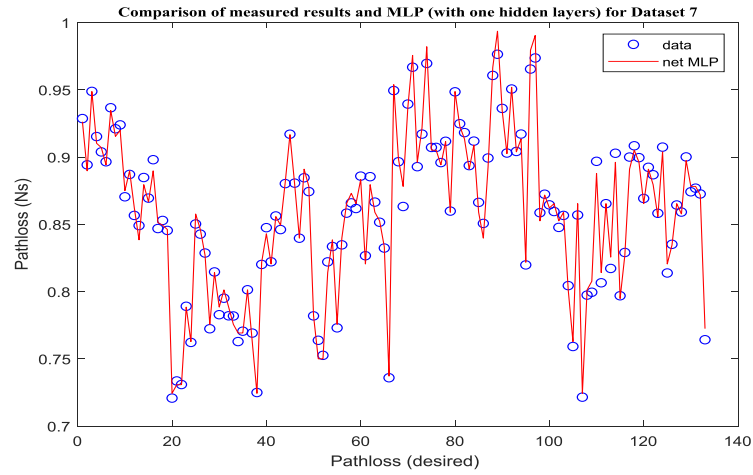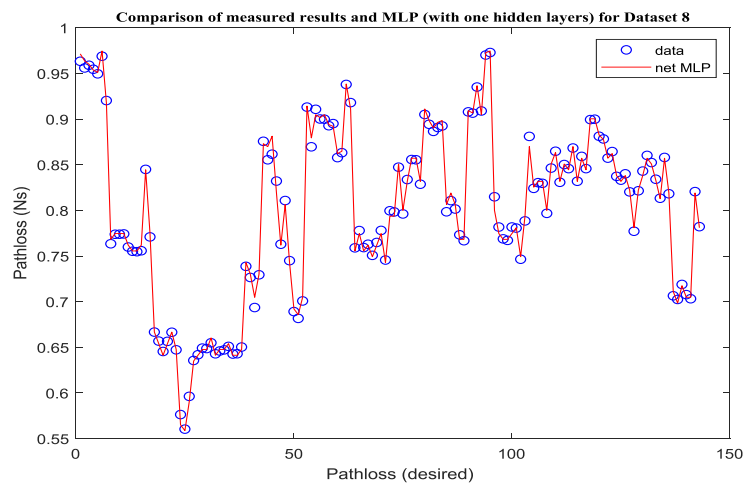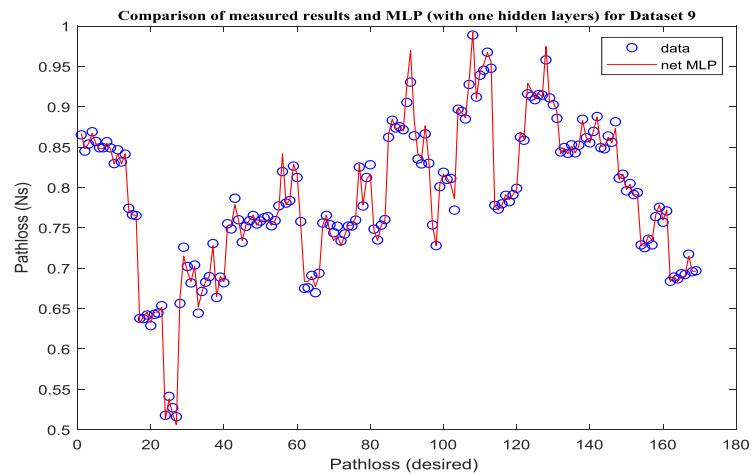**Figure 5. 38.** Comparison of measured results and MLP (with one hidden layer) for Dataset 2.
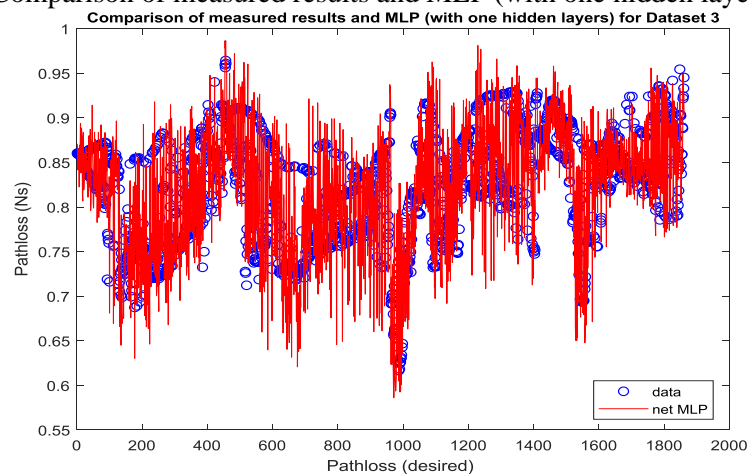
Figure 5. 39. Comparison of measured results and MLP (with one hidden layer) for Dataset 3.

95
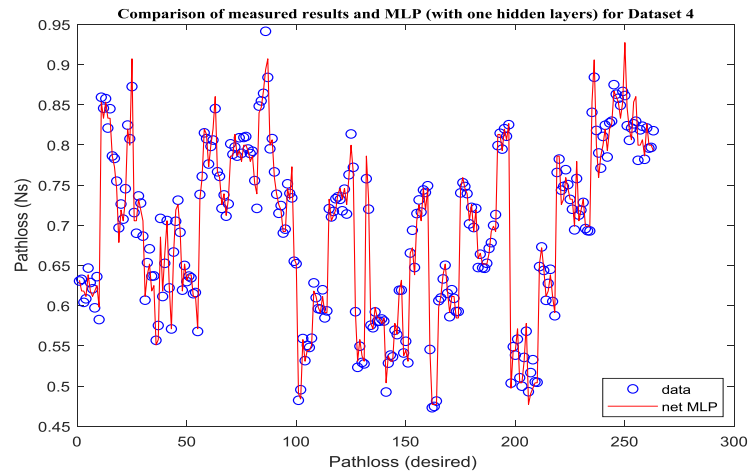
Figure 5. 40. Comparison of measured results and MLP (with one hidden layer) for Dataset 4.

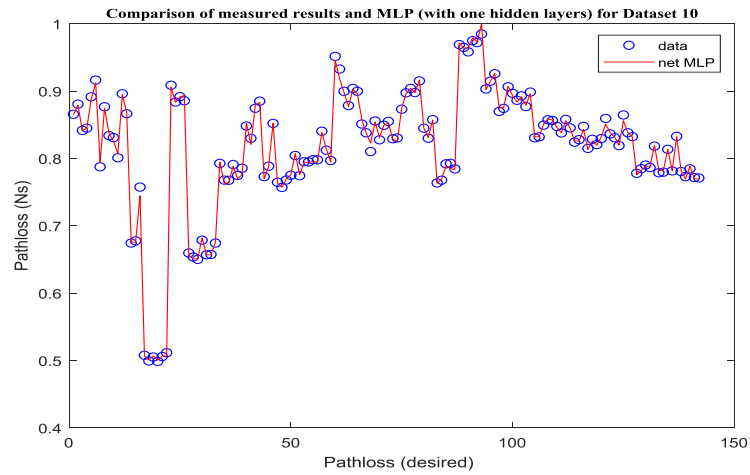**Figure 5. 41.** Comparison of measured results and MLP (with one hidden layer) for Dataset 5.

Figure 5. 42. Comparison of measured results and MLP (with one hidden layer) for Dataset 6.

Figure 5. 43. Comparison of measured results and MLP (with one hidden layer) for Dataset 7.
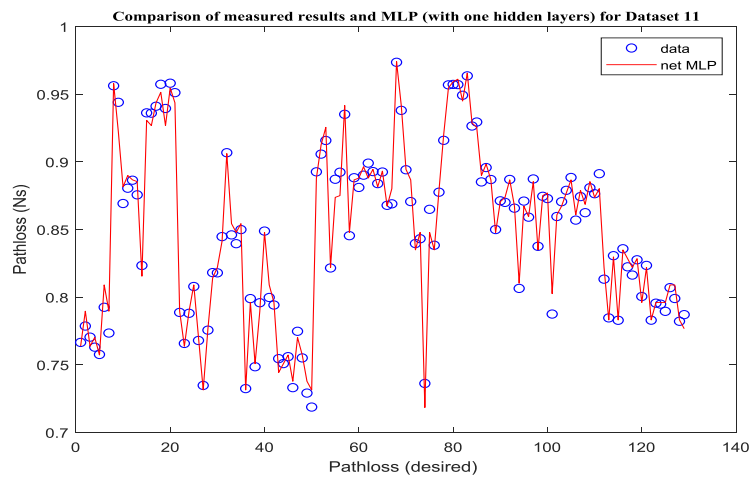

Figure 5. 44. Comparison of measured results and MLP (with one hidden layer) for Dataset 8.

Figure 5. 45. Comparison of measured results and MLP (with one hidden layer) for Dataset 9.

Figure 5. 46. *Comparison of measured results and MLP (with one hidden layer) for Dataset 10.*

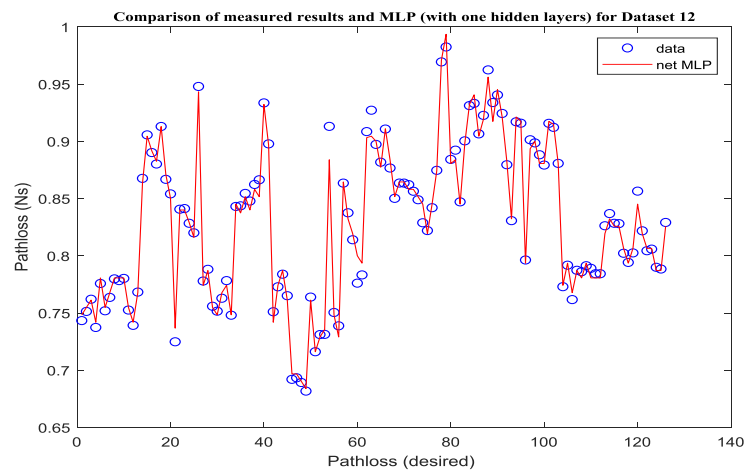**Figure 5. 47.** Comparison of measured results and MLP (with one hidden layer) for Dataset 11.

Figure 5. 48. Comparison of measured results and MLP (with one hidden layer) for Dataset 12.
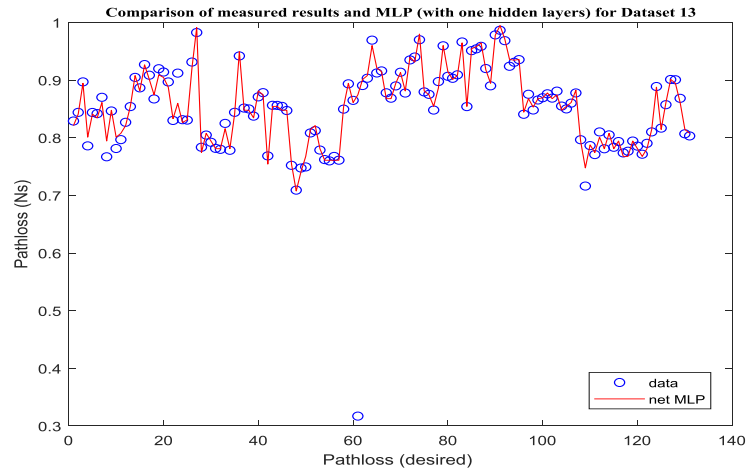
Figure 5. 49. Comparison of measured results and MLP (with one hidden layer) for Dataset 13.
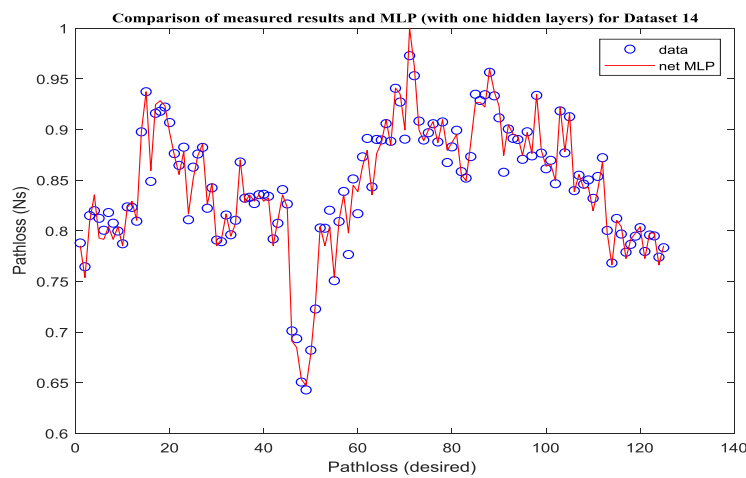

Figure 5. 50. Comparison of measured results and MLP (with one hidden layer) for Dataset 14.

After modeling the MLP network and performing the necessary optimizations, we could choose the best structure for each dataset with a hidden layer, represented in Table 5.6.

Table 5. 6. Optimized parameters for the single hidden layer MLP model's final model.

Data sets	Numbers of neurons			Number of samples for each set		
	Input layer	1ˢᵗhidden layer	Output layer	Training set	Validation set	Test set
1	4	96	1	2170	723	723
2	6	73	1	749	245	245
3	6	87	1	5586	1861	1861
4	9	46	1	791	263	263
5	11	11	1	473	157	157
6	10	83	1	1313	437	437
7	10	8	1	399	133	133
8	10	46	1	429	143	143
9	10	91	1	509	169	169
10	10	28	1	429	142	142
11	11	97	1	387	129	129

12	11	98	1	381	126	126
13	11	96	1	395	131	131
14	11	43	1	379	125	125

5.3.3. Architecture 2 (two hidden layers)

There is a correlation between the desired outputs and those obtained by the network. The performance of the optimized MLP network (with two hidden layers) was evaluated by comparing our results with actual measurements .Fig. 5.55. shows the different results of the simulations compared to the accurate measurements using trend curves better to compare the results of our model with the database.
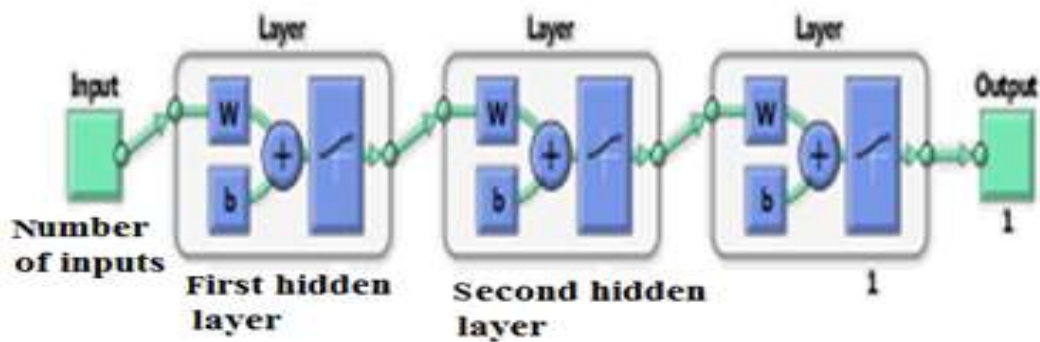

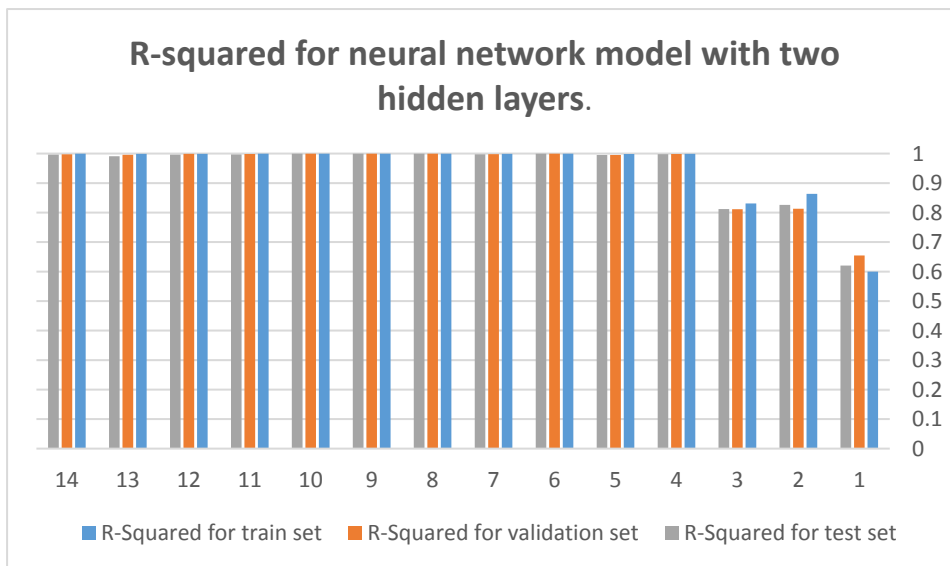**Figure 5. 51.** MLP architecture with two Hidden layers.

Figure 5. 52. R-squared for the neural network model with two Hidden layers.
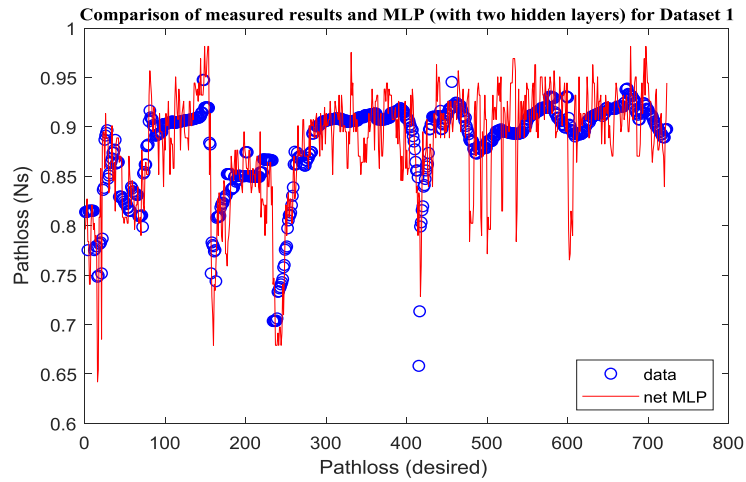
5.3.4. Final model 2 (two hidden layers)

Figure 5. 53. Comparison of measured results and MLP (with two hidden layers) for Dataset 1.
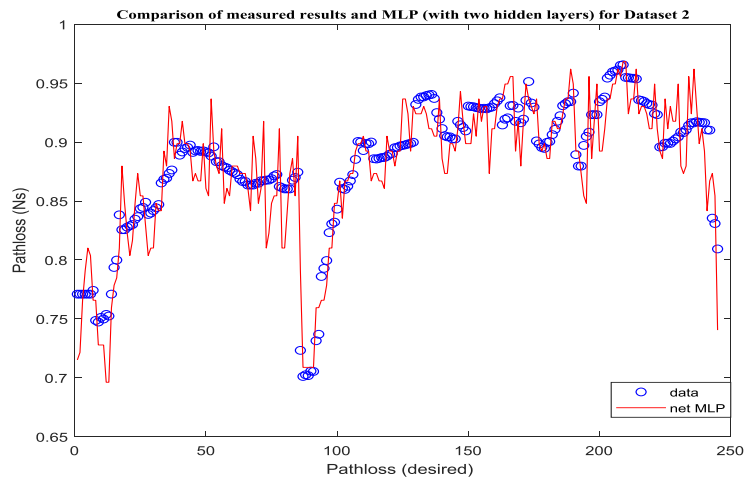

Figure 5. 54. Comparison of measured results and MLP (with two hidden layers) for Dataset 2.

Figure 5. 55. Comparison of measured results and MLP (with two hidden layers) for Dataset 3.

Figure 5. 56. Comparison of measured results and MLP (with two hidden layers) for Dataset 4.
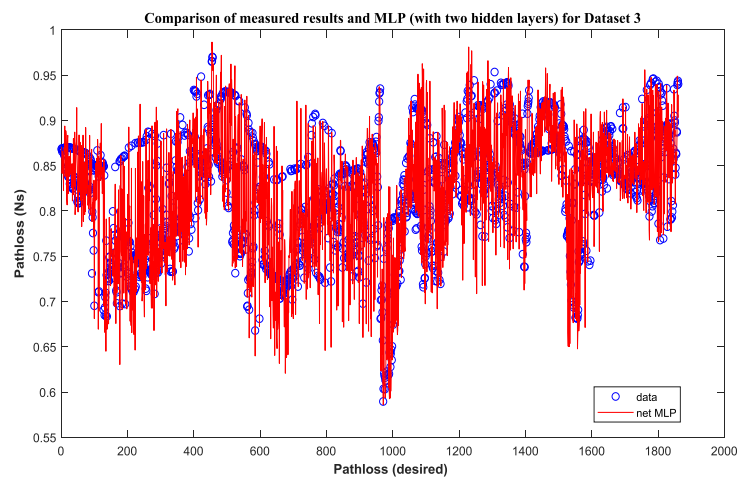

Figure 5. 57. Comparison of measured results and MLP (with two hidden layers) for Dataset 5.

Figure 5. 58. Comparison of measured results and MLP (with two hidden layers) for Dataset 6.

Figure 5. 59. Comparison of measured results and MLP (with two hidden layers) for Dataset 7.
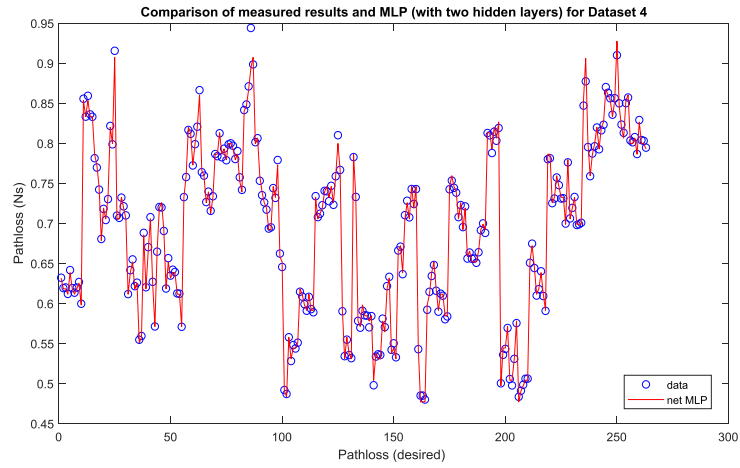

Figure 5. 60. Comparison of measured results and MLP (with two hidden layers) for Dataset 8.

Figure 5. 61. Comparison of measured results and MLP (with two hidden layers) for Dataset 9.

Figure 5. 62. Comparison of measured results and MLP (with two hidden layers) for Dataset 10.
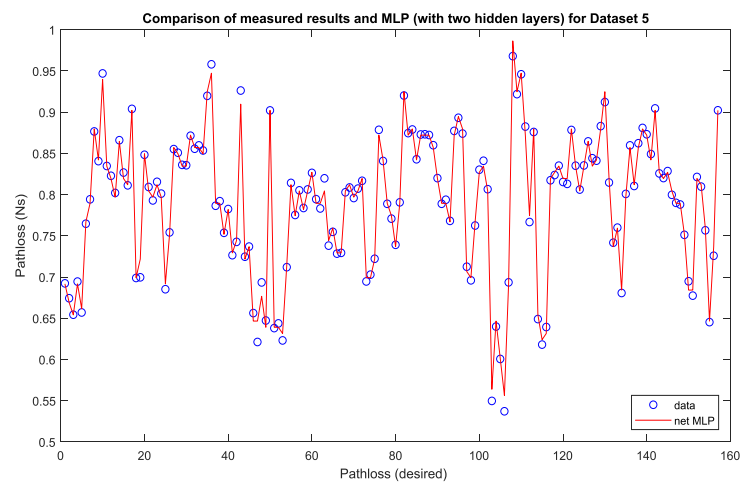

Figure 5. 63. Comparison of measured results and MLP (with two hidden layers) for Dataset 11.

Figure 5. 64. Comparison of measured results and MLP (with two hidden layers) for Dataset 12.

Figure 5. 65. Comparison of measured results and MLP (with two hidden layers) for Dataset 13.
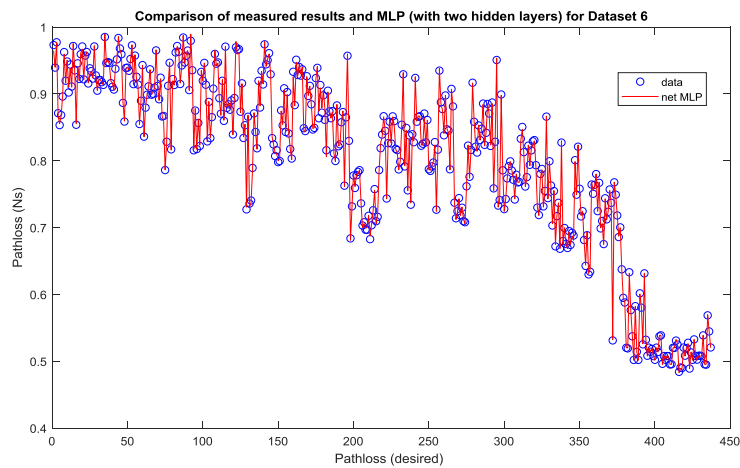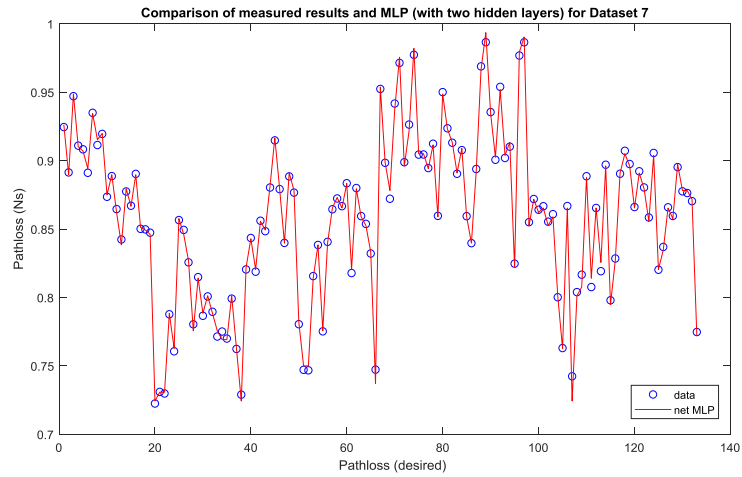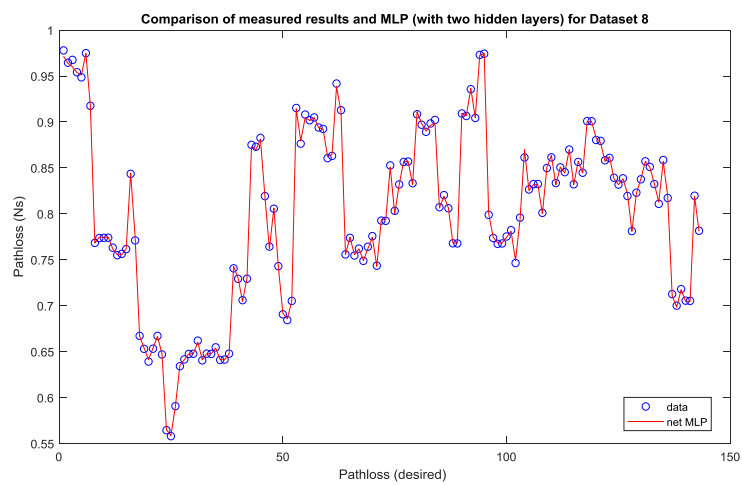

Figure 5. 66. Comparison of measured results and MLP (with two hidden layers) for Dataset 14.
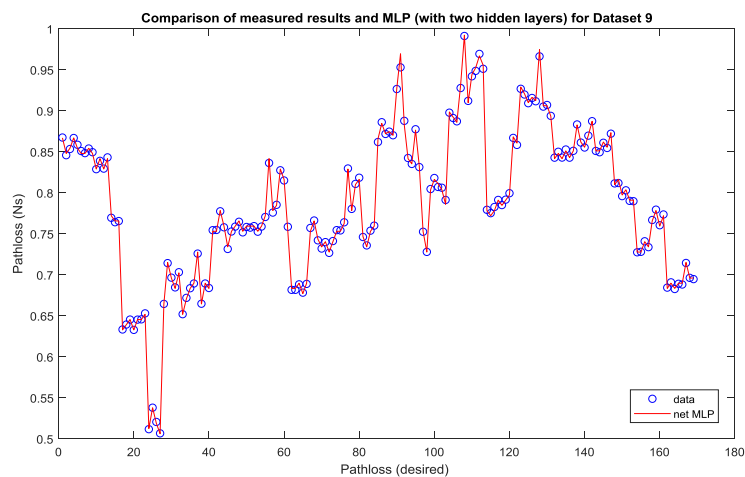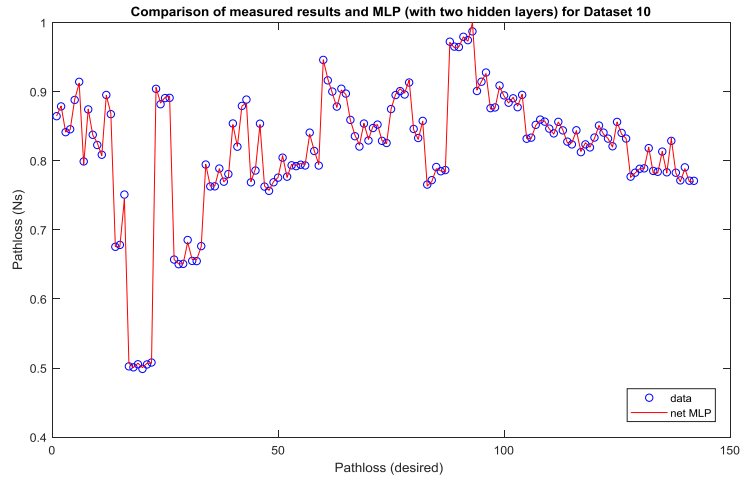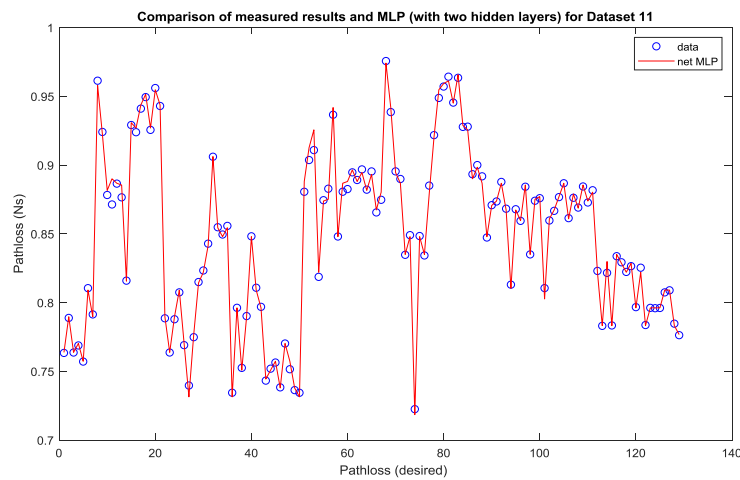
We identified the optimal structure for each dataset with two hidden layers after modeling the MLP network and making the necessary adjustments. Table 5.7. summarizes the results obtained.

Table 5. 7. Optimized parameters for the final model for the MLP model with two hidden layers.

Dataset	Numbers of neurons				Number of samples for each set		
	Input layer	1st hidden layer	2nd hidden layer	Output layer	Training set	Validation set	Test set
1	4	16	18	1	2170	723	723
2	6	20	20	1	749	245	245
3	6	50	50	1	5586	1861	1861
4	9	11	16	1	791	263	263
5	11	16	29	1	473	157	157
6	10	27	25	1	1313	437	437
7	10	10	17	1	399	133	133
8	10	16	20	1	429	143	143
9	10	16	20	1	509	169	169

10	10	10	12	1	429	142	142
11	11	30	10	1	387	129	129
12	11	7	17	1	381	126	126
13	11	20	13	1	395	131	131
14	11	37	26	1	379	125	125

5.3.5. Architecture 3 (three hidden layers)

The training, validation, and testing set were compared to the neural model response to confirm the predictive property of the optimized network structure. The R-squared is shown in Fig 5.71. There was a high agreement between the experimental and predicted results (ANS) in each scenario. Therefore, the optimized structure can predict other combinations of input variables. Fig. 5.72. - 5.85. shows a comparison between the data expected by the three-hidden-layer neural model (RNA) and those measured for different distances D (m).
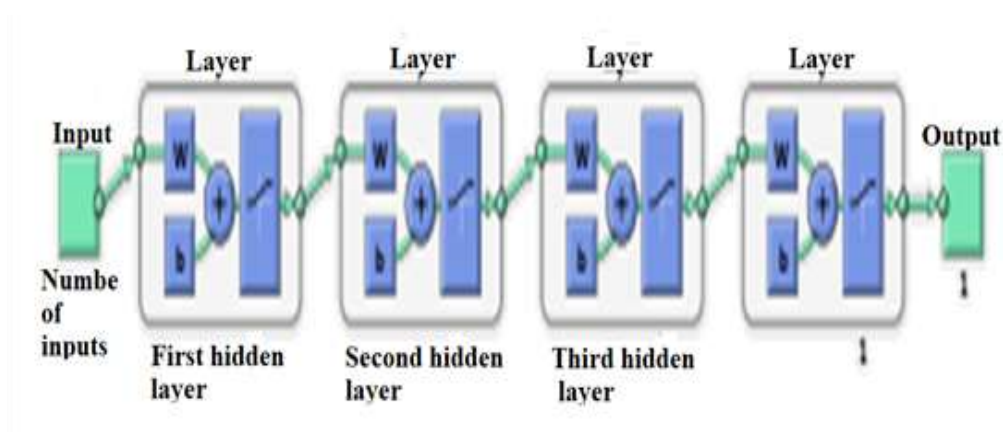
Figure 5. 67. MLP architecture with three Hidden layers.
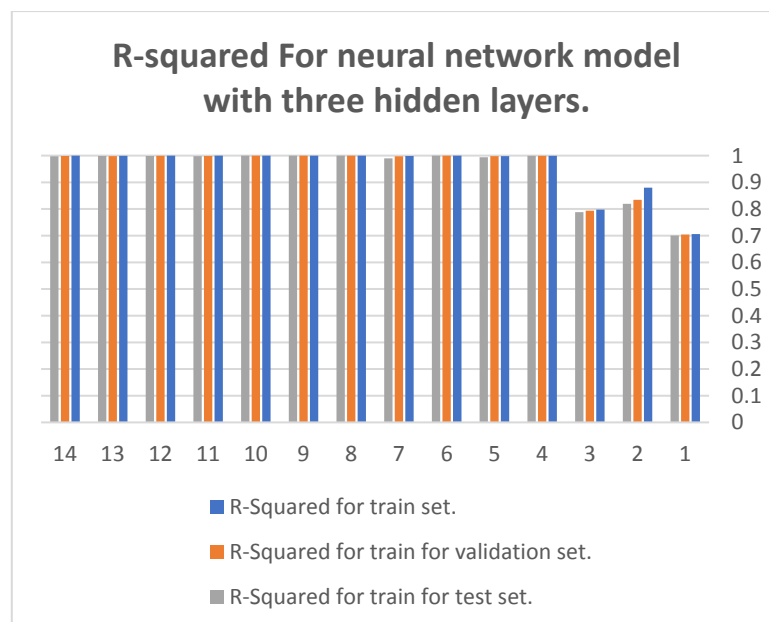
Figure 5. 68 . MLP architecture with three Hidden layers.

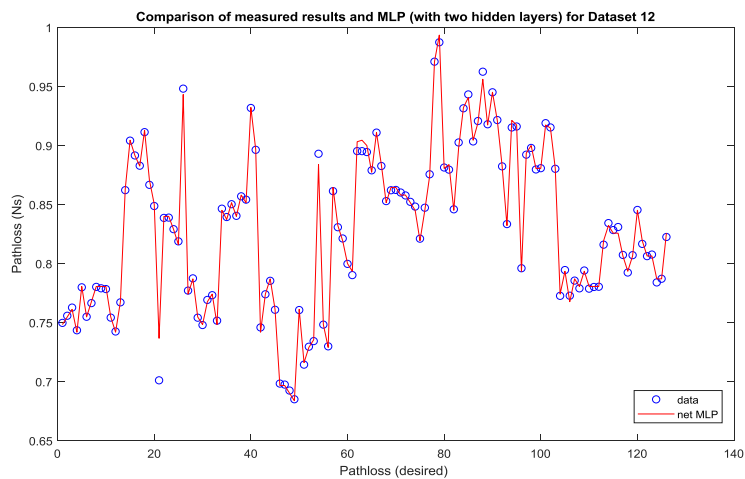## 5.3.6. Final model 3 (three hidden layers)
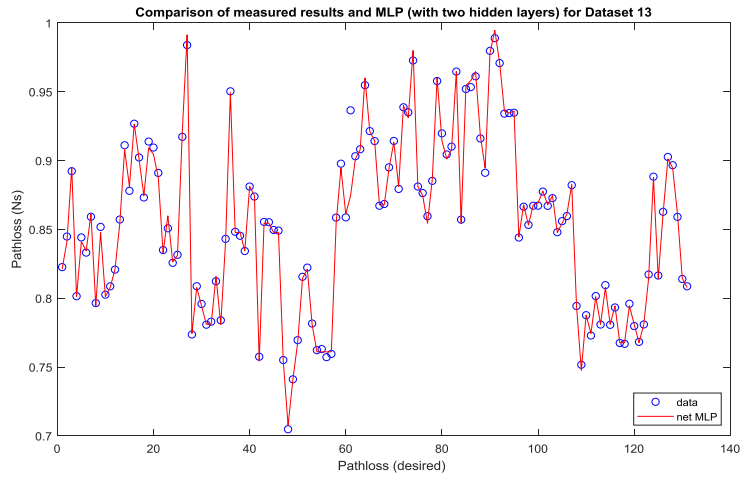

Figure 5. 69. Comparison of measured results and MLP (with three hidden layers) for Dataset 1.

Figure 5. 70. Comparison of measured results and MLP (with three hidden layers) for Dataset 2.
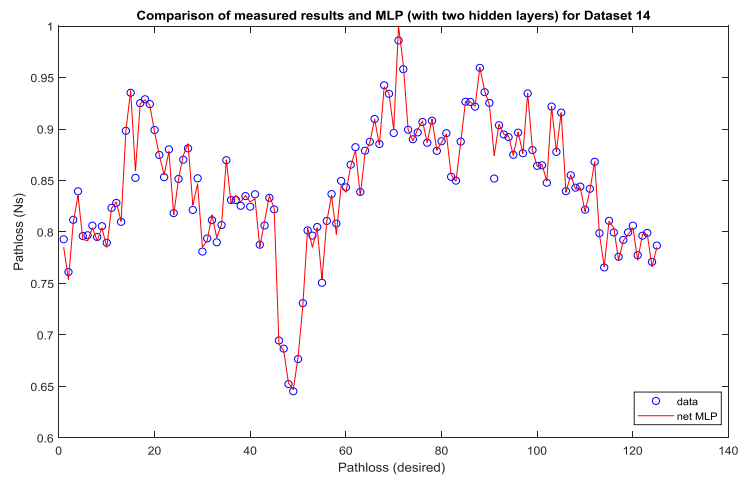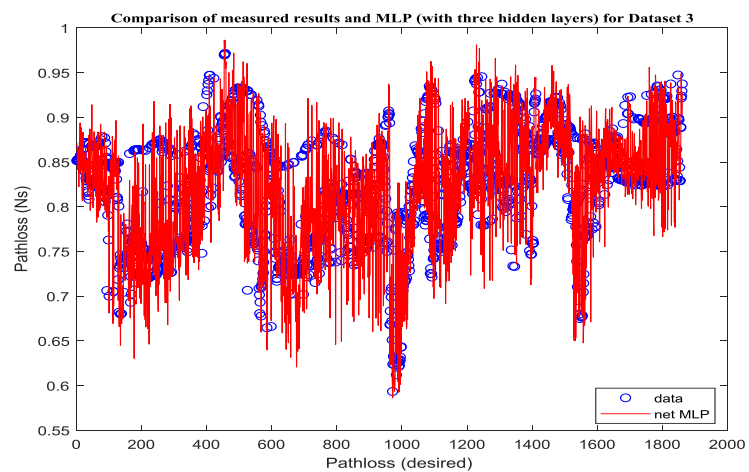

Figure 5. 71. Comparison of measured results and MLP (with three hidden layers) for Dataset 3.
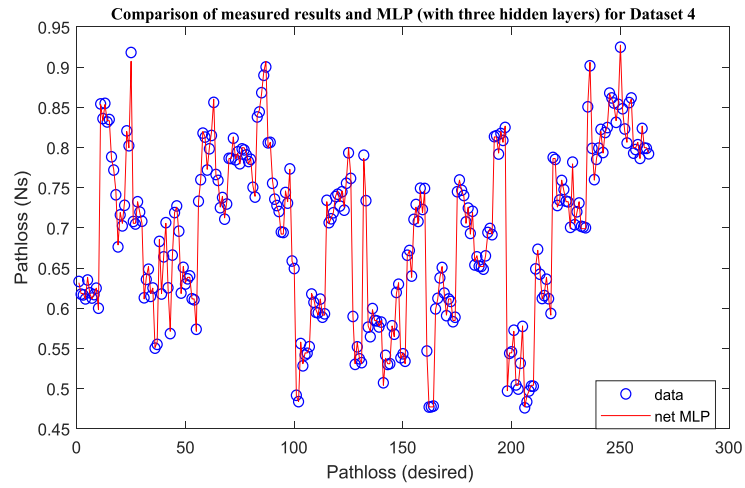
Figure 5. 72. Comparison of measured results and MLP (with three hidden layers) for Dataset 4.
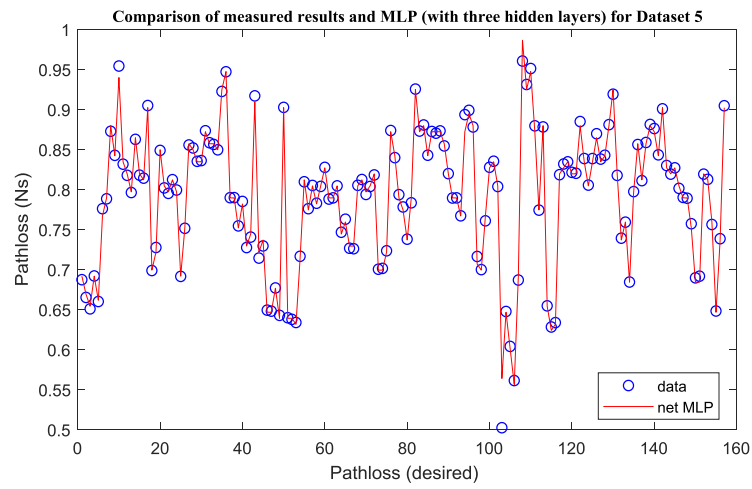
Figure 5. 73. Comparison of measured results and MLP (with three hidden layers) for Dataset 5.
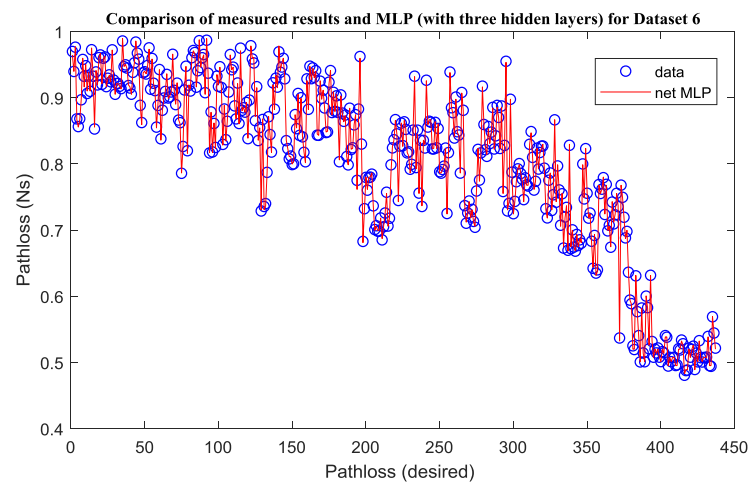
Figure 5. 74. Comparison of measured results and MLP (with three hidden layers) for Dataset 6.
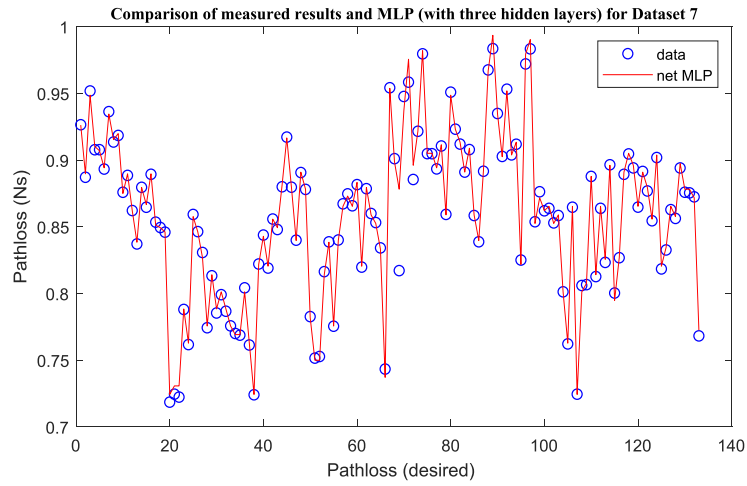
Figure 5. 75. Comparison of measured results and MLP (with three hidden layers) for Dataset 7.
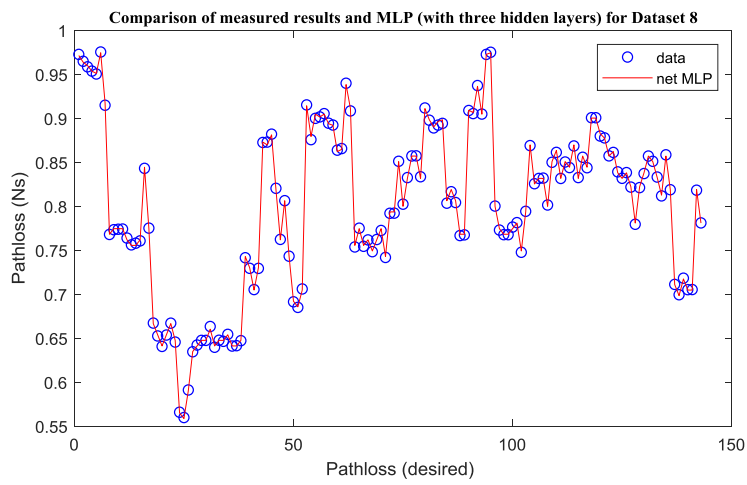
Figure 5. 76. Comparison of measured results and MLP (with three hidden layers) for Dataset 8.
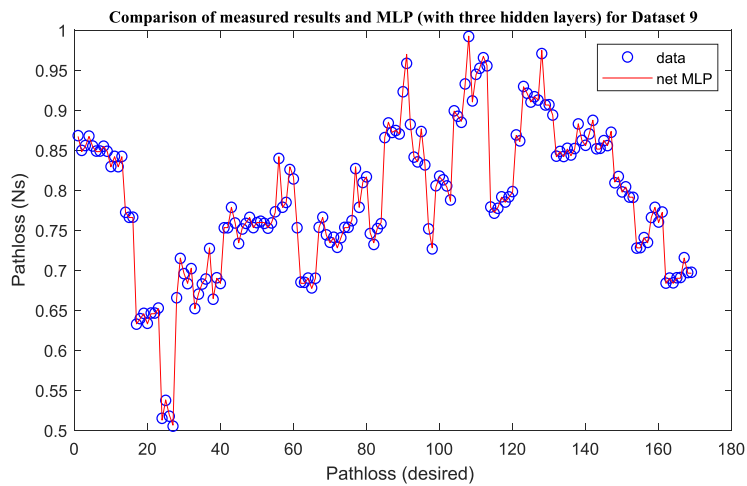
Figure 5. 77. Comparison of measured results and MLP (with three hidden layers) for Dataset 9.
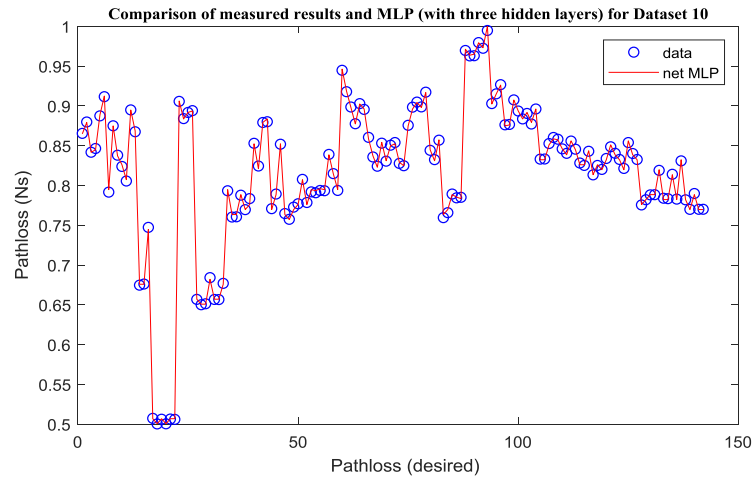
Figure 5. 78. Comparison of measured results and MLP (with three hidden layers) for Dataset 10.
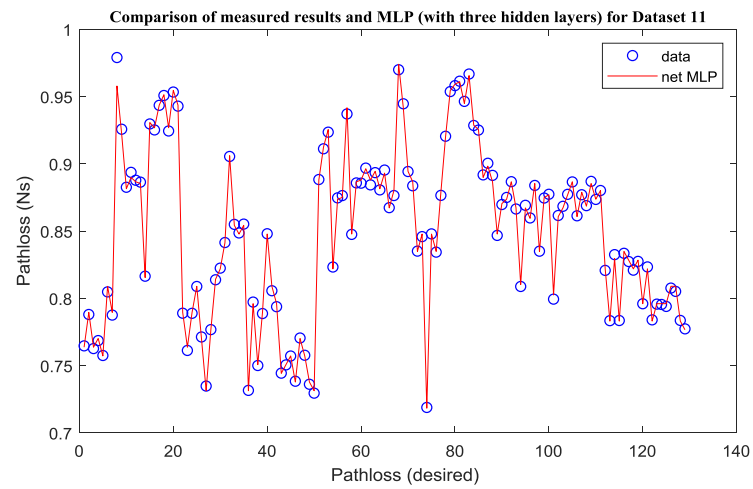
Figure 5. 79. Comparison of measured results and MLP (with three hidden layers) for Dataset 11.
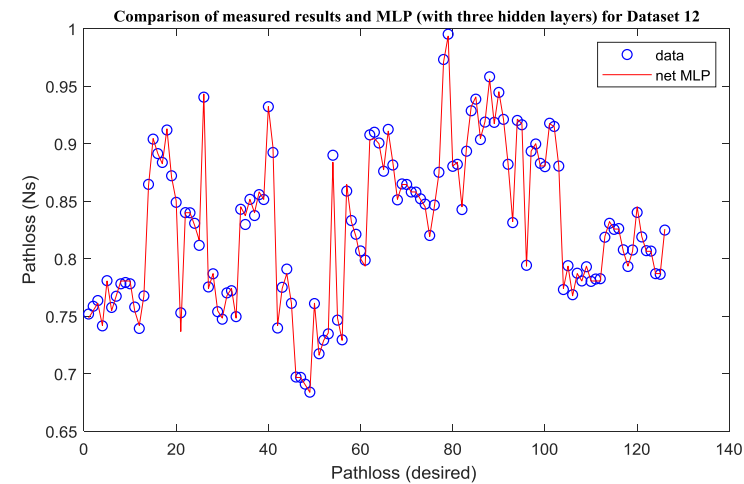
Figure 5. 80. Comparison of measured results and MLP (with three hidden layers) for Dataset 12.
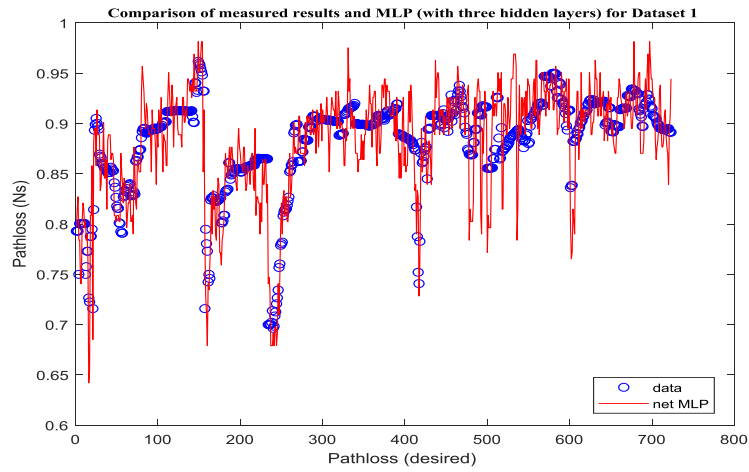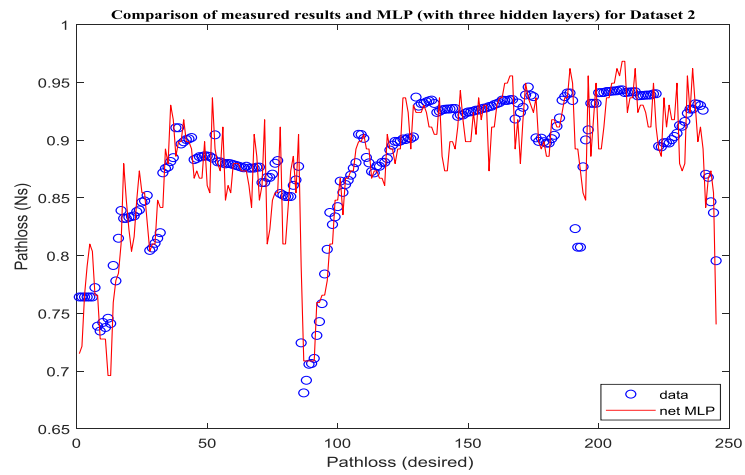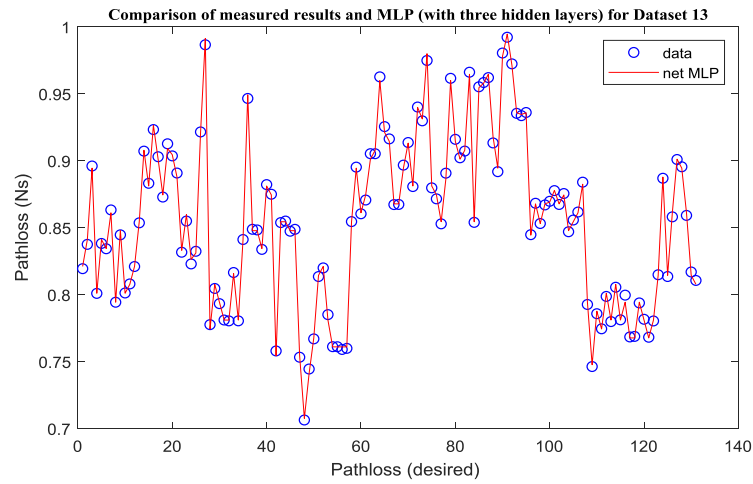
Figure 5. 81. Comparison of measured results and MLP (with three hidden layers) for Dataset 13.
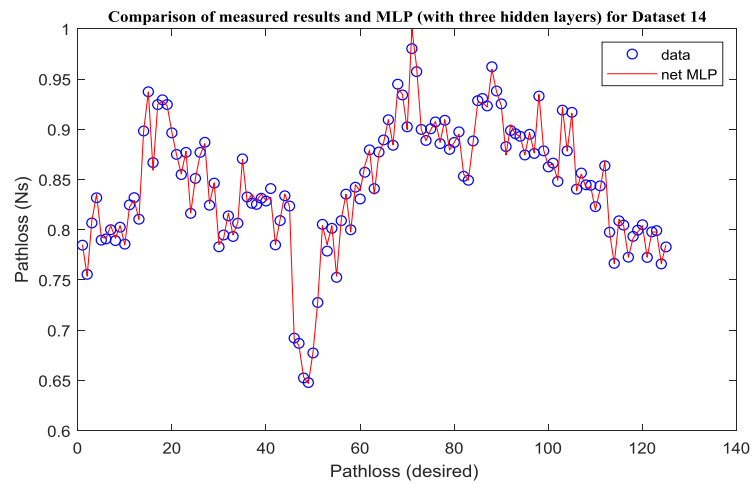
Figure 5. 82. Comparison of measured results and MLP (with three hidden layers) for Dataset 14.

Table 5. 8. Optimized parameters for the final model for three hidden layers.

Dataset	Numbers of neurons					Number of samples for each set		
	Input layer	1st hidden layer	2nd hidden layer	3rd hidden layer	Output layer	Training set	Validation set	Test set
1	4	09	10	08	1	2170	723	723
2	6	10	15	22	1	749	245	245
3	6	10	16	40	1	5586	1861	1861
4	9	05	16	35	1	791	263	263
5	11	05	18	06	1	473	157	157
6	10	12	20	36	1	1313	437	437
7	10	04	17	27	1	399	133	133
8	10	19	14	38	1	429	143	143
9	10	04	17	19	1	509	169	169
10	10	08	16	32	1	429	142	142
11	11	18	18	31	1	387	129	129
12	11	21	31	46	1	381	126	126
13	11	07	21	49	1	395	131	131
14	11	28	25	05	1	379	125	125

5.3.7. Comparison between the three architectures

The results listed in Table 5.6, Table 5.7, and Table 5.8 indicate that the number of neurons varies with the number of layers. The number of inputs plays a significant role in the accuracy and speed of the models. Fig. 5.86. shows the MSE for the three chosen architectures.
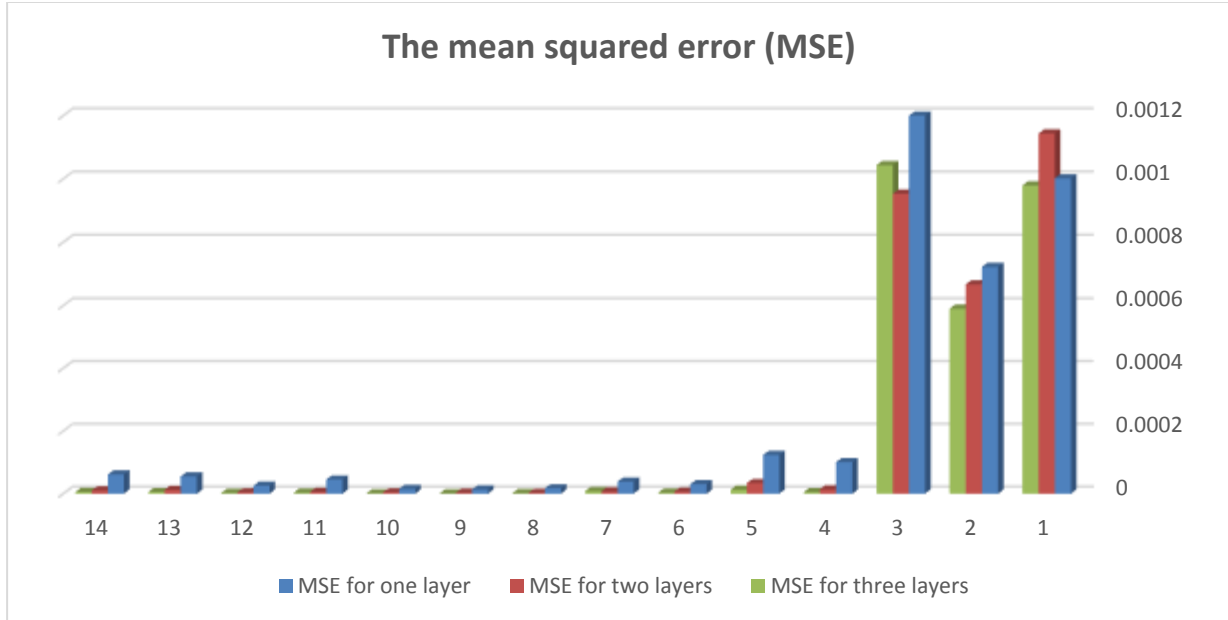
Figure 5. 83. MSE for the three neural network models.

Based on Fig. 5.86, the best architecture has three hidden layers. The error rate is directly proportional to the number of samples—the smaller the number of samples, the lower the error rate. The experiment determines the number of hidden layers and the number of neurons; for example, in dataset 3, a structure with two hidden layers performs better than one with three hidden layers. An increase in the number of neurons does not always imply an improvement in the model's performance, as, in database 7, we only needed seven neurons to get the best performance.

5.3.8. Comparison of the results obtained by our models with those obtained by empirical models

This section presents the results obtained for 14 different datasets with different parameters. The results obtained by six empirical models (Free Space Path Loss Model (FSPL), Walfisch-Ikegami model (WI), ECC-33 Model (ECC-33), COST 231-Hata model (PLC), Ericsson Model (PL999), Stanford University Interim Model (SUI)), and the type of model architecture were compared with those obtained by the MLP. The results are shown in Fig. 89-98.
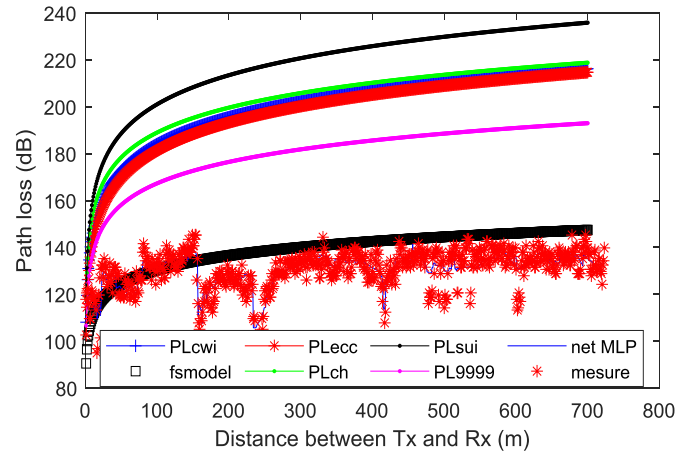
Figure 5. 84. Comparison between empirical models and MLP (with one hidden layer) for Dataset 1.
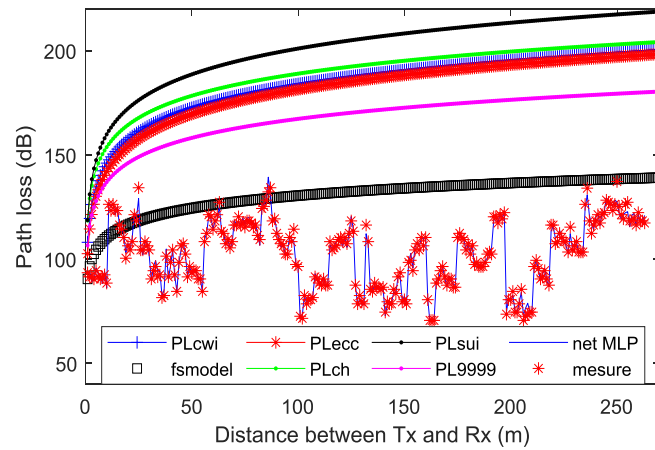
Figure 5. 85. Comparison between empirical models and MLP (with one hidden layer) for Dataset 4.
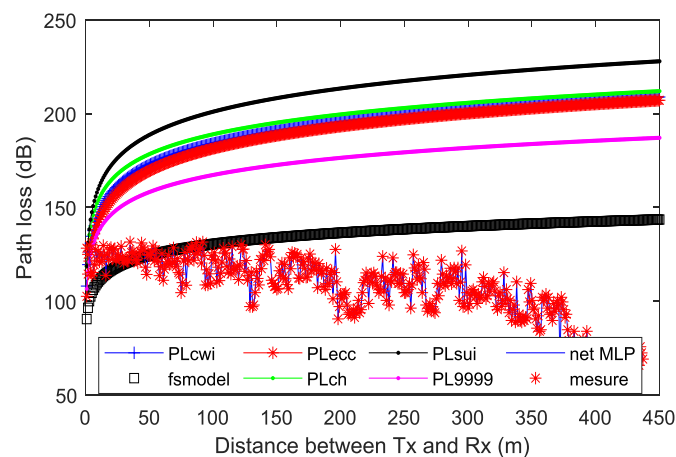
Figure 5. 86. Comparison between empirical models and MLP (with one hidden layer) for dataset 6.
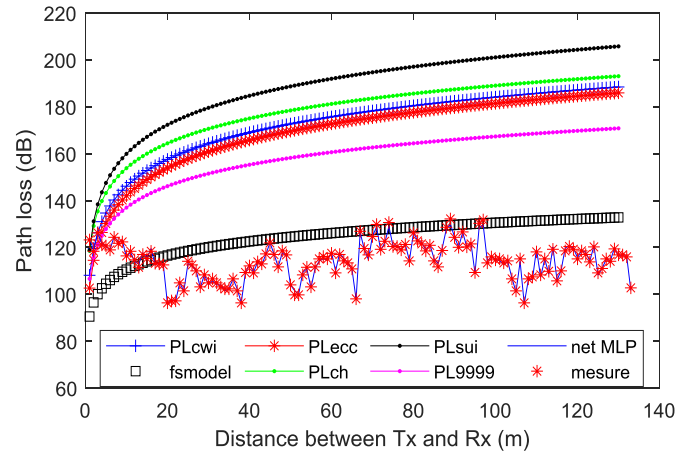
Figure 5. 87. Comparison between empirical models and MLP (with one hidden layer) for Dataset 7.
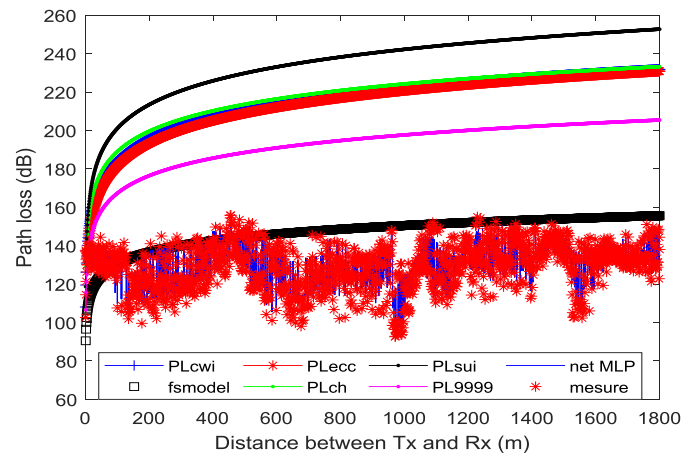
Figure 5. 88. Comparison between empirical models and MLP (with two hidden layers) for Dataset 3.
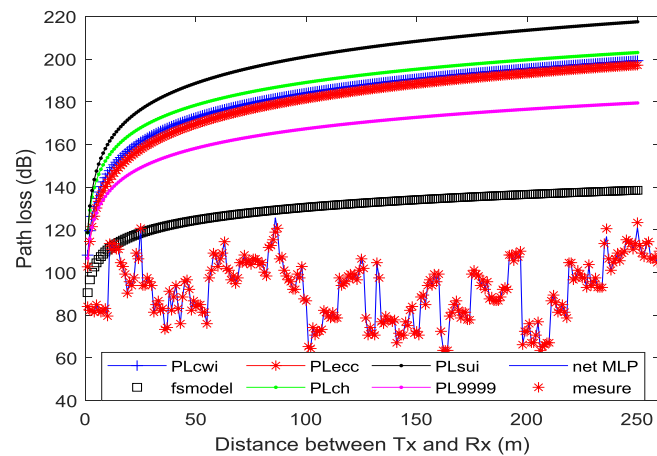
Figure 5. 89. Comparison between empirical models and MLP (with two hidden layers) for Dataset 5.
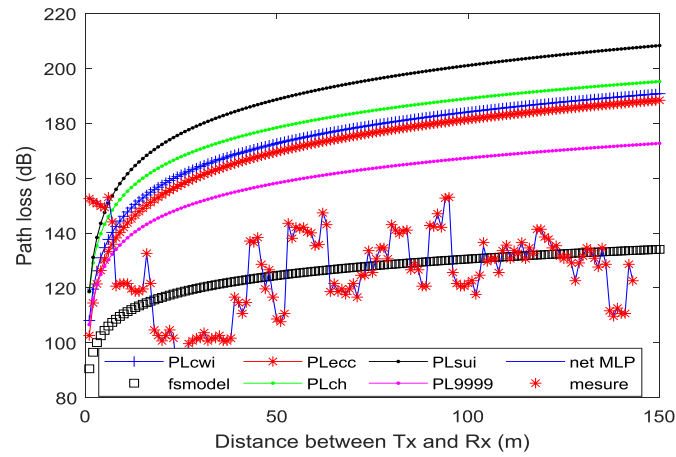
Figure 5. 90. Comparison between empirical models and MLP (with two hidden layers) for Dataset 8.
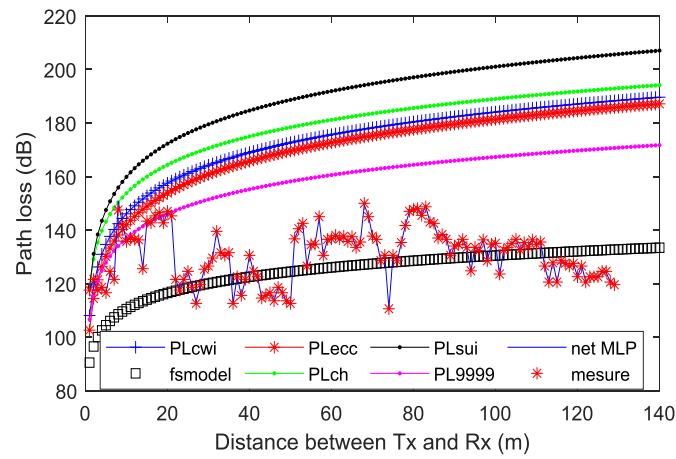
Figure 5. 91. Comparison between empirical models and MLP (with three hidden layers) for Dataset 11.
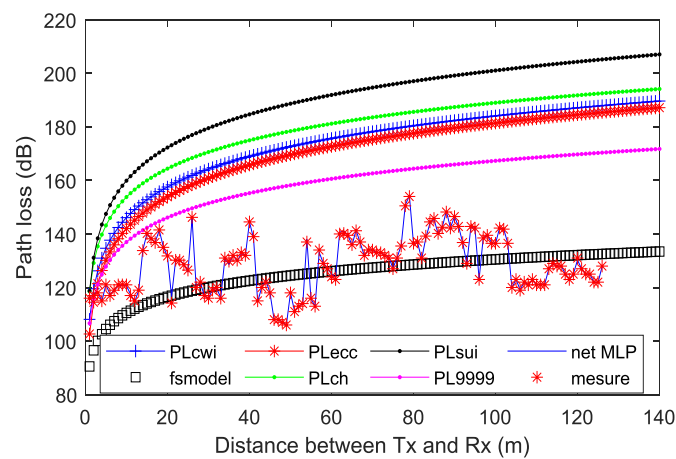
Figure 5. 92 . Comparison between empirical models and MLP (with three hidden layers) for Dataset 12.
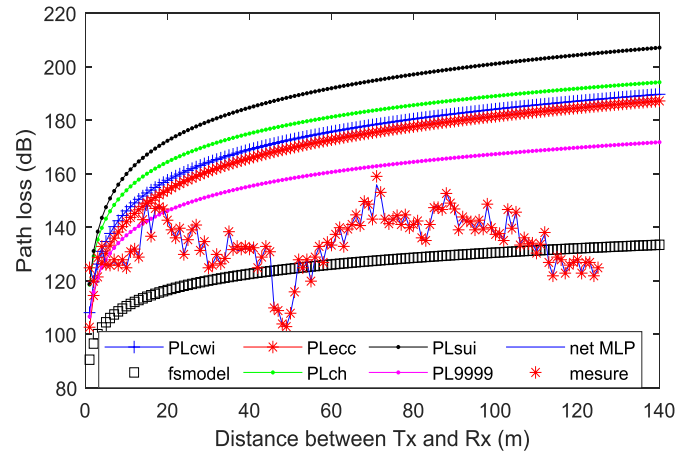
Figure 5. 93. Comparison between empirical models and MLP (with three hidden layers) for Dataset 14.

5.3.9. Analysis of the simulation

Fig. 89-98 shows that the MLP model has the lowest error value when all studied measures are included. Still, the other six empirical models overestimated the path loss and are not suggested for use in the studied context. All observed datasets and alternative designs agree with the MLP model. The neural network model (MLP) performs better than the empirical models. The graphs and error metrics analysis clearly show that the MLP model performs best. The parameters were used in the MLP models simulation to improve the models' deployment outside the initial environment where they were built. Since the models were built outside the environment under consideration, these corrective variables were employed to estimate the empirical models in this work. The parameters hr and hb represent the antenna height of the base station and the mobile station, respectively. These values were also used in the experiment. These numerical values were discovered due to the measurements performed. We used the different transmitters' base station heights in our simulations and evaluations. The actual data obtained by controlling these correction variables and the specific properties of the model were used to design and test our model. We need to know what inputs the model simulates to understand the simulation results. We divided our datasets into four primary environments (urban, suburban, rural, and indoor environments). Based on Fig. 89-98, the model proposed in this study gave the best performance. The other models were performed in the following order:

- Free space model
- Ericson model
- ECC-33 model
- Cost 231 (WI) model

- Cost 231 Hata model

- Stanford University Interim model

This result can be explained by the fact that these models were developed in a specific domain different from our datasets. The path loss prediction should always follow the actual path loss value. Moreover, these changes depend on the parameters of the dataset (distance, frequency, base station antenna height, mobile station antenna height). For example, in datasets 11 to 14), the parameters were collected in an urban area with the same frequency, distance, and mobile station, but we noticed that the path loss value changed from one set to another because the height of the base station antenna changed. The longer the transmitter antenna, the lower the path loss. This also applies to datasets 8 to 10, whose parameters were collected in the same situation, except for the BS antenna height.

On the other hand, the parameters of Dataset 4 were collected inside the building. The path loss varies depending on the obstacles inside the building, such as wall thickness, room space, and windows inside the building. Our models are the best in all cases because we feed our models with all the possible parameters to make predictions almost identical to the actual path loss values.

5.4. Conclusion

This Chapter examined neural network methods for efficient path loss prediction to address the challenges associated with empirical and deterministic path loss prediction models. An MLP model for path loss prediction has been constructed and verified, considering multi-transmitter scenarios. The inputs to the neural network algorithm change from dataset to dataset, and path loss is the output layer. The neural network model (MLP) was created on 14 datasets and compared to predictions given by six existing empirical models. The results indicate that the neural network algorithm matches the measured data well. Since the theoretical and empirical models overestimated the route loss, they are ineffective prediction models for the environment of interest. Two well-known error measures were used to validate the created model. RMSE, R2.

Interestingly, the recently presented MLP has the lowest error among all indices. The MLP model is a good fit for the measured data. The performance of the MLP outperformed the other six empirical models. In addition, by altering the number of input variables at a given time, the performance of the machine learning-based MLP model was studied. It was found that increasing the number of MLP input variables significantly increased the accuracy of the produced model. Therefore, the suggested MLP is quite effective in predicting path fading and is considered a generic data-driven model. Finally, the model can predict path loss

measurements in wireless propagation situations. Future research will focus on another neural network algorithm, namely the radial basis function (RBF) algorithm, and compare the two algorithms to improve the accuracy of signal prediction.

General Conclusion

To offer an excellent quality mobile radio service to their subscribers, mobile telephone operators carry out technical studies on these links taking into account the various attenuations. As well as the different mechanisms and phenomena of propagation come into play : reflection, refraction, transmission, diffusion, fading, multiple paths, Etc. Accurate estimation of propagation losses provides a reasonable basis for correct radio engineering design.

Several empirical attenuation prediction models have been developed, but the generalization of these models to any environment still needs to be determined. In order to get over this shortcoming, the parameters of the empirical models might be changed by actual measurements in the intended setting. Once it is inconceivable to form measurements of the environment directly, an experimenter should settle for some (possibly substantial) error. Many-path loss models are reasonable; however, their accuracy is intimately tied to the accuracy of information describing the environment and obstacles, which is rarely on the field at a clear resolution and might be pricey to collect and update. On the other hand, the models based on Artificial intelligence (AI) technologies have proved their efficacity in forecasting the losses in the wireless network.

The objective of this work is then the optimization of such a model, adjusting the parameters of the latter to obtain a minimum error between the power of the predicted and measured signal. This will make the model more accurate for attenuation prediction by global optimization techniques, including neural network algorithms. we implemented a neural network of the MLP type. After optimizing the latter, we applied the best architecture found for the rest of the work. The results of our models are precise. The curve of the latter follows the pace of the measured losses. That is to say, this curve is submerged in the cloud created by the variations of the measured loss. From this point, our MLP network successfully simulates the measured losses. Furthermore, by simply consulting the errors made by the empirical models, we conclude that the neural model is the most precise, efficient, and suitable for estimating signal losses.

Our main objective was to estimate the loss of a signal with neural networks; the results found in this dissertation prove that this objective was successfully achieved. Regardless of the technique adopted, there is much room for future research in this area, and it has the potential to have a significant influence on a lot of essential applications.

References

Aggelou, G. Neonakis, and Rahim Tafazolli. 2001. "On the relaying capability of next-generation GSM cellular networks." *IEEE Personal Communications 8* 40-47.

ALASTI, Hadi, XU, Kunjie, et DANG, Zhe. 2009. "Efficient experimental path loss exponent measurement for uniformly attenuated indoor radio channels." *IEEE Southeast 2009.* IEEE. 255-260.

ALLEN, David M. 1971. "Mean square error of prediction as a criterion for selecting variables." *Technometrics* 469-475.

Alnatoor, Moamen Adel Abdelfattah, Mohammed Omari, and Mohammed Kaddi. 2020. "Modeling Losses of Mobile Networks using Artificial Intelligence Techniques." *2020 2nd International Conference on Mathematics and Information Technology (ICMIT.* Adrar: IEEE. 212-215.

Al-Samman, Ahmed M., Tharek A. Rahman, Marwan H. Azmi, and M. N. Hindia. 2016. "Large-scale path loss models and time dispersion in an outdoor line-of-sight environment for 5G wireless communications." *AEU-International Journal of Electronics and Communications* 1515-1521.

ALSAYYARI, Abdulaziz, KOSTANIC, Ivica, OTERO, Carlos, et al. 2014. "An empirical path loss model for wireless sensor network deployment in a sand terrain environment." *2014 IEEE World Forum on Internet of Things (WF-IoT).* IEEE. 218–223.

Appelqvist, Pekka, Jere Knuuttila, and Juhana Ahtiainen. 2007. "Development of an Unmanned Ground Vehicle for task-oriented operation-considerations on teleoperation and delay." *2007 IEEE/ASME international conference on advanced intelligent mechatronics.* IEEE. 1-6.

ATHANASOPULOS. 1989. "A. Network management for the pan-European GSM cellular system." *Second IEE National Conference on Telecommunications 1989.* IET. 226–231.

Augustin, Aloÿs, Jiazi Yi, Thomas Clausen, and William Mark Townsley. 2016. "A study of LoRa: Long range & low power networks for the internet of things." *Sensors 16* 1466.

BALAPUWADUGE, Indika AM et LI, Frank Y. 2019. "Hidden Markov model-based machine learning for mMTC device cell association in 5G networks." *2019 IEEE International Conference on Communications (ICC).* IEEE. 1-6.

BALEVI, Eren et GITLIN, Richard D. 2017. "Unsupervised machine learning in 5G networks for low latency communications." *2017 IEEE 36th International Performance Computing and Communications Conference (IPCCC).* IEEE. 1-2.

BALLARD, M., ISSENMANN, E., MOYA-SANCHEZ, M. 1990. "Intelligent network application for mobile-radio systems. ." *International Symposium on Switching.* IEEE. 199–204.

BERTENYI, Balazs, BURBIDGE, Richard, MASINI, Gino, et al. 2018. "NG radio access network (NG-RAN)." *Journal of ICT Standardization* 59–76.

BHUVANESHWARI, A., HEMALATHA, R., et SATYASAVITHRI, T. 2016. "Semi-deterministic hybrid model for path loss prediction improvement." *Procedia Computer Science* 336-344.

Bojović, Biljana, Elena Meshkova, Nicola Baldo, Janne Riihijärvi, Marina Petrova. 2016. "Machine learning-based dynamic frequency and bandwidth allocation in self-organized LTE dense small cell deployments." *EURASIP Journal on Wireless Communications and Networking* 1-16.

References
_____

BROWN, Gabrial. 2017. "Service-based architecture for 5G core networks." *Huawei White Paper.*

CAI, Jain et GOODMAN, David J. 1997. "General packet radio service in GSM." *IEEE Communications Magazine* 122-131.

CAPLAN, Arnold I. 2017. "New MSC: MSCs as pericytes are sentinels and gatekeepers." *Journal of Orthopaedic Research* 1151–1159.

CARLEO, Giuseppe et TROYER, Matthias. 2017. "Solving the quantum many-body problem with artificial neural networks ." *Science* 602-606.

CHEERLA, Sreevardhan, RATNAM, D. Venkata, et BORRA, Hima Sree. 2018. " Neural network-based path loss model for mobile cellular networks at 800 and 1800 MHz bands." *AEU-International Journal of Electronics and Communications* 179-186.

COLD PREY, Mikael, KOORAPATY, Havish, BERG, J.-E., et al. 2012. "Small-cell wireless backhauling: A non-line-of-sight approach for point-to-point microwave links." *2012 IEEE Vehicular Technology Conference (VTC Fall).* IEEE. 1-5.

DALELA, Chhaya, PRASAD, M. V. S. N., DALELA, P. K., et al. 2012. *Tuning of COST-231 Hata model for radio wave propagation predictions .* Academy & Industry Research Collaboration Center.

DETTI, Andrea, MA Marsan, NB Melazzi and S. Buzzi. 2018. "Functional architecture." *5g Italy White Book: From Research To Market* 59-68.

DING, Bin, QIAN, Huimin, et ZHOU, Jun. 2018. "Activation functions and their characteristics in deep neural networks." *2018 Chinese control and decision conference (CCDC).* IEEE. 1836-1841.

DONALEK, Ciro. 2011. "Supervised and unsupervised learning." *Astronomy Colloquia.* The USA: The USA.

DONGARE, A. D., KHARDE, R. R., KACHARE, Amit D., et al. 2012. "Introduction to artificial neural network. ." *International Journal of Engineering and Innovative Technology (IJEIT)* 189–194.

ElChall, R, Lahoud, Samer, ElHelou, M. 2019. "Lora WAN Measurement Campaigns in Lebanon." *IEEE Internet of Things Journal* 2366–2378.

ERMEL, Matthias, MÜLLER, Torsten, SCHUELER, Joerg, et al. 2002. "Performance of GSM networks with general packet radio services ." *Performance Evaluation* 285–310.

Fernandes, Fabio, Alexei Ashikhmin, and Thomas L. Marzetta. 2013. "Inter-cell interference in noncooperative TDD large scale antenna systems." *IEEE Journal on Selected Areas in Communications 31* 192-201.

FORCONI, Sonia, VIZZARRI, Alessandro. 2013. " Review of studies on end-to-end QoS in LTE networks." *AEIT Annual Conference 2013.* IEEE. 1-6.

Gadh, Rajit, and F. B. Prinz. 1995. ""A computationally efficient approach to feature abstraction in design-manufacturing integration." *The Journal of Manufacturing Science and Engineering* 16-27.

GHRIBI, Brahim, LOGRIPPO,. 2000. "Luigi. Understanding GPRS: the GSM packet radio service." *Computer Networks* 763-779.

GIANNATTASIO, Gustavo, ERFANIAN, Javan, WILLS, P., et al. 2009. *A guide to the wireless engineering body of knowledge (WEBOK).* John Wiley & Sons.

References
_____

Gobbo, Nicola, Alessio Merlo, and Mauro Migliardi. 2013. "A denial of service attack to GSM networks via attach procedure." *International Conference on Availability, Reliability, and Security.* Berlin, Heidelberg: Springer. 361-376.

GOHIL, Asvin, MODI, Hardik, PATEL, Shobhit K. 2013. "5G technology of mobile communication: A survey." *2013 international conference on intelligent systems and signal processing (ISSP).* IEEE. 288-292.

GOLDSMITH, Andrea. 2005. *Wireless communications.* Cambridge : Cambridge university press.

GROSAN, Crina., ABRAHAM, Ajith. 2011. "Artificial neural networks." *Intelligent Systems.* Berlin: Springer. 281-323.

GRUM, Marcus. 2022. "WiesbadenProblem Analysis and Problem Statement." *Construction of a Concept of Neuronal Modeling.* Springer Gabler. 13-427.

GU, Guifen, PENG, Guili. 2010. "The survey of GSM wireless communication system." *2010 international conference on computer and information application .* IEEE. 121-124.

Halonen, Timo, Javier Romero, and Juan Melero, eds. 2004. *GSM, GPRS and EDGE performance: evolution towards 3G/UMTS. .* John Wiley & Sons,.

HAR, Dongsoo, WATSON, Alix M., et CHADNEY, Anthony G. 1999. "Comment on diffraction loss of rooftop-to-street in COST 231-Walfisch-Ikegami model." *IEEE Transactions on Vehicular Technology* 1451-1452.

HASHIBSIDDIQUE, Abdul, ARIFUZZMAN, A. K. M., et TARIQUE, Mohammed. 2013. " Performance study of IEEE 802.16 d under Stanford University Interim (SUI) channel." *International Journal of Computer Networks & Communications* 137.

Hata, Masaharu. 1998. "Propagation loss prediction models for land mobile communications." *ICMMT'98. 1998 International Conference on Microwave and Millimeter Wave Technology. Proceedings (Cat. No. 98EX106).* IEEE. 15-18.

HOOMOD, Haider Kadhim, AL-MEJIBLI, Intisar, et JABBOORY, Abbas Issa. 2018. "Analyzing the study of path loss propagation models in wireless communications at 0.8 GHz." *Journal of Physics: Conference Series.* IOP Publishing. 012028.

HOPFIELD, John J. 1982. "Neural networks and physical systems with emergent collective computational abilities." *Proceedings of the national academy of sciences* 2554–2558.

HROVAT, Andrej, KANDUS, Gorazd, et JAVORNIK, Tomavz. 2013. "A survey of radio propagation modeling for tunnels." *IEEE Communications Surveys & Tutorials* 658-669.

HUBBEL, Yvette C. 1997. "A comparison of the IRIDIUM and AMPS systems." *IEEE Network* 52–59.

INALTEKIN, Hazer, CHIANG, Mung, POOR, H. Vincent, et al. 2009. "On unbounded path-loss models: effects of singularity on wireless network performance." *IEEE Journal on Selected Areas in Communications* 1078–1092.

ISABONA, J, IMOIZE, A.L., OJO, S. 2022. "Development of a Multilayer Percep-tion Neural Network for Optimal Predictive Modeling in Urban Micro-cellular Radio Environments." *Applied Sciences* 5713.

References

_____

Jalal, A., and Ijaz Uddin. 2007. "Security architecture for third generation (3G) using GMHS cellular network." *2007 International Conference on Emerging Technologies.* IEEE.

JENG, S.-S., CHEN, J.-M., TSUNG, C.-W., et al. 2010. "Coverage probability analysis of IEEE 802.16 system with intelligent antenna system over Stanford university interim fading channels." *IET communications* 91–101.

KAMARUDIN, L. M., AHMAD, R. B., ONG, B. L., et al. 2010. "Review and modeling vegetation propagation model for wireless sensor networks using omnet++. ." *2010 Second International Conference on Network Applications, Protocols, and Services.* IEEE. 78-83.

KARSOLIYA, Saurabh. 2012. "Approximating number of hidden layer neurons in multiple hidden layer BPNN architecture." *International Journal of Engineering Trends and Technology* 714–717.

KHAN, Asiya, SUN, Lingfen, IFEACHOR, Emmanuel. 2010. " Learning models for video quality prediction over wireless local area networks and universal mobile telecommunication system networks." *IET communications* 1389-1403.

KNOPP, Raymond, HUMBLET, Pierre A. 2000. "On coding for block fading channels." *IEEE Transactions on Information Theory* 189-205.

KOPPELMAN, Frank S. et SETHI, Vaneet. 2005. "Incorporating variance and covariance heterogeneity in the generalized nested logit model: an application to modeling long-distance travel choice behavior." *Transportation Research Part B: Methodological* 825-853.

Laipio, Lauri. 2008. "Adjacency visualization in mobile networks."

LEE, William CY. 1998. "Mobile communications engineering: theory and applications." *McGraw-Hill Education.*

LIEW, Shan Sung, KHALIL-HANI, Mohamed, et BAKHTERI, Rabia. 2016. "Bounded activation functions for enhanced training stability of deep neural networks on visual pattern recognition problems." *Neurocomputing* 718-734.

Liitsalo, Laura, and Anne Salomaa. 2000. *The use of metadata in network management system as a social action.*

LILLICRAP, Timothy P., SANTORO, Adam, MARRIS, Luke, et al. 2020. "Back-propagation and the brain ." *Nature Reviews Neuroscience* 335–346.

LIU, Jingchu, DENG, Ruichen, ZHOU, Sheng, et al. 2015. "Seeing the unobservable: Channel learning for wireless communication networks." *2015 IEEE Global Communications Conference (GLOBECOM).* IEEE. 1–6.

MACCARTNEY, George R., ZHANG, Junhong, NIE, Shuai, et al. 2013. "Path loss models for 5G millimeter wave propagation channels in urban microcells." *2013 IEEE global communications conference (GLOBECOM).* IEEE. 3948–3953.

MCCULLOCH, Warren S. et PITTS, Walter. 1943. "A logical calculus of the ideas immanent in nervous activity." *The bulletin of mathematical biophysics* 115–133.

MEDDOUR, Djamal-Eddine, RASHEED, Tinku, GOURHANT, Yvon. 2011. "On the role of infrastructure sharing for mobile network operators in emerging markets ." *Computer networks* 1576-1591.

References
_____

MEDEISIS, Arturas et KAJACKAS, Algimanta. 2000. "On the use of the universal Okumura-Hata propagation prediction model in rural areas ." *VTC2000-Spring. 2000 IEEE 51st Vehicular Technology Conference Proceedings (Cat. No. 00CH37026).* IEEE. 1815-1818.

NAVARRO-ORTIZ, Jorge, ROMERO-DIAZ, Pablo, SENDRA, Sandra, et al. 2020. "A survey on 5G usage scenarios and traffic models. ." *IEEE Communications Surveys & Tutorials* 905–929.

Ohyane, Hidehiko, Daisuke Tanigawa, Naoki Nakaminami, and Yoshitaka Hiramoto. 2007. "Base station supporting IP transport." *NTT DoCoMo Technical Journal 9* 7-12.

OJO, Stephen, IMOIZE, Agbotiname, et ALIENYI, Daniel. 2021. "Radial basis function neural network path loss prediction model for LTE networks in multi-transmitter signal propagation environments ." *International Journal of Communication Systems* e4680.

PARWEZ, Md Salik, RAWAT, Danda B., et GARUBA, Moses. 2017. "Big data analytics for user-activity analysis and user-anomaly detection in mobile wireless network ." *IEEE Transactions on Industrial Informatics* 2058-2065.

PEREIRA, Vasco, SOUSA, Tiago. 2004. "Evolution of Mobile Communications: from 1G to 4G. ." *Department of Informatics Engineering of the University of Coimbra, Portugal* 0-20.

PEREZ, Juan S., JAYAWEERA, Sudharman K., et LANE, Steven. 2017. "Machine learning aided cognitive RAT selection for 5G heterogeneous networks." *2017 IEEE International Black Sea Conference on Communications and Networking (BlackSeaCom).* IEEE. 1-5.

PERLOVSKY, Leonid I. 2001. *Neural networks, and intellect: Using model-based concepts.* New York: Oxford University Press.

Plets, David, Roel Mangelschots, Kris Vanhecke, Luc Martens, and Wout Joseph. 2016. "A mobile app for real-time testing of path-loss models and optimization of network planning." *In 2016 IEEE 27th Annual International Symposium on Personal, Indoor, and Mobile Radio Communications (PIMRC.* IEEE. 1-7.

PLÖCHL, Matthias. 2001. "Neural network approach for modeling ammonia emission after manure application on the field." *Atmospheric Environment* 5833–5841.

POPOOLA, S.I, ATAYERO, A.A, ARAUSI, O.D, V.O. 2018. " Matthews. Path loss dataset for modeling radio wave propagation in a smart campus environment." *Data Brief 2018* 1062-1073.

POPOOLA, Segun I., ATAYERO, Aderemi A., et POPOOLA, Oluwafunso A. 2018. "Comparative assessment of data obtained using empirical models for path loss predictions in a university campus environment ." *Data, in brief* 380–393.

Rabeb, Faleh, Bedoui Souhir, Kachouri Abdermaceur, Samet Mounir. 2013. "An electronic nose for detection pollutant odorant and olfaction classification using neural network." *14th International Conference on Sciences and Techniques of Automatic Control & Computer Engineering-STA'2013.* IEEE. 174-178.

RAHEEMAH, Auda, SABRI, Naseer, SALIM, M. S., et al. 2016. " New empirical path loss model for wireless sensor networks in mango greenhouses." *Computers and Electronics in Agriculture* 553–560.

RANI, Pooja, CHAUHAN, Vinit, KUMAR, Sudhir, et al. 2014. "A review on wireless propagation models." *International Journal of Engineering and Innovative Technology* 256-261.

References

RASID, Mohd Fadlee A, WOODWARD, Bryan. 2005. "Bluetooth telemedicine processor for multichannel biomedical signal transmission via mobile-cellular networks." *IEEE transactions on information technology in biomedicine* 35–43.

REMY, Jean-Gabriel, LETAMENDIA, Charlotte. 2014. *LTE standards.* John Wiley & Sons.

RIBEIRO, Marco Tulio, SINGH, Sameer, GUESTRIN, Carlos. 2016. " Model-agnostic interpretability of machine learning." *2016 ICML Workshop on Human Interpretability in Machine Learning (WHI 2016).* New York: arXiv preprint arXiv. 1606.05386.

Rosa, Claudio, José Outes, Konstantinos Dimou, T. B. Sorensen, Jeroen Wigard, Frank Frederiksen, and Preben E. Mogensen. 2004. "Performance of fast Node B scheduling and L1 HARQ schemes in WCDMA uplink packet access." *2004 IEEE 59th Vehicular Technology Con.* 1635-1639.

ROXIN, Ana, GABER, Jaafar, WACK, Maxime, et al. 2007. "Survey of wireless geolocation techniques." *2007 IEEE Globecom Workshops.* IEEE. 1-9.

Saidi, Riad, Nada Cherrid, and Tarek Bentahar. 2020. "Study of the Prediction of Way Weakening in Mobile Radio Service: Applied to a Part of the City of Batna-Algeria." *In 2020 4th International Conference on Advanced Systems and Emergent Technologies (IC_ASET).* IEEE. 389-393.

SARIGIANNIDIS, Panagiotis, SARIGIANNIDIS, Antonios, MOSCHOLIOS, Ioannis, et al. 2017. "DIANA: A machine learning mechanism for adjusting the TDD uplink-downlink configuration in XG-PON-LTE systems." *Mobile Information Systems.*

SAUNDERS, Simon R, ARAGÓN-ZAVALA, Alejandro. 2007. *Antennas and propagation for wireless communication systems.* John Wiley & Sons.

SEIDEL, Scott Y. et RAPPAPORT, Theodore S. 1992. "91914 MHz path loss prediction models for indoor wireless communications in multifloored buildings." *IEEE Transactions on Antennas and Propagation* 207-217.

SEUNG, Sebastian. 2012. *Connectome: How the brain's wiring makes us who we are.* HMH.

SHAHAJAHAN, Mohammad. 2009. *Analysis of propagation models for WiMAX at 3.5 GHz.*

SHUAI, Nie, CHANGXING, Pei, XIANDENG, He, et al. 2011. " 3G/4G mobile communications propagation loss NPL model and network optimization scheme under shelter of vegetation." *2011 International Conference on Electronic & Mechanical Engineering and Information Technology.* IEEE. 4248-4250.

Sizun, Hervé, Pierre de Fornel. 2005. *Radio wave propagation for telecommunication applications.* BerlinHeidelbergNew York: Springer.

SMITHA, K., SIVABALAN, Arumugam, JOHN, Joseph, et al. 2009. " Modified Ceiling Bounce Model for Computing Path Loss and Delay Spread in Indoor Optical Wireless Systems ." *Int. J. Commun. Netw. Syst. Sci* 754-758.

SONG, Weinan, ZENG, Fanhui, HU, Jingzhi, et al. 2017. "An unsupervised-learning-based method for multi-hop wireless broadcast relay selection in urban vehicular networks." *2017 IEEE 85th Vehicular Technology Conference (VTC Spring).* IEEE. 1-5.

Sotiroudis, Sotirios P., Sotirios K. Goudos, Konstantinos A. Gotsis, Katherine Siakavara, John N. 2013. "Application of a composite differential evolution algorithm in optimal neural network design for propagation path-loss prediction in mobile communication systems." *IEEE Antennas and Wireless Propagation Letters* 364-367.

SPINELLIS, Diomidis. 2000. "Reflection as a mechanism for software integrity verification." *ACM Transactions on Information and System Security (TISSEC), 2000* 51–62.

SULYMAN, Ahmed Iyanda, NASSAR, AlMuthanna T., SAMIMI, Mathew K., et al. 2014. "Radio propagation path loss models for 5G cellular networks in the 28 GHz and 38 GHz millimeter-wave bands." *IEEE communications magazine* 78-86.

SURAJUDEEN-BAKINDE, Nazmat T., FARUK, Nasir, POPOOLA, Segun I., et al. 2018. "Path loss predictions for multi-transmitter radio propagation in VHF bands using Adaptive Neuro-Fuzzy Inference System." *Engineering Science and Technology, an International Journal* 679-691.

TAYAL, Mayank. 2005. " Location services in the GSM and UMTS networks." *2005 IEEE International Conference on Personal Wireless Communications.* IEEE. 373–378.

Timoteo, R, Cunha, D, Cavalcanti, G. 2014. "A proposal for path loss prediction in urban environments using support vector regression ." *Advanced International Conference on Telecommunications .* Paris, France.

TINGNAN, Bao. 2013. "The architectural differences between LTE and WiMAX." *KTH Royal Institute of Technology* 11.

VARDHAN, C. Sree, RATNAM, D. Venkat, BHAGYASREE, N., et al. 2014. "Analysis of path loss models of 4G femtocells." *2014 Eleventh International Conference on Wireless and Optical Communications Networks (WOCN).* IEEE. 1–6.

VILLAVERDE, Jorge Eduardo, GODOY, Daniela, AMANDI, Analía. 2006. "Learning styles' recognition in e-learning environments with feed-forward neural networks." *Journal of Computer Assisted Learning* 197-206.

WANG, Li-Chun et CHENG, Shao-Hung. 2018. "Data-driven resource management for ultra-dense small cells: An affinity propagation clustering approach." *IEEE Transactions on Network Science and Engineering* 267-279.

WICKRAMASURIYA, Dilranjan S., PERUMALLA, Calvin A., DAVASLIOGLU, Kemal, et al. 2017. "Base station prediction and proactive mobility management in virtual cells using recurrent neural networks." *2017 IEEE 18th Wireless and Microwave Technology Conference.* IEEE. 182-190.

WU, Jiansheng, LONG, Jin, et LIU, Mingzhe. 2015. "Evolving RBF neural networks for rainfall prediction using hybrid particle swarm optimization and genetic algorithm." *Neurocomputing* 136-142.

YANG, Jia-Qin, WANG, Ruopeng, REN, Yi, et al. 2020. "Neuromorphic Engineering: From Biological to Spike-Based Hardware Nervous Systems." *Advanced Materials* 2003610.

YELOME, Landry T., OUYA, Samuel, NDIAYE, Samba, et al. 2015. "Contribution to SMS management over 4G network in distance education context." *2015 IEEE/ACS 12th International Conference of Computer Systems and Applications (AICCSA).* IEEE. 1–6.

ZAEEM, Mohammad Nokhbeh et KOMEILI, Majid. 2021. "Cause and effect: Concept-based explanation of neural networks." *2021 IEEE International Conference on Systems, Man, and Cybernetics (SMC).* IEEE. 2730-2736.

ZAPPONE, Alessio, SANGUINETTI, Luca, et DEBBAH, Merouane. 2018. "User association and load balancing for massive MIMO through deep learning." *2018 52nd Asilomar Conference on Signals, Systems, and Computers.* IEEE. 1262-1266.

Zhang, Sai Qian, Feng Xue, N. Ageen Himayat, Shilpa Talwar, H. T. Kung. 2018. "A machine learning assisted cell selection method for drones in cellular networks." *2018 IEEE 19th International Workshop on Signal Processing Advances in Wireless Communications (SPAWC).* IEEE. 1-5.

ZHANG, Yalin, XIONG, Liang, et YU, Jia. 2020. "Deep learning-based user association in heterogeneous wireless networks." *IEEE Access* 197439-197447.